Multichannel Bioimpedance Spectroscopy: Instrumentation Methods and Design Principles

PAUL ANNUS

TUT
PRESS

TALLINN UNIVERSITY OF TECHNOLOGY
Faculty of Information Technology
Department of Electronics

Dissertation was accepted for the defense of the degree of Doctor of Philosophy in Engineering on December 02, 2009.

Supervisors: Professor Mart Min
Department of Electronics, Faculty of Information
Technology, Tallinn University of Technology

Doctor Toomas Parve
Department of Electronics, Faculty of Information
Technology, Tallinn University of Technology

Opponents: Professor Ivars Bilinskis, Academician, Latvian Academy
of Sciences

Doctor Phys. Alberts Kristiņš, Head of Laboratory
Laboratory of Electronic Engineering, Institute of Solid
State Physics, University of Latvia

Defense of the thesis: January 11, 2010

Declaration:
Hereby I declare that this doctoral thesis, my original investigation and achievement, submitted for the doctoral degree at Tallinn University of Technology has not been submitted for any academic degree.

/ *Paul Annus* /

Paljukanaliline bioimpedantsspektroskoopia: mõõtemeetodid ja disaini printsiibid

PAUL ANNUS

Abstract

Diagnostic value of electrical signals from human body and its interaction with electrical stimulus in modern medicine is unquestionable. With advancements in technology, theory and gathered experimental knowledge usage of electrical phenomena is increasingly important and realistic in medical practice. Information gathered can be used in monitoring of bodily parameters, monitoring of the state of the tissue under investigation, and lately also in real time closed loop optimization of parameters of electrical aids, such as pacemakers for example.

One of the most challenging tasks in medicine is evaluation of the condition of the human heart. Cardiovascular disease is the number one cause of death globally: more people die annually from cardiovascular diseases than from any other cause. Main diagnostic tool has been so far 12-lead electrocardiography. Unfortunately electrocardiography gives information mostly regarding electrical triggering pulses of the heart and does not directly reflect the actual mechanical pumping function. Main mechanical parameters, such as cardiac output, and stroke volume are hard to estimate even today. There are invasive methods, which are costly, and potentially dangerous. Among the most promising modern non invasive methods is ultrasound imaging, but there is another well known method - impedance cardiography, pioneered by Kubicek and Patterson for NASA in the 1960's. That non invasive method is theoretically ideal for estimation of cardiac parameters, unfortunately it has traditionally been also remarkably unreliable, and has trouble producing comparable quantitative results. Need for a cheap and noninvasive diagnostic tool nonetheless warrants further investigation in this area.

Conceptual investigation has been carried out, and design of an instrument for intracardiac spectroscopy proposed. Based on that conceptual design real instrument is designed, built, and tested. While still invasive, electrodes are placed inside heart, such an instrument allows further investigation in the area of impedance based measurements for detecting cardiac parameters, and as such gives valuable insight needed for construction of noninvasive devices, and allows also design improvements for cardiac pacemakers. Currently different versions from said device are in use in several leading laboratories worldwide.

Current thesis is concerned mostly with the design of the analog part of the device from digital to analog converters to analog to digital conversion. Suitable signals passing through tissue under investigation are discussed and some new waveforms proposed, together with general signal processing aspects. While constructed device fulfilled preliminary requirements it can be further improved. Some improvements are introduced, and directions for future work given.

Kokkuvõte

Inimkeha poolt genereeritud elektriliste signaalide ja keha ning elektromagnet-välja vastasmõju tulemusena tekkivate signaalide diagnostilist väärtust kaasaegses meditsiinis on võimatu alahinnata. Ühes teooria ja tehnoloogia arenguga, ning tänu üha täiuslikumale andmehulgale, mis on saadud läbiviidud uuringutest, muutub elektriliste signaalide kasutamine ja töötlemine praktilises meditsiinis üha tähtsamaks ja usaldatavamaks. Saadud andmed võimaldavad hinnata kudede olukorda ja keha füsioloogilisi parameetreid. Üha enam leiavad kaasaegsed signaalitöötlusmeetodid kasutust elektriliste abivahendite töö optimeerimisel reaalajas.

Üheks tähtsamaks ülesandeks meditsiinis on inimsüdame olukorra jälgimine ja vajadusel ka tema töö korrigeerimine. Südame-veresoonkonna haigused põhjustavad ülemaailmselt rohkem surmaga lõppevaid haigusjuhtumeid kui ükski teine tegur. Peamiseks diagnostikavahendiks on seni elektrokardiograafia. Kahjuks annavad elektrokardiograafi signaalid informatsiooni peamiselt südametegevust kontrollivate elektriimpulsside kohta ja ei peegelda usaldusväärselt südame tegelikku tööd vere pumpamisel. Peamised mehaanilised parameetrid, nagu südame võime verd väljutada ja tegelik löögimaht, on ka tänapäeval raskelt hinnatavad. On olemas invasiivsed meetodid, kuid nad on kallid ja potentsiaalselt ohtlikud. Võimalike mitteinvasiivsete meetodite hulgas on üks paljulubavamaid südame ultraheliuuring – ehhokardiograafia, kuid on ka üks teine hästituntud võimalus – impedantskardiograafia. Meetod töötati välja kuuekümnendatel NASA tarbeks Kubiceki ja Pattersoni poolt. Kuigi impedantskardiograafia on teoreetiliselt ideaalne mitteinvasiivne meetod, on tema praktiline rakendamine olnud seni raskendatud seoses mõõtetulemuste vähese usaldusväärsuse ja korratavusega. Vajadus mõõduka hinnaga mitteinvasiivsete diagnostikavahendite järele põhjendab jätkuvaid uuringuid impedantskardiograafia vallas.

Läbiviidud kontseptuaalsed uuringud võimaliku südame impedantsspektroskoopia seadme loomiseks on viinud disainilahenduseni. Lähtuvalt tulemustest on valmistatud ja testitud ka reaalne instrument. Kuigi tegemist on invasiivse seadmega, mõõteelektroodid asuvad südame sees, võimaldab selline seade saada väärtuslikke andmeid, mis on vajalikud mitteinvasiivsete seadmete loomiseks ja südamerütmurite töö parendamiseks. Käesoleval hetkel on seadme erinevad variandid kasutusel mitmes juhtivas laboratooriumis üle maailma.

Antud töö keskendub peamiselt seadme analoogosaga seonduvale. Alates digitaal-analoog muunduritest kuni analoog-digitaal muundamiseni. On kaalutud signaalide sobivust kudede impedantsuuringute läbiviimiseks ja pakutud välja uusi lahendusi koos sobivate signaalitöötlusmeetoditega. Kuigi konstrueeritud seade vastas algsetele nõudmistele, on teda jätkuvalt võimalik parendada. Mõned muudatustest on realiseeritud ja on hinnatud perspektiivseid suundi tuleviku tarbeks.

Acknowledgments

Contents

Frequent abbreviations, and acronyms

AC	alternating current
ADC	analog to digital converter
ASIC	application specific integrated circuit
BiMOS	bipolar metal oxide semiconductor
CMOS	complementary metal–oxide–semiconductor
CMRR	common mode rejection ratio
CPE	constant phase element
DAC	digital to analog converter
DASP	digital alias free signal processing
DC	direct current
DDS	direct digital synthesizer
DFT	discrete Fourier transform
DNL	differential nonlinearity
DSP	digital signal processing
EBI	electrical bioimpedance
ECG	electro cardiogram
FPGA	field programmable gate array
I2C	inter-integrated circuit
ICG	impedance cardiogram
INL	integral nonlinearity
LAN	local area network
LPF	low pass filter
LSB	least significant bit
LTI	linear and time invariant (system)
LXI	lan extensions for instrumentation
MLS	maximum length sequence
MSPS	mega samples per second
NSD	numerical synchronous detection
PAPR	peak to average power ratio
PAR	peak to average ratio
PCB	printed circuit board
POR	power on reset
PTP	precision timing protocol
RMS	root mean square
SAR	successive approximation
SD	synchronous detector
SNR	signal to noise ratio
SPI	serial peripheral interface
THD	total harmonic distortion
USB	universal serial bus
WHO	World Health Organization

1

1.1   **Introduction**

Exploration and admiration of the human being has probably existed as long as the human race. It is enough to look at the excitement of the small child when discovering his own body. Therefore it is of no surprise that many breakthrough discoveries are initiated by observing humans and their interactions with surrounding world. By popular myth Archimedes discovered fundamental relationship between weight of the objects in the water and the volume of water they displace when taking bath himself. Eureka. Same applies to other phenomena, among them electricity. Experiments were largely inspired by interaction between electricity and living tissue. From royal experiments with soldiers forming conductors and jumping on applied electrical charge through Luigi Galvani's experiments with frog legs to modern day.

First known version of fundamental relationship between applied voltage, body resistance, and flowing current, later known as Ohm's law, was described by Henry Cavendish in January 1781. Cavendish's discovery was born long before Georg Ohm's work, while he was experimenting with Leyden jars and glass tubes of varying diameter and length filled with salt solution. He measured the current by noting how strong was the shock he felt, when he completed the circuit with his body. Cavendish wrote that the "velocity" (current) varied directly as the "degree of electrification" (voltage). As it unfortunately happens he did not communicate his results to other scientists at the time, and his results were unknown until Maxwell published them in 1879 (Bordeau, 1982).

Results from such experiments where threefold: first they described effects of the electrical current on living tissue, secondly they allowed description of the electrical properties of said tissue, and thirdly electricity generated and communicated by the tissue were examined. While experiments in the field of electricity where transferred to other areas, such as communication of information by means of varying electrical signal parameters over the distance, and became much more

mathematical and theoretical, experiments determining effects of the electricity on human and animal subjects continued as well. At the end of 19th century Arthur E. Kennelly (1861-1939) conducted study comparing effects of direct and alternating currents (DC, AC) in the context of so-called "battle of the systems" during his work in Thomas Alva Edison's West Orange laboratory (Bush, 1940) (Brittain, 2006). In his textbook from 1895 written together with Edwin J. Houston (Houston & Kennelly, 1895) he states: "A marked difference exists between the physiological effects of an alternating and a continuous current. When a continuous current is sent through human body, chemical and physiological effects are produced, entirely distinct from those which attend the passage of an alternating current under similar circumstances. When passing through the vital organs of the body, any electric current, whether continuous or alternating, may, if sufficiently powerful, cause death. Alternating currents, however, at commercial frequencies and pressures, are much more apt to produce fatal effects on the human body than continuous currents. In New York State, alternating electric currents are used for the execution of criminals, and, when properly employed, produce absolute, instantaneous, and painless death". The later passus is clearly connected with Edison's war against AC currents. Despite of he's contempt for capital punishment it was Thomas Alva Edison who invented the electric chair to frighten people away from the use of Nikola Tesla's (1856 – 1943) AC system of electricity (Vujić, 2006). The public was shocked. Nevertheless Kennelly, since 1893 an independent consultant, continues (Houston & Kennelly, 1895) "The experiments of Tesla and others have shown that at frequencies and pressures far higher than those employed for ordinary commercial purposes, the physiological effects of alternating currents become less severe, and that at extraordinarily high frequencies, enormous pressures may be handled with impunity". It was Nikola Tesla who discovered that high voltage current could be made harmless by using alternating current scheme at very large frequencies and he predicted that it could be used for medical purposes. He also experimented with X-rays from 1894 – 1896, basically before and after the Roentgen explained their nature and origin (Vujić, 2006). Work in the same direction was continued by Kennelly in 1910, together with E .F. W. Alexanderson on the physiological tolerance of human subjects to high-frequency currents up to 100 kHz The tolerance current was defined as "the limiting currents strength which the subject could take through the arms and body without marked discomfort or distress" (Brittain, 2006). Similarities can be observed with much earlier works of Henry Cavendish. Results are actual even today. Kennelly and Alexanderson reported that a man could tolerate a current of about 500 mA at 100 kHz, but only 5 mA at 60 Hz. Limits of allowable currents are lower today, but their dependence on

frequency remains largely the same. Discussion on electrical safety and physiological effects can be found in (Webster, 1997). Still interaction with living tissue remained underexplored until the middle of twentieth century. Partly because living tissue is hard object to work with, partly because it requires simultaneous knowledge in many related areas of science, and also of course because the available technology was not yet up to the task. For example Alexanderson's radio-frequency alternator used in aforementioned experiments was largely mechanical heavy equipment. Another difficulty arises from ethical considerations. Gambling with animal or even human lives during experiments, such as the ones performed in US prisons during executions, not to mention war time crimes, raises many moral issues.

Nevertheless diagnostic value of electrical signals from human body and its interaction with electrical stimulus in modern medicine is unquestionable. With advancements in technology, theory and gathered experimental knowledge, usage of electrical phenomena is increasingly important and realistic in medical practice. Information gathered can be used in monitoring of bodily parameters, monitoring of the state of the tissue under investigation, and lately also in real time closed loop optimization of parameters of electrical aids, such as pacemakers for example. One of the most challenging tasks in medicine is evaluation of the condition of the human heart. Cardiovascular disease (CVD) is the number one cause of death globally: more people die annually from CVDs than from any other cause (WHO, 2009). Main diagnostic tool has been so far 12-lead electrocardiography (ECG). Main problem with ECG is that it gives information regarding electrical triggering pulses of the heart and does not directly reflect the actual mechanical pumping function. Main mechanical parameters, such as cardiac output, and stroke volume are hard to estimate even today. There are invasive methods, which are costly, and potentially dangerous. Among them measurement of the oxygen consumption based on Fick principle is the best known. In 1870 Adolf Eugen Fick was the first to devise a technique for measuring cardiac output. Among the most promising modern non invasive methods is ultrasound imaging, but there is another well known method impedance cardiography (ICG) pioneered by Kubicek and Patterson for NASA in the 1960's (Patterson, Kubicek, Kinnen, Witsoe, & Noren, 1964) (Kubicek, Karnegis, & Patterson, Development and evaluation of an impedance cardiac output system, 1966) (Kubicek, Patterson, & Lillehei, Impedance cardiography as a non-invasive method to monitor cardiac function and other parameters of the cardiovascular system, 1970). That non invasive method is theoretically ideal for estimation of cardiac parameters, unfortunately it is also remarkably unreliable, and has trouble producing comparable quantitative results.

Need for a cheap and noninvasive diagnostic tool nonetheless warrants further investigation in this area.

Current thesis is concerned with practical implementation of an impedance cardiograph for clinical tests. General overview is given on various subjects associated with the task. Design considerations of the apparatus are discussed, and some indications are given for further improvement.

1.2 Analog versus digital realm

When considering scientific experiments one can separate object, interaction with object, observation of results, conversion, signal processing, reasoning and often some form of feedback. It is generally assumed that digitizing and digital signal processing are relatively modern and recent phenomena, and it was preceded by its purely analog counterpart. While there is some truth in that, closer examination reveals also discrepancies. Considering Henry Cavendish's (HC) experiment leading to discovery of first known form of Ohm's law it is possible to draw following picture (Fig. 1.):

| | | t₁ | t₂ | t₃ | t₄ | t₅ |
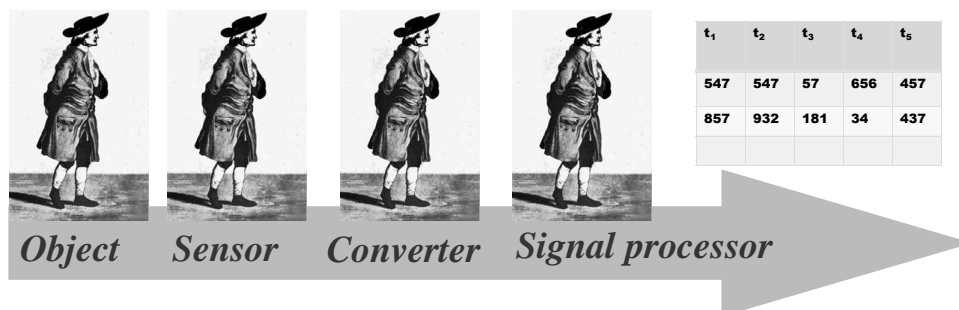
Fig. 1. Flow of the experiment data processing: from object under investigation through sensing, processing and converting the data, to documentation of the results.

Whereas experimenter HC injects current into object HC, sensor HC reads results, coverts them, processes data, and draws conclusions. While at first glance such an experiment has nothing to do with digital signal processing it is not entirely true. First an excitation. Since experiment was done with Leyden jars it is safe to assume that the delivered current was more like a short pulse, then long term stabile signal. Secondly HC could not perform all the tasks entirely simultaneously. Therefore

again it is relatively safe to assume that sensing was not continuous in time, but at discrete time intervals, likely somewhat synchronous to introduced pain. Next sensed signal is probably best described, even if somewhat fuzzily, as quantized. For example: not really painful, painful and very painful. And such a discrete, both in time and in value, observations and conclusions are later converted back into analog domain, by stating aforementioned law. Later experiments replaced excitation with more stable sources, starting with Galvani elements, and voltaic piles which still exhibited large changes in time, and made experiments difficult to repeat. Major breakthrough came probably when Estonian-German physicist Thomas Johann Seebeck discovered thermoelectricity in 1821. Only after Seebeck published his findings could Georg Simon Ohm use thermocouples in his famous experiments (Velmre, 1971), as they provided a more stable voltage source, and formulate in 1827 his famous law (Ohm, 1827). Much later sinusoidal generators, first electromechanical, followed. Human body was replaced with either man made or natural objects, indication of results with Deprez-Carpentier voltmeter or similar apparatus. All very analog in nature. Nevertheless, as soon as reading of the results happened digitalization took place. Up until the introduction of analog signal processing elements, and ultimately analog computers, but at the end there was still a human being reading and analyzing the results. So in time human being moved right on the picture, but never disappeared entirely, up until very recently when digital computers took over, and analog to digital conversion was introduced in hardware. With advances in technology such a converter unit started to move towards the left end of the picture, or closer to the object under investigation. In another words it was never the question whether to use analog or digital sensing and signal processing, but at which point, and how exactly should the conversion happen:

Fig. 2. Where to convert data from analog to digital domain.
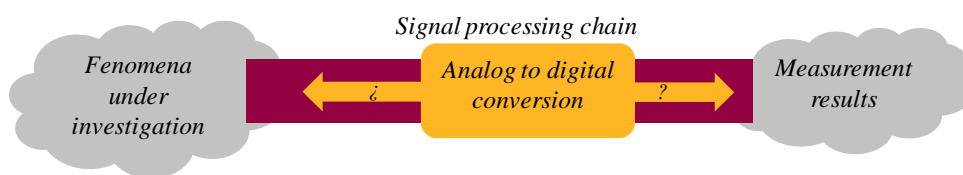
To confuse matters further one could argue, that in real world every signal, and signal processing unit is analog in the nature, or to some extent vice versa digital, if quantum physics is involved. In fact both statements are gaining even more field when latest chip making technologies are involved, and transistors in digital processors are starting to behave erratically.

Still the question regarding where to digitize is very actual even today, when it is possible to convert between analog and digital domains at almost arbitrary position within signal processing chain. Some of the reasons warranting investigation in that area are need for more accurate measurements, conservation of energy, and last but not least cost of implementation. Optimization between these parameters is mainly empirical.

1.3 **Black box**

Before describing exact methods for signal processing, and apparatus it is relevant to have reasonable description of the object under investigation, and its parameters. It is well known that linear, time invariant (LTI) systems can be completely described by their response $h(t)$ to excitation with Dirac delta:

$$\delta(t) = \begin{cases} +\infty, & t = 0 \\ 0, & t \neq 0 \end{cases} \tag{1.1}$$

There is third rule the function must follow, i.e. the area should be equal to 1:

$$\int_{-\infty}^{\infty} \delta(t)dt = 1 \tag{1.2}$$

Dirac delta function $\delta(t)$ is a purely mathematical construct introduced by theoretical physicist *Paul Dirac*. As such it is impossible to use $\delta(t)$ directly in real life measurements. Fortunately based on the third rule it is possible to create real signals, which behave reasonably well. First of all if excitation pulse is relatively short compared to time where $h(t) \neq 0$, and its area is 1 then it can be viewed as sufficiently similar to $\delta(t)$. Secondly integral of the $\delta(t)$ is very useful function itself:

$$H(x) = \int_{-\infty}^{x} \delta(t)dt \tag{1.3}$$

This Heaviside step function was introduced by Oliver Heaviside, and is relatively easy to create and use, if ambiguity at *x=0* is resolved. If for an arbitrary excitation *x(t)* the response *y(t)* can be calculated as convolution between *x(t)*, and systems impulse response *h(t)*, or $y(t) = h(t) * x(t)$, where *h(t)* is response of the system in case of $x(t) = \delta(t)$, then evolution function of the dynamical system $\int h(t)dt = h(t) * H(t)$, and form that *h(t)* can be easily determined. Second way to use $\delta(t)$, is to consider that:

$$\delta(t) = \lim_{a \to 0} \frac{1}{a} \left(sinc(t/a) \right) \qquad (1.4)$$

$sinc(x) = \sin(\pi x)/\pi x$, or normalized $sinc$ function is often used in modern signal processing.

That very powerful mathematics can be exploited if the system under investigation is linear and time invariant. In real life it is never entirely true. In fact it is principally impossible to measure a system without interacting with it and involuntarily changing its parameters due to that fact. All systems exhibit to certain extent different behavior depending on the magnitude of the applied stimulus, and parameters do change with time. In best case it is called aging and is usually very slow process, in worst case fast random fluctuations in parameters appear. Nevertheless LTI systems theory is widely used and with very good results. Only way to do it is to have certain knowledge regarding the system under investigation, and apply some restrictions while performing measurement. Or in another words model of the system should be created, and simplified according to certain rules. First of all any non-linear system can be considered as being piecewise linear. If the approximately linear region is reasonably narrow introduced errors can be negligible. Secondly: even if the system under investigation changes its parameters in time, it is usually possible to consider reasonably short time intervals, during which changes are again negligible. Typical modulations in parameters of biological tissues are well within frequency range on some hundred Hz, and therefore if the measurement timeframe is shorter then some ms then resulting errors are acceptably small.

Restrictions and simplifications are in fact essential in any model used by sciences, as well as some a priori knowledge regarding the system under investigation. If nothing is known about the object, then severe problems arise. First of all trying to relate all possible inputs to the system to outputs from the system is theoretically impossible, because the set of possible inputs is not countable. Secondly without more knowledge then input signals and corresponding output responses, even when limiting examination to continuous systems, where output responses are close to each other when input signals are, it is generally impossibly difficult task to deduce required rule between them. And furthermore things that humans do not expect to see remain often unnoticed, automatically filtered out by brain, therefore unknown rule may remain undetected even if in plain view. If there is some useful knowledge beforehand, then not just the input sequence can be limited, but also the model simplified. Perfect model of any object is the object itself, and as such is useless for system analysis, or in another words if we have full knowledge about

the object, needed for the perfect model, then there is no need to examine it at all. Humans do not have an overwhelming knowledge, and therefore object as its own model is not just useless, but also impossible. According to Albert Einstein only God needs not play dice. From his letter to Max Born: "I, at any rate, am convinced that He does not throw dice." (Born, 1971). Perhaps it is not strange that similar concepts as in systems theory are also in use in semiotics. Juri Lotman (Lotman, 2005) writes that for any meaningful communication between two subjects to take place these subjects must be dissimilar, and also similar to certain extent, or in another words their language spaces must intersect, but not coincide. Furthermore any valuable, non trivial, information exchange can happen only between non coinciding subspaces. This brings up unavoidable, actually valuable and enriching, errors in translation. Much like Karl Poppers assertment that hypothesis, proposition, or theory is scientific only if it is falsifiable. Looking for optimal choice of the models is directly linked to the understanding that they inevitably introduce errors, but also help in avoiding them. At the end any good model is inevitably falsifiable.

1.4   **Impedance and admittance**

Let's consider Linear Time Invariant (LTE) system, with sinusoidal excitation *i(t)*, impulse response *h(t)*, and output *u(t)*:
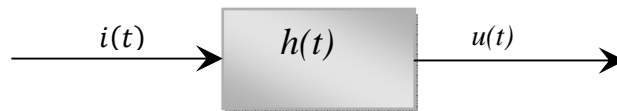
Fig. 3. LTI with excitation current *i(t)*, and output voltage *u(t)*.

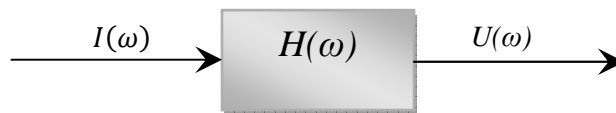And equivalent presentation of such a system in frequency domain:

Fig. 4. Same LTI as in Fig 3 presented in frequency domain.

Equation $u(t) = i(t) * h(t)$ in time domain is transformed into $U(\omega) = I(\omega) \cdot H(\omega)$, where frequency response $H(\omega) = \mathcal{F}h(t)$, or Fourier transform of the impulse response. Obviously it can be rewritten in the form:

$$H(\omega) = \frac{U(\omega)}{I(\omega)} = Z(\omega) \qquad (1.5)$$

That equation for sinusoidal currents was first defined by Oliver Heaviside in July 1886: electrical impedance or simply impedance, describes a measure of opposition to a sinusoidal alternating current. Or in another words impedance impedes current flow.

From modern point of view only small step was missing: usage of the complex numbers. Complex numbers were first conceived and defined by the Italian mathematician Girolamo Cardano, who may have borrowed some of the concepts from Niccolò Fontana Tartaglia, or perhaps because Cardano found them rather useless can be largely contributed to Rafael Bombelli's L'algebra (Bombelli, 1569). The term complex number was introduced by Carl Friedrich Gauss nearly two centuries later. It is safe to say that, introduced into electrical calculations several hundred years after Cardano, complex numbers revolutionized perception of how circuits work. In 1893 in his famous paper "Impedance" (Kennelly, 1893) Arthur E. Kennelly wrote: "…the working theory of alternating currents can be made as simple as working theory of continuous currents" through the use of the impedance concept and complex quantities. At the International Electrical Congress in Chicago in 1893 Charles Proteus Steinmetz made one of his greatest contributions to the Electrical Engineering community, a lecture and presentation describing the mathematics of alternating current phenomena and introduced the term phasor for his simplified mathematical representation of an electricity waveform (Brittain, 2006). Discussing Kennelly's paper Steinmetz cited: "Any circuit whatever, consisting of a combination of resistances, non-ferric inductances and capacities, carrying harmonically alternating currents, may be treated by the rules of unvarying currents, if the impedances are expressed by complex numbers:

$$a + bj = r(cos\varphi + jsin\varphi), \qquad (1.6)$$

the algebraical operations being then performed according to the laws controlling complex quantities.", and continues: "It is well known that points of a plane can be represented by complex quantities in their rectangular representation

$$a + bj, \qquad (1.7)$$

or their polar representation

$$re^{j\varphi} = r(cos\varphi + jsin\varphi), \qquad (1.8)$$

And use has been made hereof repeatedly in the mathematical treatment of vector quantities. It is, however, the first instance here, so far as I know, that attention is drawn by Mr. Kennelly to the correspondence between the electrical term "impedance" and the complex numbers.

The importance hereof lies in the following: The analysis of the complex plane is very well worked out, hence by reducing the electrical problems to the analysis of complex quantities they are brought within the scope of a known and well understood science." (Kennelly, 1893)

So instead of rather "complex" functions usage of complex numbers results in following equation, where Z is impedance, R resistance, and X reactance:

$$\dot{Z} = R + jX = \boldsymbol{Re\dot{Z}} + j\boldsymbol{Im\dot{Z}} \tag{1.9}$$

Thus it is possible to divide impedance Z into real and imaginary parts. On the complex plane arbitrary $\dot{Z}$ can be seen as vector with length $\left|\dot{Z}\right|$, and phase angle φ:
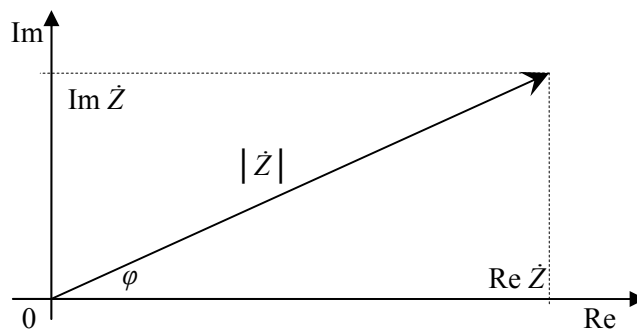
Fig. 5. The impedance vector and its real and imaginary parts.

Where $\left|\dot{Z}\right| = \sqrt{\mathrm{Re}\,\dot{Z}^2 + \mathrm{Im}\,\dot{Z}^2}$, and $\varphi = \arctan(Im\dot{Z}/Re\dot{Z})$. Let's consider two simple circuits. First series connection of resistor R and capacitor C:
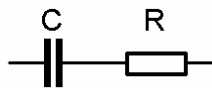
Fig. 6. The simplest RC circuit, a capacitor and a resistor are in series.

Impedance of the circuit can be expressed as $\dot{Z} = R + 1/j\omega C = R - j\,1/\omega C$. When $Re\dot{Z} = R$, and $Im\dot{Z} = -1/\omega C$ are known at one frequency it is possible to

calculate them, and consequently also impedance $\dot{Z}$ at any arbitrary frequency, since impedance values on complex plane draw strait line parallel to imaginary axis at the distance of R from it, starting at $-j\infty$ when $\omega = 0$ and ending at real axis at R when $\omega = \infty$. Therefore the phase angle is negative. This means that the voltage as dependent variable is lagging the current, which is general rule in capacitively behaving circuit, since $i = C(du/dt)$. When drawing phasor diagram for capacitive circuit it is often convenient to mirror image over real axis, and therefore move image into first quarter. It is denoted by – sign near imaginary axis. Things get somewhat more complicated when three element circuit is considered:
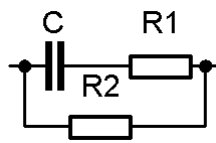
Fig. 7. Three element RC circuit, commonly used to discuss impedance of the tissue, also as Cole type A circuit.

In order to characterize circuit it is not enough anymore to make one measurement at single frequency. On phasor diagram frequency dependent impedance vector of the series connection of resistor and capacitor with parallel resistor is drawing a semicircular line:
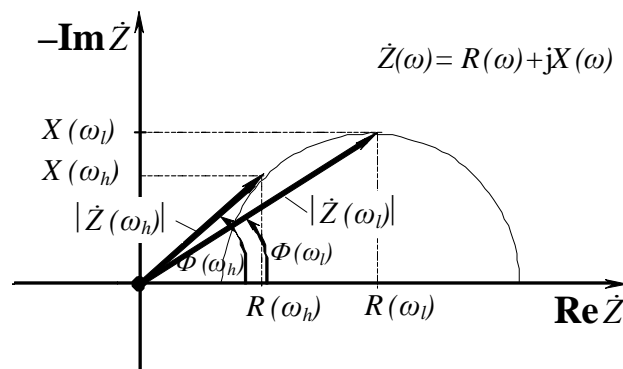
Fig. 8. the phasor diagram of the Fig. 7 Fig. 8circuit at two frequencies, low ωl and high ωh .

Instead of impeding one can also discuss that certain objects and substances are admitting current. Admittance is therefore an inverse of the impedance $\dot{Y} = 1/(\dot{Z}) = \boldsymbol{Re}\dot{Y} + j\boldsymbol{Im}\dot{Y} = G + jB$, where G is conductance, and B susceptance. Susceptance was first called permittance by Oliver Heaviside who introduced most of the terms here at the end of 19th century.

1.5 Dielectrics

Objects can be roughly characterized as conductors, insulators, or semiconductors according to their electrical properties. A dielectric, a material that can be penetrated by electric field, is traditionally an insulator. Arthur Robert von Hippel (1898 – 2003), one of the pioneers in the study of dielectrics, ferromagnetic and ferroelectric materials, writes in (von Hippel, 1988): "The present great debate on the structure of water and its changes with temperature, pressure, and solutes has produced a bewildering variety of models, all more or less supported by the same thermodynamic, spectroscopic, conduction, and diffraction data." Among great names involved in study of polar dielectrics is certainly Peter Debye (1884-1966), teacher of von Hippel who formulated following relaxation equation:

$$\dot{\varepsilon}(\omega) = \varepsilon_\infty + (\varepsilon_0 - \varepsilon_\infty)/(1 + j\omega\tau_0) \qquad (1.10)$$

Where $\dot{\varepsilon}(\omega)$ is complex permittivity of a medium, ε_∞ is permittivity at very high frequency, ε_0 is static permittivity at very low frequency, and τ_0 is the time constant of the relaxation process. Under linear conditions and for the same material, admittance Y, impedance Z and permittivity ε all contain the same information, differently presented, and are based on Maxwell equations. Maxwell equations are extremely robust and valid also for non-linear, non-homogenous and anisotropic systems. James Clerk Maxwell (1831 –1879) himself used the concept of quaternions displaced later by vector analysis, for which Heaviside can be largely credited. It was also Heaviside who compacted the equations to well known modern form. In part III of "A dynamical theory of the electromagnetic field", which is entitled "General equations of the electromagnetic field", Maxwell formulated twenty equations, which were in 1884 by Heaviside replaced by a set of four simplified equations, known today as Maxwell's equations. Rewriting of Debye's relaxation equation in more familiar impedance based form results in following:

$$\dot{Z} = R_\infty + \frac{1}{G_p + G_p j\omega\tau} \qquad (1.11)$$

Where $\tau = C/G_p$. Resulting Debye circuit with ideal components (Martinsen & Grimnes, 2005) can be seen in Fig. 9:
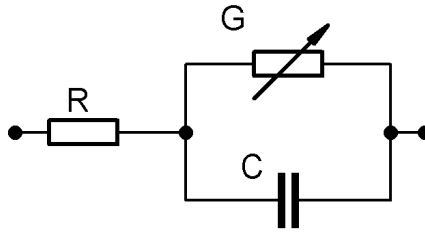
Fig. 9. Three element RC circuit according to Debye model, also as Cole type B circuit.

In his 1928 paper (Cole, Electric Impedance of Suspensions of Spheres, 1928) Kenneth Stewart Cole (1900 – 1984) argues that according to Otto Julius Zobel (1887 –1970) "certain types of two terminal networks … can be made equivalent both in impedance and in phase angle for all frequencies. As a result of this such circuits containing any number of resistances and a capacity, can be made equivalent to either one of two simple circuits" Cole continues, that "the number, location, and magnitude of the elements of such a circuit cannot be determined solely by electrical measurements made at the terminals, and that the number of circuits which can be made to fit a given set of data is probably limited only by the patience…". In fact Debye circuit in Fig. 9 behaves exactly as circuit in Fig. 7, or in another words: circular line is drawn on the complex plane, with center at the real axis. That brings up more general problem. From that point it is obvious, that internal structure of the object under investigation cannot be guessed purely by measurements, but requires deeper knowledge regarding object, and its behavior. And battle for adequate equivalent schematics of the tissue goes on even today. It is hard task to draw a picture, which both behaves adequately, according to measurement results, and also has a valid physical meaning. The problem with Debye theory, which was originally developed for polar gases and dilute solutions of polar liquids, was that "there is a considerable amount of experimental evidence to indicate that equations … are not correct description of the observed frequency dependence of such processes" (Cole & Cole, Dispersion and Absorption in Dielectrics, 1941). Solution proposed by Kenneth S. Cole, and Robert H. Cole in their famous paper, was an introduction of a parameter α:

$$\dot{\varepsilon}(\omega) = \varepsilon_\infty + (\varepsilon_0 - \varepsilon_\infty)/(1 + j\omega\tau_0)^{1-\alpha} \qquad (1.12)$$

The effect of parameter α is that center of the circular line in phasor diagram is shifted from the real axis, resulting in fact in flatter line. Constant phase element (CPE) was introduced instead of an ideal capacitor in Debye's model. And as they write "The remarkable fact is that the experimental results are so generally ex-

pressed by an empirical formula involving a single new constant α". Unfortunately it has been probably one of the most controversial equations. Stress should be on words empirical and experimental. Many works are concerned with the meaning of α, and resulting equivalent circuits. An interesting criticism and alternative to Cole-Cole model is proposed in recent paper by Grimnes and Martinsen (Martinsen & Grimnes, 2005). Nevertheless in the frames of the current work it is important to note that within certain frequency limits ω_l and ω_h Debye's ideal model is behaving very similarly to more complex representations. The three-element equivalent is roughly valid over few decades:
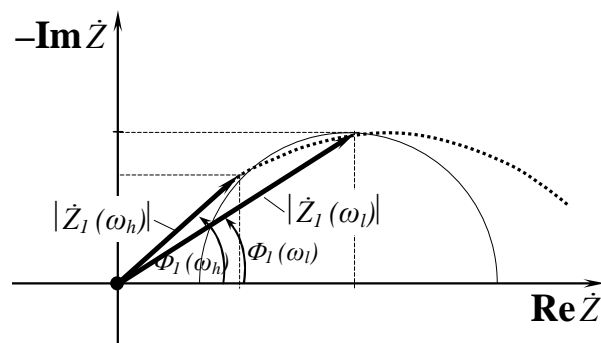
Fig. 10. the phasor diagram of the real impedance (dotted line) compared to simplified ideal model of Debye.

1.6 Impedance of the tissue

First explanation how the cellular structure of biological material can be connected with equivalent circuits can be contributed to Hugo Fricke and Sterne Morse (Fricke, 1925). As Kenneth Cole explains (Cole, Electric Impedance of Suspensions of Spheres, 1928) "their measurements of the resistance and capacity of suspensions of red blood cells at various frequencies could accurately fitted to a circuit of type A (Fig. 7), where they thought of R_2 as due to the suspending medium, R_1 to interiors of the corpuscles, and C to the capacities at their surfaces". Drawing wider picture Herman P. Schwan says (Schwan, 1999) "Fricke, Cole and Curtis laid the basis of our understanding of the β-dispersion. They did this by applying the relevant Maxwell equations to cell suspensions surrounded by membranes".

Fig. 11. Derivation of the impedance of the typical cellular tissue sample, where r_i is an intracellular resistance, r_e is an extracellular resistance, and C_c is capacitance between cellular membranes (Min, Parve, Ronk, Annus, & Paavle, Synchronous Sampling and Demodulation in an Instrument for Multifrequency Bioimpedance Measurement, 2007).
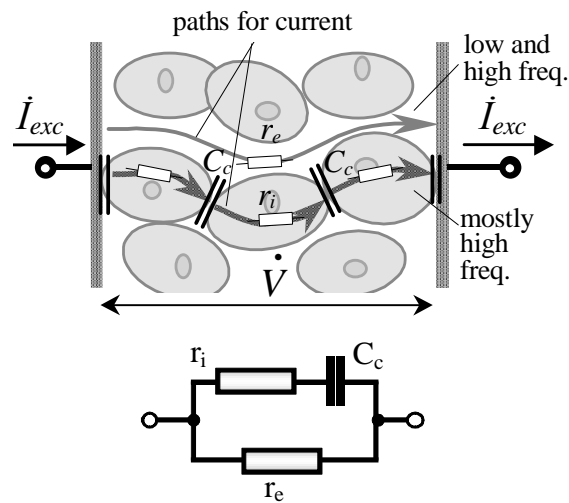
Schwan himself laid the foundations for understanding of an α-dispersion, and γ-dispersion. Motivation behind existence of several distinct dispersions is based on a fact that different mechanisms are behind the behavior of biological material impedance at vastly different frequencies. Appearing between frequencies from mHz to roughly some hundred Hz an α-dispersion being probably the most controversial, and needing further research and elaboration. As explained by Grimnes and Martinsen (Grimnes & Martinsen, Bioimpedance and Bioelectricity Basics, 2008) it is mostly due to counterion effects (perpendicular or lateral) near the membrane surfaces, active cell membrane effects and gated channels, intracellular structures (e.g. sarcotubular system.), ionic diffusion, and dielectric losses (at lower frequencies the lower the conductivity). Maxwell–Wagner effects appearing in β-dispersion deal with processes at the interfaces between different dielectrics. If Fricke's model is extended towards increasing frequency smaller and smaller entities have their impact on the distribution from passive cell membrane capacitance, to intracellular organelle membranes, and protein molecule response. Whole β-dispersion can be observed from kilohertz to ca 100 MHz, and as explained is tightly related cellular and sub cellular structure of the biological materials. Lastly γ-dispersion from 100 MHz to 100 GHz is mostly due to dipolar mechanisms in polar media such as water, salts and proteins.
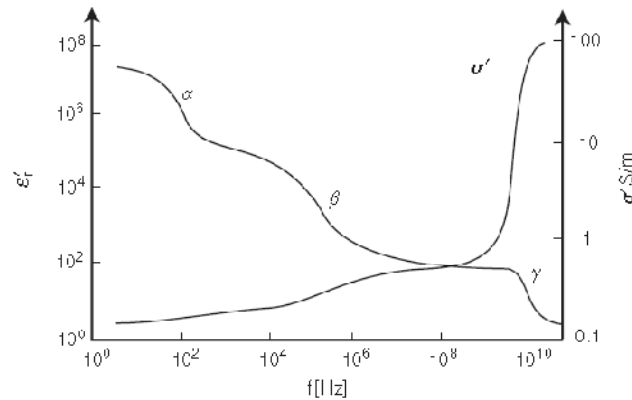
Fig. 12. Classical picture illustrating α, β, and γ dispersions of inphase conductivity and permittivity, as clearly separated Cole–Cole-like systems. Permittivity in biological materials typically diminishing with increasing frequency (Grimnes & Martinsen, Bioimpedance and Bioelectricity Basics, 2008),

In spite of the long study of electrical properties of the biological materials Schwan while describing advanced methods for measurement still makes an important statement (Schwan, 1999): "The problem with most of these techniques is the complexity of the human body and its distribution of tissues of varying conductivity and permittivity, anisotropic properties at that. Even with sophisticated numerical techniques, it is almost impossible to do justice to this situation. The impedance signals received depend critically on this complex arrangement and simple models will not suffice". In any case impedance of the human tissue varies largely both in frequency, and also depending which tissue and how is measured. Some indications for expected parameters can be found in literature, like (Gabriel, Lau, & Gabriel, 1996). Electrical impedance $\dot{Z}$ of biological objects or electrical bioimpedance (EBI) is measured with the aim to get information about the biological processes taking place inside the living organism. From the general point of view of the measurement, there is no significant difference between the EBI and other impedances, like the impedance of chemical cells, etc. But as biological objects are structurally complicated, the bioimpedance has also complicated equivalent circuit. Situation is further complicated by the fact, that it is possible to measure directly only the active and reactive components R and X of the complex impedance (or G and B of the complex admittance), which are mutually in quadrature. To be used for mathematical conversions R and X must be measured with required accuracy. For test purposes equivalent schematics was constructed to mimic heart muscle behavior in frequency range from 100 Hz to 10 MHz. Complexity and frequency characteristics can be observed on Fig. 13:
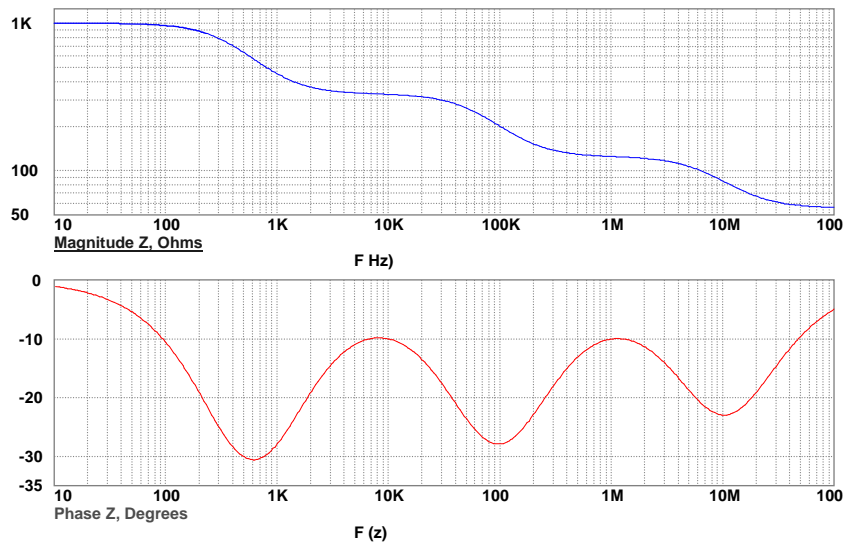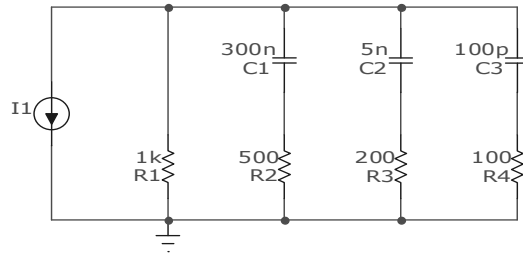
Fig. 13. Test circuit for modeling and testing heart muscle tissue impedance measurement solutions.

Reasons causing specifics in the means for EBI measurement come from the fact, that in medical devices for specific applications different biological processes are of interest. So also the demands to the measurement process and to the results of this process can differ significantly. Considering heart tissue in frequency range from kilohertz to megahertz, results are expected to be less than 1000 ohm. Simulation results of the heart tissue impedance are shown on Fig. 14 (Gordon, 2007).
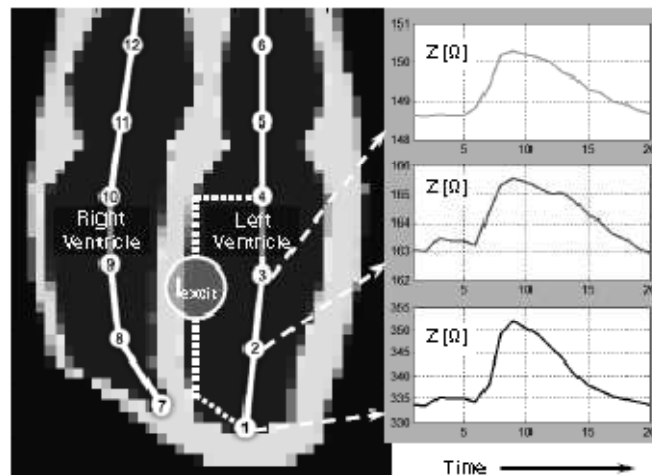
Fig. 14. Cross-section of the first frame of 3D dynamic model. Numbers 1-12 represent electrodes in the simulation inside heart. Electrodes 1 and 4 are used for excitation. Impedance variation is shown for electrodes 1, 2 and 3 in reference to electrode 4 (Gordon, 2007).

There is another factor which is rarely mentioned in connection with impedance of biological objects, but nevertheless affects measurement results – temperature. Any and all materials and substances change their electrical parameters as a function of temperature, and even though subject under investigation is ultimately a human, and therefore homoeothermic, keeping more or less stabile temperature, temperature still varies, and will influence measurement results. Even more when patient in unhealthy state is investigated. It warrants simultaneous temperature measurements in order to make comparison between different tests.

1.7   Measurement of EBI, basic considerations

Let's start with object under investigation, and connections to it. Simplest way to make the measurements is on Fig. 15:
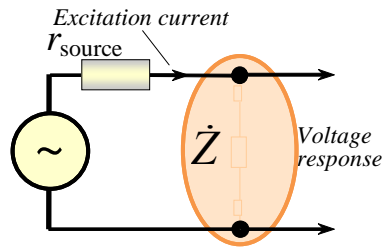
Fig. 15. Basics of the bioimpedance measurement: current injected, and voltage at the terminals is measured.

Unfortunately it is rather useless for practical measurements. In addition to problems mentioned above there are additional difficulties to be dealt with. First of all connections to the object. In case of biological tissue connection is achieved with electrodes. Even without considering electrode construction in detail it is apparent that they have their own contribution to measured impedance, further complicated by the complex interface between electrode and the object. Not surprisingly a typical linear equivalent circuit for electrode on skin surface is Cole type B circuit (Fig. 9) (Northrop, 2004). To certain extent their impact can be minimized with method traditionally contributed to William Thomson, better known as Lord Kelvin (1824 –1907). While Kelvin bridge, invented the in 1861 to measure very low resistances, was certainly an important step, first true tetrapolar (Fig. 16) measurements of electrolytic resistivity were probably conducted by Jonas Ferdinand Gabriel Lippmann in 1873 (Geddes, 1996). Friedrich Wilhelm Georg Kohlrausch should also be credited for his contribution in the area of precision measurements of electrolytes (Geddes, 1996).

Fig. 16. Measurement of the bioimpedance with Kelvin type electrodes.

If current source can be considered near ideal ($r_{source} \gg \dot{Z}$), and if voltage response is picked up by an ideal voltmeter ($Z_{in} \approx \infty$), then electrode impedances will have negligible effect on measured result. Let's examine four lead measurement configurations in more detail (Fig. 17):

Fig. 17. Impedance measurement setup with unwanted parasitics shown.

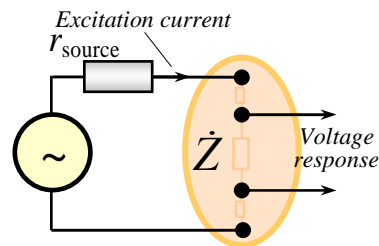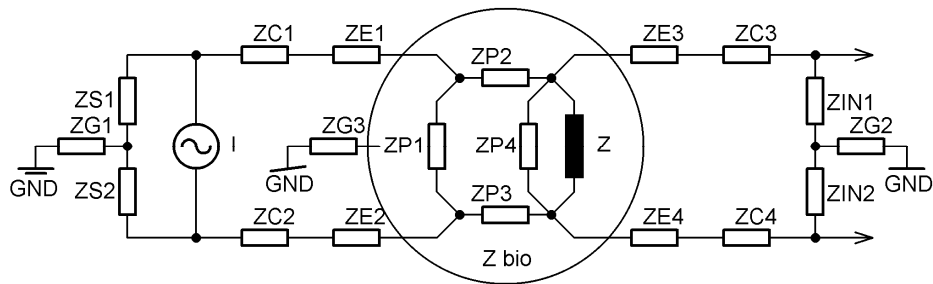Current source *I* has its internal impedance, which even if high in good design, is certainly not absent, and furthermore it is frequency dependent. In good current source Z_{S1} and Z_{S2} are equal, and very high relative to impedance of the biological object under examination Z_{bio} , and current sources ground connection is at least symmetrical to output leads. Ideally floating current source should be used, but it is technically very challenging. Next impedances of the leads Z_C, and electrodes Z_E are connected in series with current source, which inevitably reduce the maximum output swing of the real source, and if not carefully planned could also have considerable effect on the magnitude and phase of the output current. Biological object Z_{bio} adds to possible error sources several parasitic impedances Z_P. They do depend on the electrode placement, construction, and ultimately on an object composition itself. Current injected into complex and usually anisotropic biological object will have, besides intended current path through part of interest Z, several current paths which could render results useless, or at least very difficult to interpret, if not considered very carefully. Impedances of the voltage pickup electrodes Z_E, and leads Z_C, in conjunction with input impedance of the voltage measurement unit Z_{IN} will further distort measurement results.

Separate ring of problems is formed by ground connections, and associated connecting impedances Z_G. Partly because of the possible common mode voltages appearing in case of asymmetries, partly because outside environment will inevitably inject into measurement setup noise, and disturbances. In symmetrical circuit, sources of outside signals between separate grounds will add common mode voltage which can be reduced with well designed circuitry, but certainly not eliminated, if however circuit is not symmetrical signals became differential, and will pass through to the signal processing unit, possibly making havoc in the measured results due to non-idealities of the signal processing chain. It is important to note that, while all these sources of errors can be considered, and their effects reasonably minimized, they will be inherently present in any measurement setup.

- 20 -

Using four lead or Kelvin type tetrapolar connection to object does not eliminate impedance of the leads, impedance of the connecting electrodes, and problems related to the complexity of the biological materials, it will only reduce error contribution of these factors if carefully planned. There are many good sources discussing these effects such as (Grimnes & Martinsen, Sources of Error in Tetrapolar Impedance Measurements on Biomaterials and Other Ionic Conductors, 2006). Therefore achievement of high accuracy, and most importantly repeatability, of impedance measurements is very hard if not impossible task to handle in wide frequency band. Fortunately long term average of Z, or base impedance is rarely interesting in itself. Instead relative variations in Z have often a diagnostic value, either shorter time modulations or longer term wander.
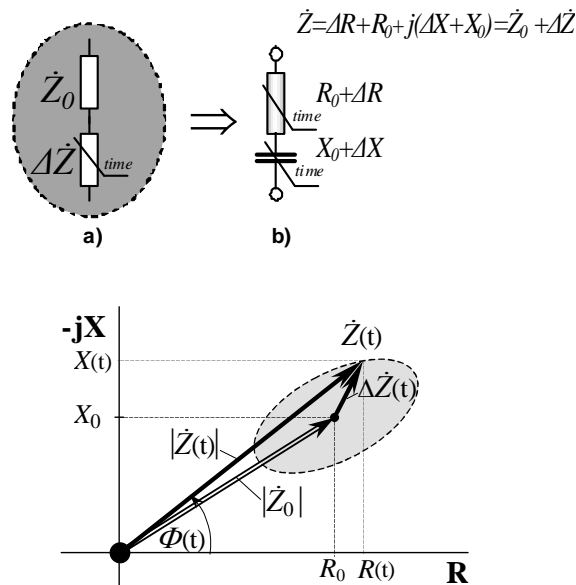
Fig. 18. Time varying impedance and its phasor diagram.

These variations in Z can be contributed to many sources in living tissue, such as mechanical movements in body parts, including, but not limited to, heartbeat, blood flow, breathing, and movement of limbs. Secondly slower variations in tissue should be considered. It can happen because of very long processes, like aging, but also due to various abnormalities in operation, like appearance of tumors, blockage of blood flow, or ultimately because of disintegration of the cellular structure of the biological material.
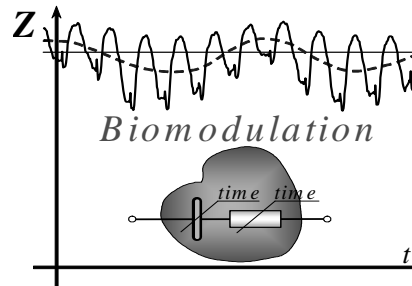
Fig. 19. Typical picture of biomodulation of the impedance, mostly cased by breathing, and heartbeat.

If heart tissue is considered then two main contributors to changes in EBI are heart beating, and breathing. In connection with measurements it is important to note that separation of these two processes by signal processing is not an easy task. If an healthy subject's heartbeat is usually faster than breathing, then when examining pathologies they can have overlapping frequency spectra, and in severe cases breathing can be even faster than heartbeat. Several techniques are proposed to tackle the problem. One of the most promising is usage of the adaptive shape locked filtering of these two highly varying signals (Krivoshei, 2009). Formation of the resulting waveform, and resulting current paths in case of impedance measurements for aiding pacing process can be seen in simplified image Fig. 19, and Fig. 20.
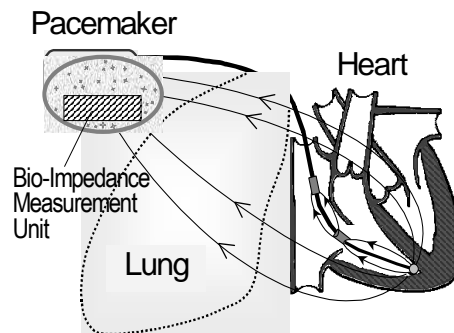
Fig. 20. Path of the current through lungs and heart for bioimpedance measurement (Min, et al., 2007).

One of the biggest challenges warranting intracardiac impedance measurements is estimation of the hearts stroke volume. It is typically multielectrode invasive measurement. Electrode placement inside the heart can be seen schematically in Fig. 21.
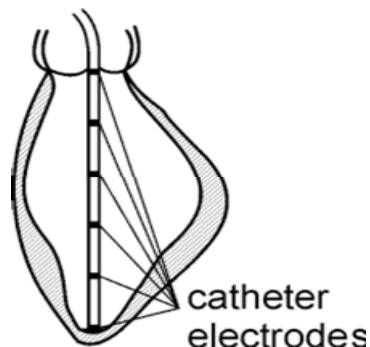
Fig. 21. Electrode placement for measurement of the intracardiac impedance (Min, et al., 2007).

Conducting invasive measurements inside heart is challenging task. Due to intricate nature of heart tissue it is generally not enough to use one set of electrodes, and one measurement channel. In certain cases as many as 16 electrodes are used, and furthermore impedances between arbitrary sets from these 16 electrodes are measured in order to get eligible picture of the underlying biological processes. Task is further complicated by fact that measurement itself should not interfere with the normal heart operation in any way. Allowed current levels should be kept at very low safe levels. Typically some microamperes, depending on measurement frequency. In case of pacing aids severe energy constraints should be considered as well. Fortunately the last problem is not so important if impedance is measured during open chest surgery, where outside apparatus can be used. Nevertheless security and dependability requirements for such an apparatus are very high.

1.8   Voltage pickup basics

Simplified measurement setup from Fig. 16 is considered again, and additional components are added for further discussion Fig. 22. Current is transmitted through the tissue, it seeks path of least resistance, developed response voltage is measured, and impedance to this current is estimated. Voltage response from voltage pickup electrodes is first conditioned by amplifier *G*. In order to minimize adverse effects from the surrounding environment it is strongly preferred to use instrumentation amplifier with fully differential high impedance input. It is familiar from other bioelectricity measurement systems, such as ECG measurement, but similarity is only apparent. Usual frequency range for ECG measurement is well below 1kHz.
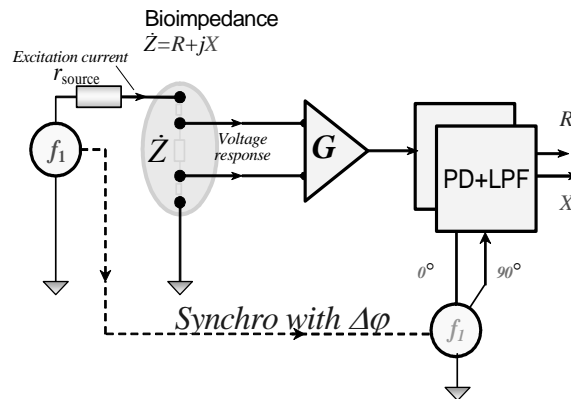
Fig. 22. Measurement of the bioimpedance with Kelvin type electrodes, and with synchronous signal processing.

In case of EBI measurement, that range is typically extended to several hundred kilohertz, and preferably even further, up to some megahertz. There are no off the self instrumentation amplifiers available for such a wide frequency range. Further, since the input signal is typically very low, in micro- and millivolt range, noise parameters of such an amplifier should be exemplary. In order to comply with possibly large disturbances at the input it should be able to work linearly also when common mode signals in volt range are present at the input. While high common mode rejection ratio (CMRR) is relatively easy to achieve at lower frequencies, problems became apparent in kilohertz, and megahertz frequencies. Design of such an amplifier is not a trivial task, but it is entirely possible to achieve good results.

Bigger problems become apparent when multielectrode configuration with arbitrary electrode selection is considered. It is not possible to introduce switching matrix between electrodes and voltage pickup amplifier, except when switching is done manually, which is not an option for fully automatic modern device. In modern electronics fast and reliable switching is achieved with CMOS switching elements. Unfortunately they do introduce several parasitic elements into measurement path. Most notably inherent capacitance, which from one side prevents ideal decoupling between switch sides, when switch is disengaged, and also reduces higher frequency components, by forming RC low pass filter. It is apparent that when very high input impedance of the amplifier is considered, then parallel capacitance destroys it immediately. On the other hand, if the switch is behind amplifier, where low impedance coupling to the switch can be achieved, differential configuration of the input stage is almost impossible. One compromise is to use low noise, highly linear voltage followers at the first stage, and fully differential channel after the switch matrix.

- 24 -

In order to achieve best signal to noise ratio (SNR) maximum amplification should generally be at the beginning of the signal path. At the same time wide range of input voltages should be considered, and therefore some gain control should be applied. In case of 16 electrodes, it means that 16 gain controlled wideband, low noise amplifiers should be used, which is not very economical, and also affects energy consumption of the system. Even bigger problem is that these amplifiers would amplify both the differential signal of interest, and possibly much stronger common mode signal. Therefore amplification should be limited to comply with larger signal, in order to stay within linear range.

These controversial requirements dictate that amplification at the first stage should be kept minimal even if it is not favorable when SNR is considered, and main contribution to gain will come after switching matrix in fully differential channel.

1.9   Aspects of the signal processing

After preliminary conditioning, impedance conversion, switching, and amplification, signals are introduced into processing engine. If the current waveform is taken for reference, and therefore the phase angle $\varphi_I = 0$, then calculations are very simple $\dot{Z} = \dot{V}/\dot{I} = Re(\dot{V}/\dot{I}) + jIm(\dot{V}/\dot{I})$. It gets even simpler if I is normalized, and division with 1 can be omitted. Impedance can be measured in two ways, either by detecting its magnitude and finding voltage phase angle with current, or by measuring directly *Re* and *Im* parts of response voltage, by finding correlation coefficients with reference sinusoid, and reference cosinusoid 90 degrees apart. It can be easily achieved by multiplying response with inphase, and quadrature sinusoids to excitation signal, and by low pass filtering (LPF) the result. If response signal with amplitude A, and phase angle φ_u is considered, and reference signal amplitude is unity, then from elementary trigonometry for *Re* channel:

$$A \sin(\omega t + \varphi_u) * \sin(\omega t) = \frac{A}{2} * \cos(\varphi_u) - \frac{A}{2} * \cos(2\omega t + \varphi_u) \qquad (1.13)$$

And after ideal LPF double frequency component is completely removed and DC result will be $A/2 * \cos(\varphi_u)$, and consequently for the *Im* channel result will be $A/2 * \sin(\varphi_u)$.

In real world things are more complicated than that. Since the excitation signal passes through various schematic components and impedances, the reference phase

angle is not 0 degrees anymore. So first of all certain frequency and setup dependent correction $\Delta\varphi \neq 0$ should be introduced and used during calculations. It can be roughly estimated by analysis, but better yet it can be measured during calibration phase, when know Z, usually suitable R, is placed into circuit. With same calibration procedure also an inherent amplitude error can be corrected. It is important to bear in mind that these corrections are frequency dependent, and should be calculated for all frequencies of importance separately.

One of the questions needing an answer during design phase is placement of an analog to digital converter (ADC) within signal processing chain. If ideal or arbitrarily good components could be used then placement of the ADC is arbitrary, when considering real components restrictions apply. Let's start first with analog synchronous demodulation, following analog low pass filtering, and then conversion into digital domain following outputs R and X on Fig. 22. Usually biomodulation of the impedance signal can be in the range from 0,1%, or even lower, when noninvasive measurements are considered on the surface of the object, to some tens of percent from whole signal if invasive local measurements are considered, such as measurement of the heart functions during open chest surgery. Frequency range of these modulations is well below some hundred hertz, and therefore sampling frequency of let's say 1kHz is fully satisfactory in a view of Nyquist–Shannon criterion, and even with modest filtering. There is ample of good quality AD converters from many different manufacturers at this relatively low frequency. 24 bit low distortion converters will allow measurement of 0,1% modulation, even if some dynamic margin is left, with 10-12 bit resolution, which is usually more than enough. Low frequency low pass analog filtering before converter will also considerably reduce disturbances from surrounding environment. There are still some drawbacks. One of which is that correct analog multiplication is difficult task to handle. Real multipliers have linearity problems, and their accuracy is not sufficiently good. Therefore multiplication of two sinusoids is often replaced with multiplication of the response sinusoid with square wave signals. It can be easily accomplished with CMOS switches, and with very good results. Problem with such a multiplier is in the frequency composition of the square wave signal. Such a multiplier is sensitive not only to the fundamental harmonic, but also to higher harmonics, and allows also noise leakage into result. So very clean sine wave excitation signal should be used, and non-linearity of the object under investigation should not cause significant higher harmonics in the response signal. Biggest problem however comes from different angle. In case multichannel measurement of the impedance is needed, like with multiple electrodes in living heart, amount of analog multipliers needed is multiplied by channel number. If at the same time

simultaneous measurement at several different frequencies is required, amount of multipliers needed is further increased (Fig. 23. Multifrequency analyzer with massively parallel synchronous demodulator circuits.. If four channel measurement at eight different frequencies simultaneously is performed, then required amount of multipliers is 4*8*2=64 (two multipliers for each channel and at each frequency for *Im* and *Re* values), which is at least not trivial anymore. Added to that also low pass filters are required for each channel, and not surprisingly separate AD converters, or multiplexing of the inputs to converter.
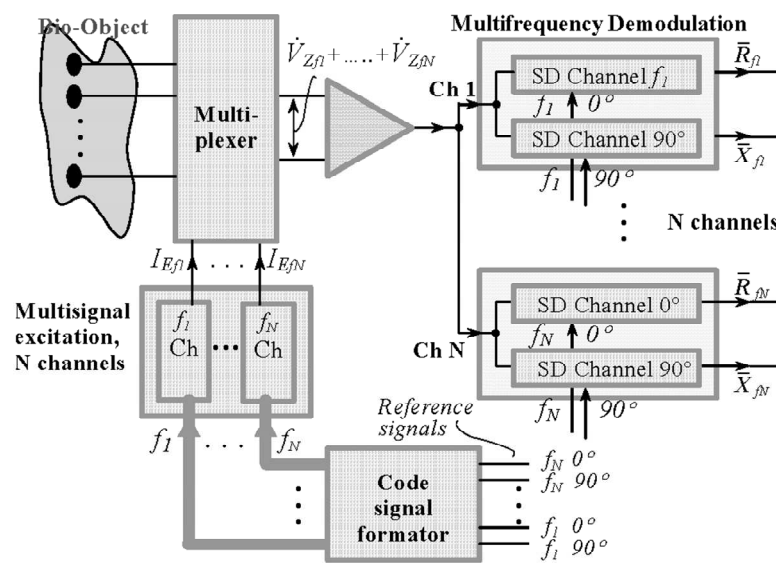
Fig. 23. Multifrequency analyzer with massively parallel synchronous demodulator circuits.

While space, unwanted leakage of the signals between different parts and energy consuming in analog domain is critical in many designs, multiplication, and filtering in digital domain is just a question of computing power, cleverness of the signal processing methods and algorithms and only to lesser extent also power consumption. More importantly digital signal processing is relatively easily scalable. By moving digitalization of the signal towards the beginning of the signal processing channel new problems emerge. Lets first consider speed issues. Digitalization at 1 kHz is rather trivial task with modern component base. When millions, or even billions, of samples per second are required, then digitalization becomes considerably more problematic. While digitizers exist at gigasample per second speeds, they are far from the precision of their lower frequency counterparts, and resolution is usually limited with 8 bits. Added to the problem of the reduction of precision and resolution is the need to digitize also the so called carrier signal. Not

the near DC result of multiplication, as it is with analog multipliers followed by the low pass filters, but the full response sinusoid will appear at the input of the converter. Further all the possible disturbances from surrounding environment will add to the problem, and reduce available dynamic range. Impact of the carrier can be minimized by the usage of so called compensation method. Practical work in that area (Annus, Lamp, Min, & Paavle, 2005) has shown that 6-8 bit improvement can be achieved, by subtracting carrier from the response signal. Method requires knowledge of the amplitude and phase of the response signal.

An interesting digitalization option is so called synchronous sampling (Pallas Areny & Webster, 1993) . It is possible to adjust sampling positions according to the known excitation signal. If samples are taken from the points where excitation signal has zero and maximum values, real and imaginary parts of the response signal can be calculated by simple addition and subtraction of the relevant samples. In addition the additive component can be found with similar mathematics, which may be beneficial for simultaneous ECG/ ICG measurement (Min, Parve, Ronk, Annus, & Paavle, Synchronous Sampling and Demodulation in an Instrument for Multifrequency Bioimpedance Measurement, 2007).
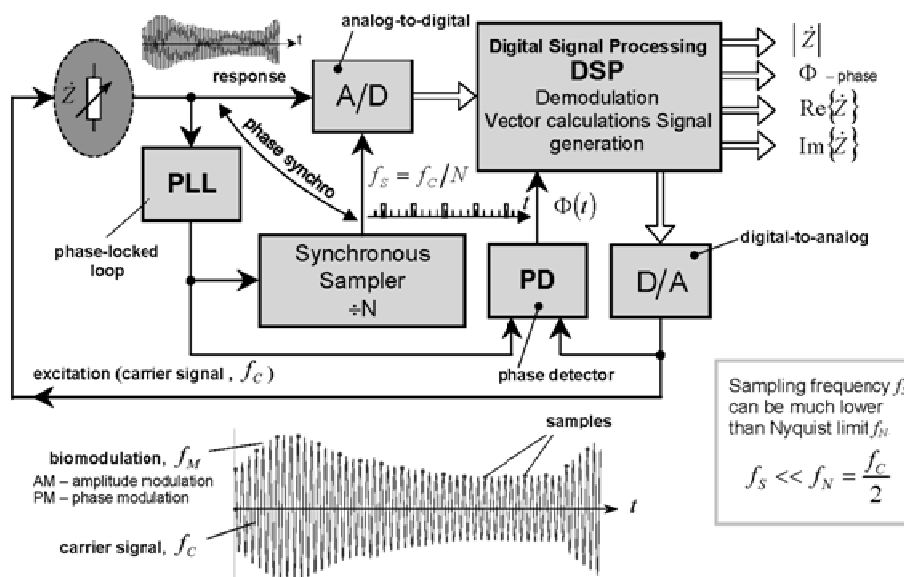

Fig. 24. Measurement of the bioimpedance with digital synchronous undersampling and signal processing.

Restrictions posed by fundamental Nyquist–Shannon limit (Jerri, 1977) can be reduced with synchronous undersampling (Fig. 24) and careful choice of excitation frequencies (Min, Land, Märtens, Parve, & Ronk, 2004), and further by applying

more complicated digital alias free signal processing (DASP) (Bilinskis, 2007) methods. However there is another fundamental limit. Signal to noise ratio achievable after digitizing depends, among other things, on number of samples available. It can be roughly estimated that SNR will improve with $\sqrt{n}$, where n is number of available samples for calculation.

1.10 Impact of noise and disturbances

While conducting real impedance, or in broader view in fact any measurements unwanted side effects do occur. Some of them are caused by very fundamental physical effects, some of them sneakily leak in unavoidably from surrounding environment, and some are just plainly caused by non ideal apparatus and methods. There is something common in all of these: their impact can be minimized according to some criterion, but it is not possible to completely avoid errors caused by unwanted side effects. Johnson–Nyquist noise, or thermal noise, is generated by the random thermal agitation of the charge carriers inside any electrical conductor at equilibrium, and it happens regardless of any applied voltage. Thermal noise is approximately white, meaning that the power spectral density is nearly equal throughout the frequency spectrum. Additionally, the amplitude of the signal has very nearly a Gaussian probability density function. It was first measured by John Bertrand Johnson at Bell Labs in 1928 (Johnson J. B., 1928), and later explained in detail by Harry Theodor Nyquist (Nyquist, 1928), Johnsons coworker at the time. Thermal noise is distinct from shot noise, which consists of additional current fluctuations that occur when a voltage is applied and a macroscopic current starts to flow. For the general case, the above definition applies to charge carriers in any type of conducting medium, like ions in an electrolyte, not just resistors, however it is usually modeled as a voltage source representing the noise of the non-ideal resistor in series with an ideal noise free resistor, in a way known today as Thévenin equivalent circuit.

In reality such a circuit was first derived by Hermann von Helmholtz in his 1853 paper and its application was illustrated. Thirty years later Léon Charles Thévenin working for France's Postes et Télégraphes, published the same result (Johnson D. H., 2001) apparently unaware of Helmholtz's work. In the context of this thesis it is interesting to note that in 1853 Helmholtz, while being an associate professor of physiology at Königsburg, published in Poggendorf's Annalen a paper "Some laws

concerning the distribution of electric currents in conductors with applications to experiments on animal electricity." It was based on his note published year before. In this paper, Helmholtz described how locations of electromotive force generators can be determined form measurements of currents and voltages in muscle tissue. He described how the recent works of Kirchhoff, Gauss, Ohm and others can help to determine how the "animal electricity" flows.

For practical measurement tasks is useful to write equation describing root mean square (RMS) value of the voltage generated by Thévenin noise source:

$$v_n = \sqrt{4k_B T R \Delta f} \qquad (1.14)$$

Where k_B is Boltzmann's constant in joules per Kelvin, T is the resistor's absolute temperature in degrees of Kelvin, R is the resistor value in ohms (Ω), and Δf is the bandwidth in hertz over which the noise is measured. The noise source can also be modeled by a current source in parallel with the resistor, called the Norton equivalent circuit. As it was with Thévenin's equivalent there is certain amount of controversy involved in who actually described it first. Hause-Siemens researcher Hans Ferdinand Mayer published in November 1926 an article "On the equivalent-circuit scheme of the amplifier tube.", in which he describes the transformation between Thévenin and an equivalent current source based circuit. At the same month Edward Lawry Norton, an accomplished Bell Labs engineer wrote internal technical report at Bell Labs called "Design of Finite Networks for Uniform Frequency Characteristic", where a short paragraph describing the current-source equivalent appears (Johnson D. H., 2001).

The RMS value of the noise current of the Norton equivalent circuit based noise generator can be simply written as:

$$\iota_n = \sqrt{\frac{4k_B T \Delta f}{R}} \qquad (1.15)$$

Thermal noise in an RC integrating circuit is referred to as kTC noise, and has an unusually simple expression, as the value of the resistance drops out of the equation. This is because higher R contributes to more filtering as well as to more noise. The noise is not caused by the capacitor itself, but by the thermodynamic equilibrium of the amount of charge on the capacitor so the inherent Johnson noise of an RC circuit can be seen as an effect of the thermodynamic distribution of the number of electrons on the capacitor, even without the involvement of a resistor. Formula for the RMS noise voltage generated in such a filter is:

$$v_n = \sqrt{k_B T / C} \qquad (1.16)$$

Typically these low pass *RC* circuits appear in many places during synchronous demodulation (Karvonen, Riley, & Kostamovaara, 2001). Thermal noise is intrinsic to all objects and as such it manifests itself at every step of impedance measurement. Starting with the noise of the current generator, through impedances of the cables, electrodes, bio-object itself, to the noise generating input impedance of the voltage pickup amplifier. While it may be almost impossible to calculate the actual value of the resulting noise of all contributing elements it is important to note its wide frequency band, omnipresence, and consequences on signal processing.

Another category of signals disturbing measurement process are generated outside of the measurement setup. Some of them are manmade, such as mains leakage, high energy signals from defibrillators, and electrical knives, some are not. Common to them is that measures can be taken to minimize them. Invented in 1836 by Michael Faraday, Faraday cage or Faraday shield is an enclosure formed by conducting material, or by a mesh of such material. Such an enclosure blocks out external static electric fields. A Faraday cage's operation depends on the fact that an external static electrical field will cause the electrical charges within the cage's conducting material to redistribute themselves so as to cancel the field's effects in the cage's interior. This phenomenon is used, for example, to protect electronic equipment from lightning strikes and other electrostatic discharges. Faraday cages can't block static and slowly varying magnetic fields such as Earth's magnetic field. To a large degree though, they also shield the interior from external electromagnetic radiation if the conductor is thick enough and any holes are significantly smaller than the radiation's wavelength. While effective it may prove difficult to place a patient inside such an enclosure, and it does not guard from disturbances generated inside enclosure during medical procedures, and by medical apparatus.

There are still measures to minimize the effects of the external disturbing electromagnetic fields on the measurement result. First of all measurement apparatus itself and all the connections to and from it can, and preferably should, be shielded. Unavoidable connections to other equipment can be suitably filtered, and in some cases replaced by the optical cables, not susceptible for electromagnetical pickup. Later would also serve as a safety precaution for the object under measurement. Signals picked up by the object under investigation could be reduced by suitably placed low impedance ground connections. Unfortunately often these connections are forbidden by other rules and regulations, mostly due to safety issues.

Another way to reduce capacitively coupled perturbancies is extensive usage of differential measurement methods. In case of differentially coupled amplifier chances are that most of the coupled signals appear as common mode voltage at the input. Problems with such an approach are linked with limited linear range of the amplifier input, as well as with low common mode rejection ratio (CMMR) at higher frequencies of interest. Situation still can be improved when amplifier units ground is connected with patient in three electrode pickup scheme, or if the patient is actively driven in phase with the disturbing common mode voltage. It is discussed in many papers over the time, and used in many instruments. Good overview can be found in (Boone & Holder, 1996). If the amplifier unit is suitably isolated, safety restrictions may not apply, additionally safety resistors could be inserted.

1.11 Multifrequency and multisite measurement considerations

As stated above biological material can be highly anisotropic, and not homogenous. Therefore measurement between certain distinct set of electrodes can be highly misleading. Often it is counterbalanced by conducting measurements between many different electrodes. Such a measurement can be done sequentially in time, but if biomodulation of the signals is of importance simultaneous measurements are needed. One way to achieve this is to conduct measurements at several slightly differing frequencies. In this case impedances between different points can be separated, and values will not vary much due to almost identical frequencies:
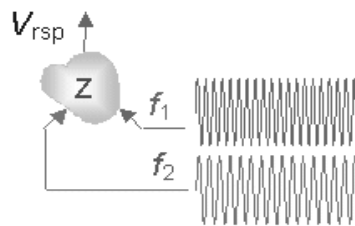

Fig. 25. Impedance measurement in case of two currents with slightly differing frequencies f_1, and f_2, injected from different points.

Similar but different task is accomplished when impedance variations at vastly different frequencies are measured. From discussion of the impedance of the biological tissues is evident that different processes can be characterized at

different frequencies. Current path depending on excitation frequency will result in impedance measured having different information content:
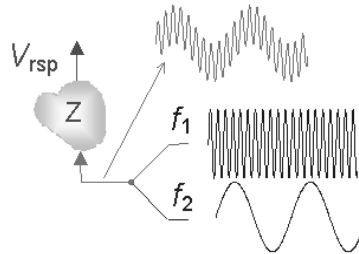

Fig. 26 Impedance measurement in case of two currents with highly differing frequencies f_1, and f_2, injected from the same point.

In even more complex cases multisite and multifrequency measurement are needed simultaneously. One of the difficulties associated with such a measurement setup, namely multiplication of the amount of required signal processing units, is briefly discussed already. Question arises whether it is possible to optimize such a complex measurement by applying different signals and processing methods.

1.12 **Signals and processing revisited**

According to definition electrical impedance Z, or simply impedance, describes a measure of opposition to a sinusoidal alternating current (AC). In its complex form $\dot{Z} = \dot{V}/\dot{I} = R + jX$, and it is frequency dependent. It is therefore evident from definition that impedance can be, and in fact should be, measured with sinusoidal excitation current. Are there at all other possibilities when choosing excitation signals? Fortunately the question here is answered already by Johann Carl Friedrich Gauss in 1805 and Jean Baptiste Joseph Fourier in 1807 (Heideman, Johnson, & Burrus, 1984). Gauss did discover what is essentially known today as fast Fourier transform (FFT), and is generally contributed to James William Cooley and John Wilder Tukey. Famous paper, published in 1965 by Cooley and Tukey, describes very similar FFT algorithm, which led to an explosion in digital signal processing (Duhamel & Vetterli, 1990). So in fact Gauss's work preceded even Fourier's own groundbreaking theories, and as it often happens was almost forgotten for coming hundred and fifty years. In their invited paper P. Duhamel, and M. Vetterli note quite rightfully: "Considering this history, one may wonder how many other algorithms or ideas are just sleeping in some notebook or obscure publication…" (Duhamel & Vetterli, 1990). Gauss developed his computationally

efficient method for interpolation of the orbits of celestial bodies. Fourier in turn was interested in heat propagation, and claimed essentially that any continuous periodic signal could be represented as the sum of properly chosen sinusoids. That claim proved to be both bold and revolutionary, and rather controversial as well. It ignited dispute between the reviewers of his paper. While Pierre-Simon Laplace, who in turn formulated Laplace's equation, and pioneered the Laplace transform which appears in many branches of mathematical physics, and is more general then Fourier's counterpart, was voting for publishing of the paper, Joseph-Louis Lagrange adamantly protested against it. Protests were based on the fact that such an approach could not be used to represent signals with sharp corners, or in another words with discontinuous slopes, such as square waves. Dispute lasted up to 1898, when Josiah Willard Gibbs published a paper on Fourier series in which he discussed the example of what today would be called a sawtooth wave, and described the graph obtained as a limit of the graphs of the partial sums of the Fourier series. Interestingly in this paper he failed to notice the phenomenon that bears his name, and the limit he described was incorrect. In 1899 he published a correction to his paper in which he describes the phenomenon and points out the important distinction between the limit of the graphs and the graph of the function that is the limit of the partial sums of the Fourier series. Maxime Bôcher gave a detailed mathematical analysis of the phenomenon in 1906 and named it the Gibbs phenomenon. In essence both Lagrange and Fourier were right. While it is not possible to construct signals with sharp corners from sinusoids it is possible to get so close that the difference in energy between these signals is zero. If real signals from nature are concerned instead of exact and purely mathematical curiosities problem is even smaller. So for all practical signal processing tasks it is indeed possible to state that any real signal can be constructed from sinusoids. In signal processing terms all non sinusoidal signals with fundamental frequency do have higher sinusoidal harmonics. It apparently also answers the question regarding measurement of the impedance: any real signal can be used for measurement of the impedance, provided that its spectral composition is considered.

But before going any further is probably good to answer the question why it is useful to consider other then sinusoidal excitations. For a single frequency measurement simpler hardware and simpler signal processing, and ultimately lower cost and energy consumption can be the moving factors. While sinusoidal excitation is best by definition several alternative waveforms can be considered with acceptable results. Simplest alternative is square wave signal or signal which can be described by the Rademacher function (Fig. 27). One of the possible definitions of the Rademacher function $f_n(x)$ is the sign of $sin(2^n\pi x)$, for a non-negative integer

n. For *n=1* therefore $\mathcal{R}(t) = sign(\sin(2\pi t))$, where $\mathcal{R}(t)$ denotes here a Rademacher function.
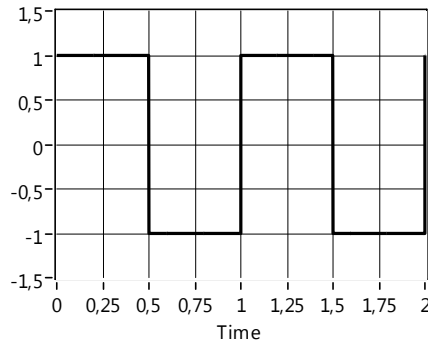

Fig. 27. the Rademacher function of n=1, or just simply an odd square wave.

In order to see the difference between square wave and sinusoid it is convenient to consider the Fourier series of the square wave with amplitude 1. Since function is odd, i.e. $-f(x) = f(-x)$, Fourier series of the function will contain only sinusoidal members (frequency *f=ω/2π*):

$$f(t) = \frac{4}{\pi}\sum_{n=1}^{\infty} \frac{\sin((2n-1)\omega t)}{2n-1} = \frac{4}{\pi}\left(\sin(\omega t) + \frac{1}{3}\sin(3\omega t) + \frac{1}{5}\sin(5\omega t) + \cdots\right)$$

(1.17)

Unfortunately severe problems appear if measurements with square waves are conducted. The measurement is no longer conducted on single well defined frequency, but instead produces results also on higher harmonics. It could be largely ignored if during signal processing multiplication is conducted with sinusoidal signals, unfortunately as it was discussed above, often it is accomplished with same rectangular signal instead, and energy form all the higher harmonics is summed to the fundamental, and becomes undistinguishable. Also spectral impact from non linearity's of the object (or apparatus) cannot be separated from desired response signal. Spectra resulting from such a multiplication can be seen on Fig. 31 with dotted line. There is another way of looking at how the errors appear (Kuhlberg, Land, Min, & Parve, 2003). Let's consider phase sensitivity characteristics of the synchronous demodulator (SD):
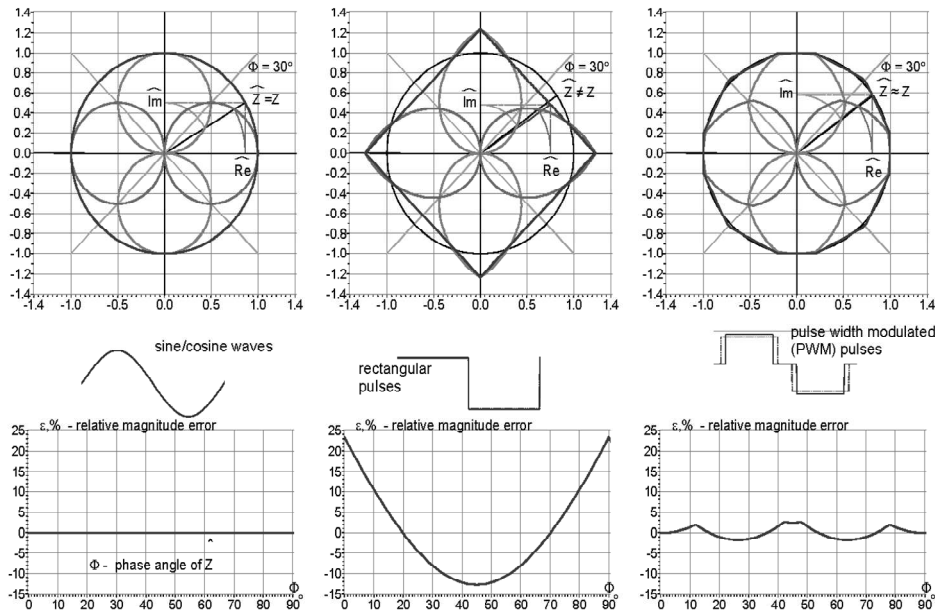
Fig. 28. Quality of synchronous demodulation in case of different signal waveform. From left to right sine wave, square wave, and modified square wave.

From Fig. 28 it is clear that synchronous demodulator produces different results in case of fully square wave system and in case of sinusoidal system. Fortunately there is very simple method for reducing errors introduced by higher harmonics. Let's consider sum of two square waves with same frequency and amplitude, one of them shifted in phase by β degrees, and another - β degrees. Such a double shift is preferable, since resulting function is again odd. In signal processing odd functions are more natural, because negative time is usually meaningless, and signals start at t=0. Care must be taken that in many mathematical textbooks, and more importantly in different programs, even functions are considered instead. Should the summary phase shift 2β be equal to the half period or odd multiply of half periods of any higher harmonic such a harmonic will be eliminated from the signal, since sum of to equal sinusoids with 180 degree shift is zero. Main difference with simple square wave is in appearing third level with zero value, so it is reasonable to call them shortened square waves. More generally spectra of these signals can be derived from Fourier series:

$$f(t) = \frac{4}{\pi} \sum_{n=1}^{\infty} \frac{\cos((2n-1)\beta)\sin((2n-1)\omega t)}{2n-1} = \frac{4}{\pi}\left(\cos\beta\sin(\omega t) + \frac{\cos 3\beta}{3}\sin(3\omega t) + \frac{\cos 5\beta}{5}\sin(5\omega t) + \cdots +\right)$$

(1.18)

Two of these shortened square waves are of special interest. In order to remove 3rd and 5th harmonics from the signal (as they cause most significant errors) 18 degree and 30 degree shifts are useful. First of them is void of 5th, 15th, etc harmonics, and second 3rd, 9th, 15th etc. harmonics. Both of these three level signals with amplitude A are shown on Fig. 29. The third level does not introduce much added complexity from signal processing view. Both generation with digital logic, and also synchronous rectification with CMOS switches is straightforward (Min, Kink, Land, & Parve, 2006).
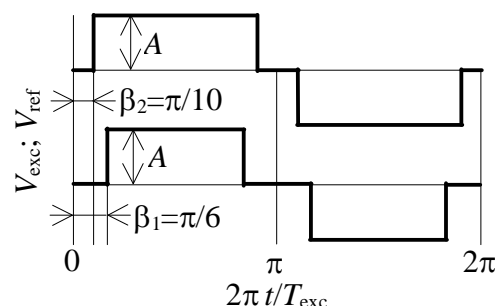
Fig. 29. 18, and 30 degree shortened signals with amplitude A (Min, Kink, Land, & Parve, 2006).

If one of them is used as excitation signal and other as rectifying reference result will be much cleaner spectrally then it was with simple square waves, Fig. 31 white rectangles. These two waveforms were chosen, because complete elimination of certain harmonics was desired. One possible optimization approach would be to find shortened square wave with lowest summary energy of higher harmonics. Relative dependence of the energy of the higher harmonics from shortening angle can be seen on Fig. 30:
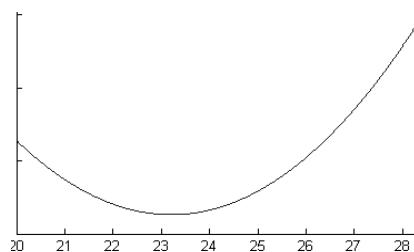
Fig. 30. Relative dependence of the energy of the higher harmonics from shortening angle.

If shortened square wave is used only in synchronous demodulator, then choice of 22,5 degree of shortening is obvious. Compared previously discussed shortened

square waves generation of such a signal requires much lower clock frequency, at least 30 times higher than resulting signal versus 8 times higher, and consequently is more energy efficient, or alternatively allows usage of higher frequency signals at the same clock rate.
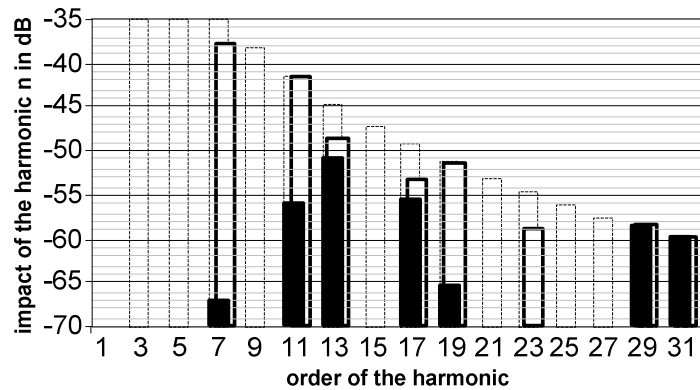
Fig. 31. Impact of the harmonics, in case of ordinary square wave (dotted line), simple shortened square wave (white boxes), and multilevel shortened square wave (black boxes) (Annus, Min, & Ojarand, 2009).

If 18 degree and 30 degree shortened signals are considered, then apparently there are still coinciding higher harmonics in both signals. Could the same summing procedure produce further improvement without much added complexity, if more square waves are added together? The answer is yes. If third summed waveform is added into palette, namely 42 degrees shifted then combination of these three gives very promising results. Three interesting and still simple signals are considered as combinations of previously mentioned summed signals. First and most obvious is sum of 18, 30, and 42 degrees shortened signals with signs 1,-1, and 1. Resulting waveform is on Fig. 32, and spectra of the result is on Fig. 33. Spectra of the signal on Fig. 32 . Result is already remarkably cleaner compared to simple square wave. It could be one of the candidates for use in demodulators, besides simpler 22,5 degree shortened square wave, when excitation is sinusoidal.
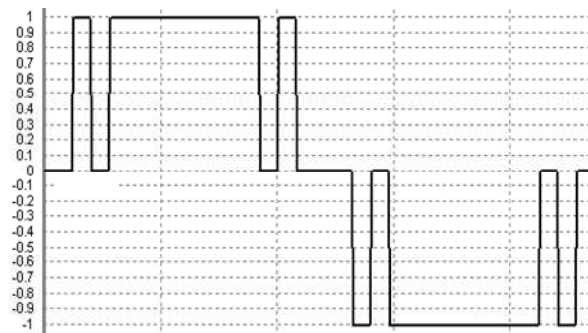
Fig. 32. Resulting waveform from summing of three shortened signals with weights 1, -1, and 1 (Annus, Min, & Ojarand, 2009).
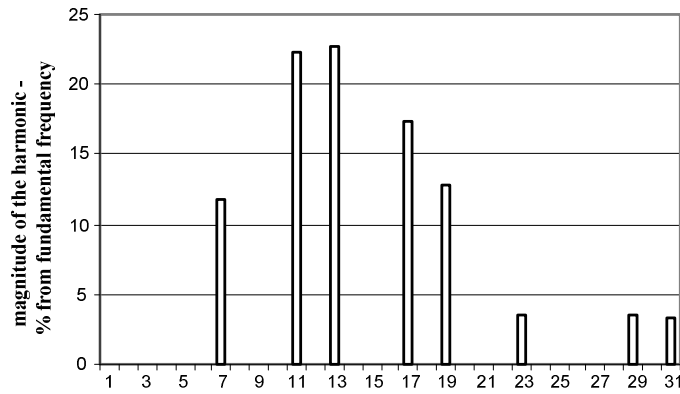
Fig. 33. Spectra of the signal on Fig. 32 (Annus, Min, & Ojarand, 2009).

If on the other hand excitation is also shortened square wave, then following pair of signals is suggested (Annus, Min, & Ojarand, Shortened square wave waveforms in synchronous signal processing, 2008). First of them is sum of all three components with coefficients 1,1, and 1, Fig. 34. Spectra of this summed signal is on Fig. 35.

- 39 -
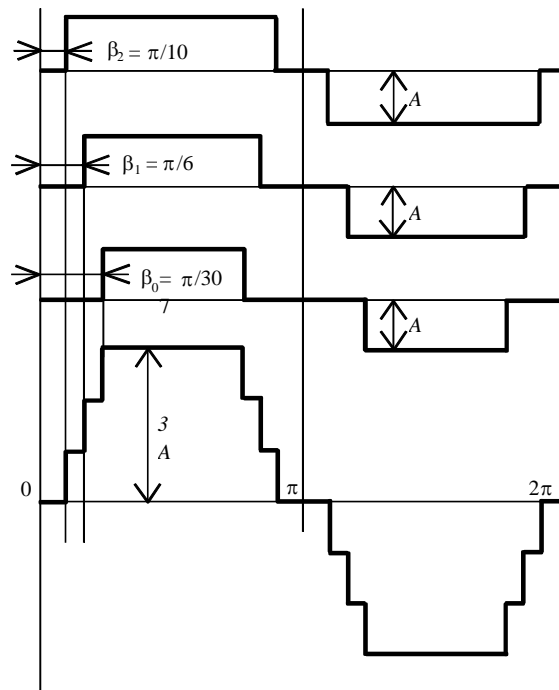
Fig. 34. Sum of three shortened waveforms with coefficients 1, 1, and 1 (Annus, Min, & Ojarand, 2009).
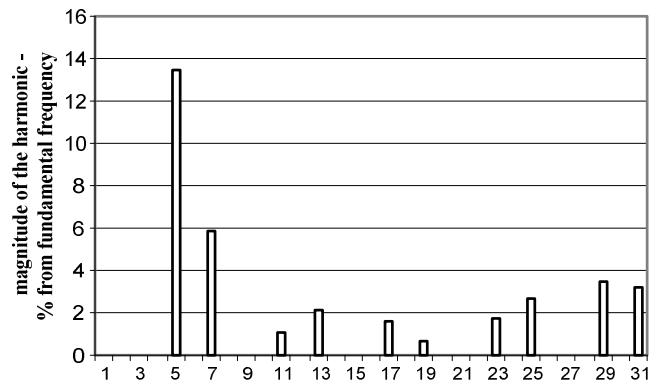
Fig. 35. Spectra of the signal on Fig. 34 (Annus, Min, & Ojarand, 2009).

Suitable counterpart summed with coefficients 2, -1, and 1 is on Fig. 36, and spectra on Fig. 37:
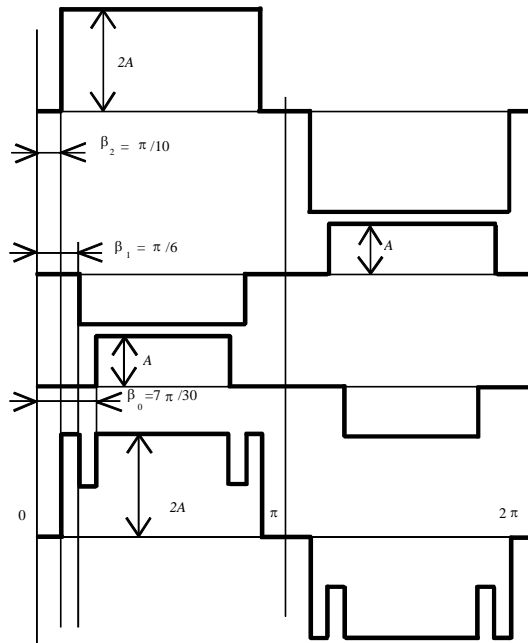
Fig. 36. Sum of three shortened waveforms with coefficients 2, -1, and 1 (Annus, Min, & Ojarand, 2009).
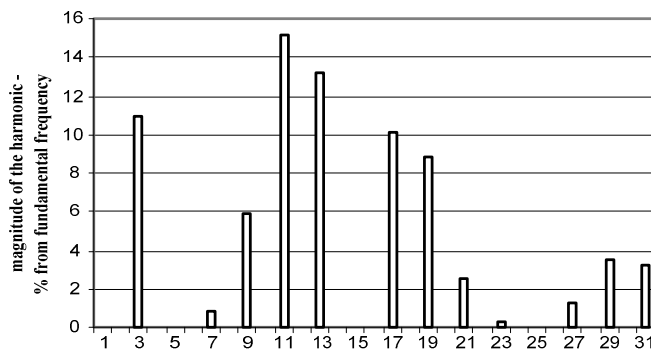
Fig. 37. Spectra of the signal on Fig. 36 (Annus, Min, & Ojarand, 2009).

Comparison of the multiplication results (Fig. 31) shows significant improvement over previous result. Nevertheless same clock speed penalty still applies as with simpler solution.

Entirely different approach for elimination of higher harmonics by summing square waves is based on fact, that as square wave can be represented by sum of indefinitely many sinuses according to Fourier series, almost same is true also in reverse

order, i.e. sine wave can be approximated with many square waves with different frequencies added together.

One way of achieving it is described in (Min, Parve, & Ronk, Design Concepts of Instruments for Vector Parameter Identification, 1992). Simple piecewise (over number of system clock periods) constant approximation of the sine wave values is used. Waveforms with relatively small number of different levels (3,4,5) are used, and as with already described shortened square wave method different waveforms are suggested for multiplication, resulting in cleaner multiplication product. Values of separate discrete levels are determined according to:

$$a_q = \sin((\tfrac{\pi}{4m}(2q-1)) \qquad (1.19)$$

Where m is the total number of approximation levels, and $q = 0, 1, 2, ..., m$ is the approximation level number. Spectral composition of these approximated harmonic functions can be found according to the following equation:

$$k_h = 4mi \pm 1$$

Where k_h is the number of the higher harmonic, which exist in the spectra, and $i = 1,2,3 ...$ If two such signals with number of levels m_1 and m_2 are multiplied, then coinciding harmonics k_c can be found according to:

$$k_c = 4(m_1 m_2)j \pm 1 \qquad (1.20)$$

Where $j = 1,2,3 ...$ If two waveforms with m=3, and m=4 are considered, then first coinciding harmonics are 47th, 49th, 95th, 97th, 143rd, 145th, etc. As with shortened square waves clock frequency should be relatively high, and furthermore these waveforms are relatively sensitive to level errors, which prohibits usage of higher m values, and manifests itself in reappearing higher harmonics.

There is another more mathematical approach (Wei & Zhang, 2000). It involves Möbius function $\mu(n)$, which is 1 if n=1, $(-1)^r$, if n is the product of r distinct primes, and 0 if n is divisible by prime square. If Fourier coefficients $A(n)$, and $B(n)$ of an even and odd functions with period 2π are completely multiplicative, as it is true for square waves, $A(n) = (-1)^{(n-1)/2}1/n$, and $B(n) = 1/n$ for n=1,3,5,…, then for sinusoidal function it is possible to write:

$$\sin x = \sum_{n=1}^{\infty} \mu(n)B(n)Y(nx) = Y(x) - \tfrac{1}{3}Y(3x) + \cdots + \tfrac{\mu(2n-1)}{2n-1}Y((2n-1)x) + \ldots$$
$$(1.21)$$

Where $Y(x) = \sum_{n=1}^{\infty} B(n) \sin nx$, or odd square wave. It is interesting to note that many common waveforms in electronics have completely multiplicative Fourier coefficients, and can be used to construct sine waves in similar manner.

Most practical sine wave approximation in electronics is achieved by method called direct digital synthesis (DDS) (Cushing, 1999). It involves lookup table of sine values for one period, or simply addressable memory, and is based on rotating phase vector pointing to that table, which does rotate based on value of the phase register, and certain constant M describing how many bits should the phase register increment on each step. Output of the phase to amplitude converter can drive digital to analog converters, or can be used for digital processing. Frequency of the output sine wave of such a DDS unit is:

$$f_{out} = M f_{clk}/2^n, \tag{1.22}$$

where f_{clk} is system clock frequency used to increment phase accumulator, n is a width of the phase accumulator in bits, and M is frequency control word. Practical limit for the output frequency is roughly 40% of the system clock frequency. Nyquist–Shannon sampling theorem would allow 50%, but depending on the output filter design it can only be lower for real devices. Another practical consideration to bear in mind is that output amplitude of DDS is frequency dependent due to sampling, and follows $\sin(x)/x$ curve, or more precisely:

$$A(f_{out}) = \frac{\sin\left(\frac{\pi f_{out}}{f_{clk}}\right)}{\frac{\pi f_{out}}{f_{clk}}}, \tag{1.23}$$

1.13 Spectroscopy considerations

First of all impedance of real objects can rarely be considered purely resistive. Furthermore when measuring purely resistive loads it is possible to use even simpler excitation signals then sinusoidal, namely direct current (DC). If on the other hand impedance varies with frequency, as it usually does, single frequency measurement is not enough to fully describe object under test. In complex cases, like measuring electrical properties of biological specimens, sweeping over entire frequency band may be warranted with our sinusoidal excitation. Sweeping on the other hand is usually slow, and prohibits examination of faster changes in object under investigation. So sweeping does not work in case of the investigation of the

biomodulation. In that case different signals can be used, from simpler sum of many sinusoids, to more exotic waveforms.

Generally speaking the method for investigating simultaneously both the frequency characteristics of the impedance and time characteristics of the same impedance is called joint time-frequency analysis. There is a fundamental limit when highest resolution in both domains is required: Gabor-Heisenberg uncertainty principle:

$$\Delta t \Delta \omega \geq 1/2 \qquad (1.24)$$

Accuracy in both time and frequency domains cannot be arbitrarily high simultaneously. As it turns out the eigenfunctions of the Fourier operator give the best resolution in both domains (Soares, Oliveira, Cintra, & Campello de Souza, 2003) (Gabor, 1946). Best known of them being Gaussian. Entire new field for investigations opens up with joint time-frequency analysis for finding optimal signals to conduct it. Very interesting practical uncertainty limits can be found in (Udal, Kukk, & Velmre, 2009). Promising, but not discussed here in detail, are different wavelets, chirplets, and other signals suitable for time-frequency joint optimization.

Let's consider spectroscopy with sinusoidal excitation signals. Single sinusoid is technically feasible signal, and can be reproduced quite accurately, however it becomes increasingly costly to use simultaneously many sinusoidal signals. There is another drawback associated with simultaneous use of multiple sinusoidal signals – crest factor. The crest factor or peak-to-average ratio (PAR) or peak-to-average power ratio (PAPR) is equal to the peak amplitude of a waveform divided by its root mean square (RMS) value:

$$C = {|x|_{peak}}/{x_{rms}} \qquad (1.25)$$

With single sinusoid crest factor is $\sqrt{2} \approx 1,414$. By summing two or more sinusoidal signals together the crest factor can take many different values, generally bigger then 1,414.

Why is crest factor so important? Two reasons worth considering are: nonlinear behavior of the object under investigation, and dynamic range of the measurement apparatus itself. Real objects can rarely be described as linear. It means that different excitation levels do not produce linearly dependent responses. For practical purposes measurement signals are usually kept within narrow range of amplitudes where object behaves approximately linearly. It is clear that such an

approximation is better the narrower the range is kept. In worst case high energy pulses can even permanently alter or destroy the object under investigation, and that is certainly not acceptable when performing measurements for example on living human tissue.

Also dynamic diapason of the apparatus is limited. From the lower side by omni-present noise signal. If the measurement signal is completely buried in the noise and cannot be restored any more the measurement is void. Upper limit is ultimately determined by breakdown of the circuitry, or at least with the level when measurement apparatus itself becomes non linear. Form that it is clear that large peaks in excitation signal should be avoided, as well as very low level components which get lost in noise. Fig. 38 is to give an impression of what happens when just eight sinusoidal signals, one octave apart from each other in frequency, each with equal amplitude 1, and with the same initial phase are summed together. The crest factor of this signal is 2,26538, and it is clearly worse than crest factor of a single sinusoid. For comparison Gaussian white noise is shown on Fig. 39. Crest factor can be optimized, but it is not a trivial task.
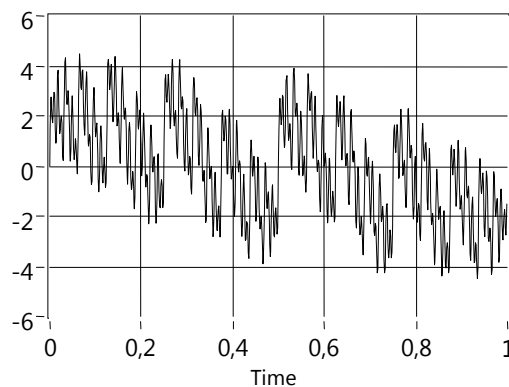
Fig. 38. Sum of eight sinusoidal signals with different frequency.
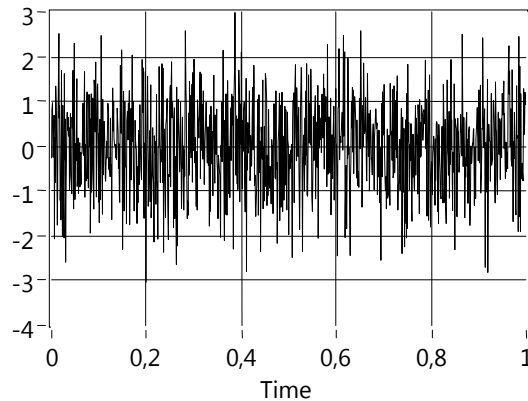
Fig. 39 Gaussian white noise as signal.

When performing short time computations over longer periodic signals the signal is measured only for a limited time. Generally it is not possible to tell what happens outside of this timeframe, or window. Assumption that most algorithms make, is that signal repeats itself exactly as it appears in such a window, which poses a number of problems. If sinusoidal signal is sampled in a time interval not equal to exact number of periods then sharp discontinuities appear, and consequently spectra of such a signal appears not only on single frequency but in much wider area, which is commonly called spectral leakage. If there are many sinusoids, with different frequencies, leakage can interfere with the ability to distinguish them spectrally. In another words smaller components can be hidden completely, or distinction between separate components can just be blurred. One way to fight this problem is to apply smoothly diminishing windows, instead of sharply edged rectangular window. There are many known functions which behave reasonably well as windowing functions, such as Blackman, Hamming and Hann functions for example. However two problems do appear when smooth windowing is used. First of all it takes more computing power due to the multiplication of the response with the window function, and secondly frequency resolution is lowered. Later means also that noise leakage into the result is higher. Fortunately problem largely disappears if rectangular widow is exactly as long as some exact number of full periods of the signal, provided of course that the disturbing signals are not too large. From one side it is easy to achieve in case of synchronous measurements, on the other it poses strict restrictions on the choice of the measurement frequencies.

- 46 -

There is additional benefit in using excitation signals with integer number of periods in sampling window. Number of samples can be drastically reduced by applying non uniform synchronous undersampling methods (Min, Land, Märtens, Parve, & Ronk, 2004) resulting lowered energy consumption, among other things. The drawback is that certain samples can be very close in time, and therefore hard to digitize, and aliasing effects should be considered very carefully. Also noise level will increase compared to uniform, non undersampling techniques.

What are the alternatives to sinusoidal excitation in wideband analysis? Among simplest waveforms, signals derived from square wave are of great interest, such as maximum length sequences (MLS). Good overview of MLS techniques can be found in (Cohn & Lempel, 1977). From crest factor point of view they have the best crest factor achievable namely 1. Secondly they are very easy to generate keeping in mind today's digital realm. There are many other alternatives (Min, Pliquett, Nacke, Barthel, Annus, & Land, 2008) .One of the most promising signals is square wave chirp, and its modifications (Min, Paavle, Annus, & Land, 2009).

1.14 Sourcing current

As it was mentioned previously sourcing a current for measurement of impedance is preferable over sourcing voltage, or at least in ideal world. Real circuitry has its limits. It is important to distinguish between limitations in the current source circuitry itself, and limiting parasitic outside of the current source. Looking back at the Fig. 17. Impedance measurement setup with unwanted parasitics shown.only Z_{s1}, Z_{s2}, Z_{g1}, and I are directly related to the current source. From design point of view also Z_{c1}, and Z_{c2} could be added, as they form part of the circuitry, and to some extent measures can be taken to eliminate adverse effects caused by these impedances. Electrode impedances and parasitic paths in the object under investigation however form a totally different group of problems. Not shown on Fig. 17 are leakage impedances from electrode wires to earth, and also from entire current source circuitry to noise sources which to some extent are part of the circuitry. So in real life current source is far from being just and ideal I. Added to the complex of problems are limitations due to active components of the circuitry, and limits imposed by supply lines.

Let's first examine problems outside of the current source itself. Research in the field of long lines is one of the first issues early adopters of electricity, and

especially communications had to deal with. Mathematical analysis of the behavior of electrical transmission lines grew out of the work of James Clerk Maxwell, Lord Kelvin and Oliver Heaviside. In 1855 Lord Kelvin formulated a diffusion model of the current in a submarine cable. The model correctly predicted the poor performance of the 1858 trans-Atlantic submarine telegraph cable. In 1885 Heaviside published the first papers that described his analysis of propagation in cables and the modern form of the telegrapher's equations (Weber & Nebeker, 1994). Without going into detail of this well know issue the, telegrapher's equations, like all other equations describing electrical phenomena, result directly from Maxwell's equations. In a more practical approach, one assumes that the conductors are composed of an infinite series of two-port elementary components, each representing an infinitesimally short segment of the transmission line. From impedance measurement point of view the most important component, omnipresent in all types of cabling is capacitance between two wires. In typical shielded wires (to minimize external disturbances) it can easily reach hundreds of picofarads, and by forming RC integrator together with high output impedance of the current source is very serious obstacle. Fortunately there is a long known remedy called active driving of the shield (Graeme, 1973). Problem with active driving is that it can be very complicated when multielectrode system is considered, where each electrode can assume the role of both the excitation source and voltage pickup. Practical experiments show that instability is often very difficult to tackle with. Nevertheless in simpler systems actively driven shield, often together with another outer shield for noise reduction, is useful solution.

Different set of problems and solutions is connected to current source itself. From modeling point of view real current source can be seen as Thévenin circuit, where ideal voltage source is connected series with high impedance, and as Norton circuit, where ideal current source is connected parallel to high impedance. Thévenin type of presentation leads to current source which is probably easiest to construct. Good quality voltage sources can be made in wide range of frequencies and voltages, and by adding series resistor simplest current source is derived. Still several problems are apparent. Voltage source is limited by supply range. It can be doubled in bridged connection, but achieving voltages over some tens of volts is usually not feasible in embedded electronics. Resistor on the other hand needs to be much larger then impedance under examination. These two requirements are contradictory if arbitrary current levels need to be achieved. Large resistors do also add rather large thermal noise contribution which is very unfortunate when small signals need to be measured. In reality compromise can be achieved by using load dependent correction. It can be achieved by measuring real transfer characteristics

with known loads, or alternatively by continuous measurement of the excitation current (Wang, Xu, & Wang, 2005). One strong benefit is related to safety. Since the resistor is connected in the worst case to the supply line, then strong upper limit exists for generated current. If frequency dependent current limitation is required, then that is similarly easy to achieve, as shown on Fig. 40 (Annus, Lamp, Min, & Paavle, 2005).
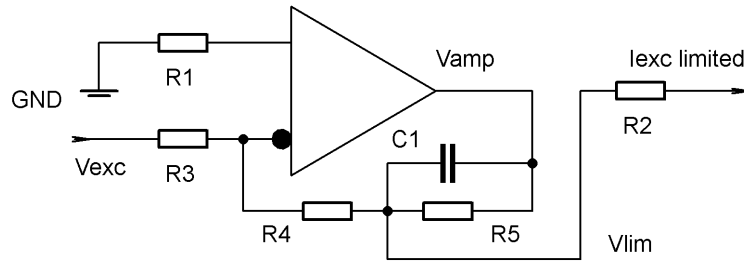

Fig. 40. Frequency dependent current limitation in current source circuitry (Annus, Lamp, Min, & Paavle, 2005).

It is evident that at lower frequencies the impedance of the parallel connection of the capacitor C_1, and resistor R_5 is mostly due to resistivity of the R_5, and output voltage V_{lim} is limited by resistive divider:

$$\max_{\omega \to 0} V_{lim} = \max_{\omega \to 0} V_{amp} R_4/(R_4 + R_5), \qquad (1.26)$$

V_{amp} being limited by supply rails. At higher frequencies division lessens, and output voltage can swing near the supply rails. Cleverness of the circuit lays in fact that, while the limitation is frequency dependent, the transfer function $V_{lim}/V_{exc} = -R_4/R_3$ is almost frequency independent.

There are many different active current source designs. Usually they are based on operational amplifiers, and consequently appeared together with the first devices. One of the known designs from early sixties is Howland current source. It was invented by Bradford Howland from MIT around 1962 (Pease, 2008). Historically it has been described as very clever circuit which is almost useless (Horowitz & Hill, 1989). Nevertheless several modifications of Howland circuit have been used successfully for impedance measurement (Chen, Lu, Huang, & Cheng, 2006), (Hong, Rahal, Demosthenous, & Bayford, 2007), (Bertemes-Filho, Brown, & Wilson, 2000) and many others. Second common type is the so called load in the loop circuit, where impedance under measurement is essentially placed in the feedback loop of an inverting amplifier, and the current in the load is proportional with the input voltage of the amplifier (Boone & Holder, 1996), (Annus, Krivoshei, Min, & Parve, 2008), etc. Third design is centered on current mirroring, and is

mostly used in chip design (Kasemaa & Annus, 2008). In fact there are many other possibilities, such as supply current sensing based current sources, different multiamplifier designs, circuits based on so called diamond structures, current conveyors, and finally already mentioned current measuring and correction circuits (Wang, Xu, & Wang, 2005), auto-balancing bridge method (Agilent Technologies, Inc, 2009) and others. General discussions on wide bandwidth current source parameters can found foe example in (Seoane, Bragos, & Lindecrantz, 2006), and discussions of the load in the loop circuits in (Annus, Krivoshei, Min, & Parve, 2008).

Form practical point of view two active current sources have been extensively investigated. Designs based on Analog Devices AD8129/30 differential-to-single-ended amplifiers with extremely high CMRR at high frequency, largely based on (Birkett, 2005), and simple four transistor bridged circuits (Annus & Kipper, Sümmeetriline vooluallikas, 2007). Simplest four transistor circuit has been tested and implemented with good results (Paavle, Annus, Kuusik, Land, & Min, 2007). Such a circuit (Fig. 41 Simplified schematics of the four transistor bridged V/I converter) is well suited for measurements with the aforementioned shortened square waves.
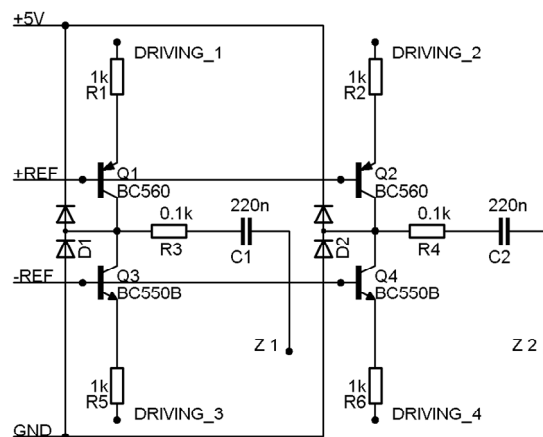
Fig. 41 Simplified schematics of the four transistor bridged V/I converter (Annus & Kipper, Sümmeetriline vooluallikas, 2007)

Inputs *Driving 1-4* are connected to digital outputs of processor circuit, and impedance under investigation between electrodes at Z_1, and Z_2. Practical tests have shown, that even this simplest common base design works at excitation frequencies from some tens of hertz up to 100 kHz, and with excitation currents from 1uA to

1mA. Capacitors C_1, and C_2 effectively block DC component at the output, resistors R_3 and R_4 together with D_1, and D_2 protect the output, and *Ref+* together with *Ref-* are connected to low impedance stabile voltage sources.

Common to active current sources is that the maximal achievable upper frequency limit is around 10MHz in case of better circuits. Output impedance while very good at lower frequencies, and can reach tens of megaohms, will fall into few kiloohm range, and the phase is shifted. Typical parameters can be even worse. Form safety point of view a failure in active circuit may result in increased output current, which should be considered with great care. It seems reasonable that when lower impedances, below 1 kΩ, are expected, and lower currents, in the rage of few microamperes, are used, then simplest resistive Thévenin circuit is preferred. Many current source errors can be modeled and measured, and reverse calculations can be performed to compensate them. Main target is to assure by design, that these errors will not vary much during operation of the instrument, otherwise compensation can be either difficult, or impossible. One of the most important factors is the temperature dependence of the values of the components. It can be minimized by usage of high quality components, but temperature compensation is important as well.

1.15 Safety and reliability

Safety of the patient and surrounding medical personnel is of utmost importance, when using electrical devices in healthcare environment. Electrical currents can enter the body in various ways. In case of bioimpedance measurement they are deliberately injected into the body of the patient, and therefore great care must be taken to keep them within safe limits. Even more dangerous situation can arise, when circuit is completed through the mains. In both cases at least double protection is required, so that any single fault cannot cause harm to humans. Several standards deal with requirements for medical apparatus. Modern devices should usually comply with IEC60601-1 safety standard for medical instruments (IEC). Most important aspects include verification of protective earth, dielectric strength, insulation resistance, and leakage current. Later can be subdivided between earth leakage, patient leakage, and enclosure leakage. Body phantom circuit is defined by IEC60601-1 for simulation of the body's impedance during tests. It consists of 1kΩ resistor in parallel with serial connection of the 10kΩ resistor and 15nF

capacitor. Typical requirements for placement of the isolation barriers, and their limiting values for intracardiac impedance measurements are shown on Fig. 42.
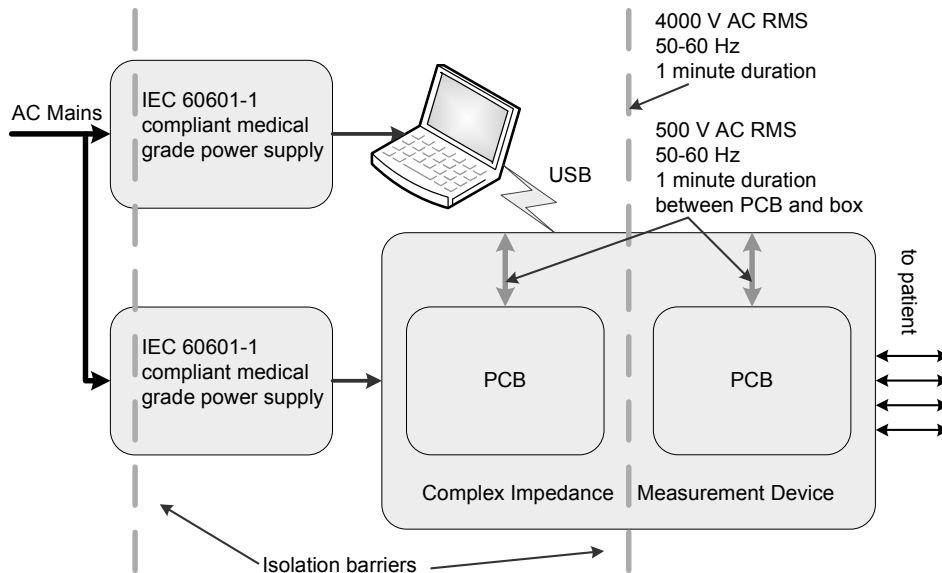
Fig. 42. Electrical Isolation Diagram.

Complying with double isolation requirements two isolation barriers are connected in series between AC mains and patient. First is IEC60601-1 compliant isolation inside medical grade power supply, and it is followed by internal barrier inside measurement instrument. All the components inside instrument should be well isolated from enclosure as well. It is clear from the picture that any additional directly connected apparatus, such as PC and networked devices connected to PC, should use medical grade power supplies as well. Secondary isolation within device, between analog and digital signals chain components, is serving also as a measure against noise leakage. Secondary isolation can also be seen on Fig. 68 showing main printed circuit board, together with analog signal processing modules.

Leakage current limits, and their dependence on the fault conditions are also given in table 1. Fig. 43 shows a graph of the current limitation versus frequency from IEC 60601-1, complemented with the curve of current limiting by the electronic circuit of forming the excitation signal.

During normal operation device is subjected to various disturbances form operation theatre. Among them probably the most destructive is connected with occasional

defibrillation process. None of them should be able to destroy the device. Furthermore operation of the device should resume when such a disturbance is removed, and occurrence of the disturbance should be clearly marked in the resulting dataset. Device must be able to identify and remove also pacing signals. For protection from outside high energy surges gas surge arresters are used at the patient connecting leads. For doubled protection they are followed also by current limiting resistors, and clamping diodes.

Current	Normal Condition*	Single Fault Condition*
Patient Leakage Current (individual electrodes)	0.01 mA	0.05 mA
Patient Auxiliary (total for all electrodes)	0.01 mA d.c. 0.01 mA a.c	0.05 mA d.c. 0.05 mA a.c.
Enclosure Leakage	0.1 mA	0.5 mA
Mains Voltage on Patient or on Applied Part	N/A	0.05 mA

* all current limitations refer to root-mean-square (RMS) value of the current

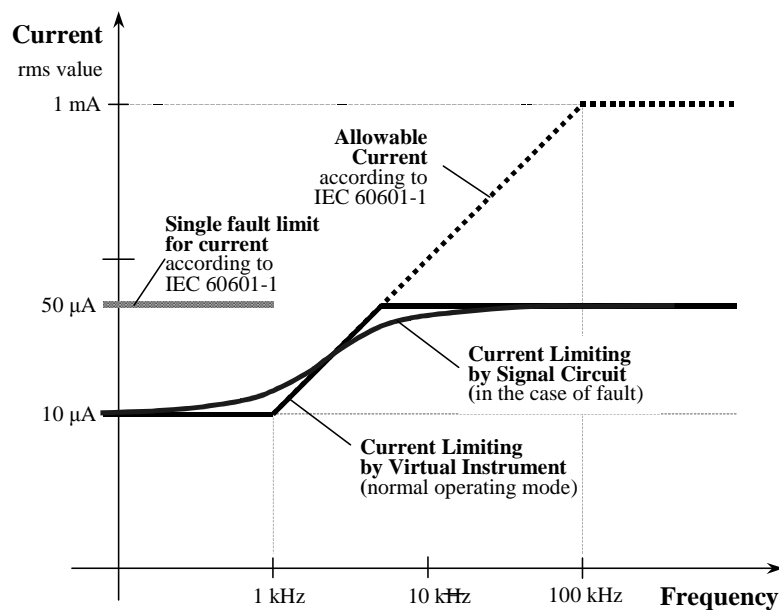Table. 1. Safe leakage currents.

Fig. 43. Maximum allowable measurement current versus frequency. (blue line shows actual physical limiting in the instrument).

2

2.1 Description of the design task and general solution

For improvement of the pacing devices set of experiments was planned in one of the leading laboratories in the field. It required device for invasive measurement of heart tissue impedance variations at different locations, and at different frequencies simultaneously. Several design constraints were imposed by the laboratory. The instrument had to be fully contained within a single substantially rectangular enclosure no greater than 10000cm3, with no side longer than 300 mm. The instrument had to be connected by universal serial bus (USB) to personal computer (PC). If USB power supply, limited by standard at this time to max 500mA, would have been inadequate, then connection to additional separate medical grade power supply (certified to IEC 60601-1) was required. Single patient connector was mandatory, and instrument had to fully contain all the components within said single enclosure. 16 leads to electrodes were required, each of them arbitrarily connectable to any of the four differential current source outputs or four differential voltage pickup inputs. Excitation on at least 8 different frequencies simultaneously was required, and furthermore grouping of the excitation sources was envisaged. Grouping should allow injection of 2 excitation signals into each current source, 4 signals into two arbitrary sources or all 8 of them into single excitation channel. Excitation range from 1 kHz to at least 1 MHz was mandatory. In addition to that safety restrictions applied. The complex-valued physiological impedance instrument had to be classified as a Class II Type CF device per IEC 60601-1. IEC 60601-1 specifies the minimum dielectric withstand voltage for the device to be 4000 VAC (RMS) at 60 Hz for duration of 1 minute. IEC 60601-1 and AAMI ES1 also specify the allowable safe leakage currents, given in table 1, in mA RMS. Leakage currents also applied to intended currents delivered as part of the operation of the device. For frequencies above 1 kHz, the measurement current limit value had to be multiplied by the numerical value of the frequency in kilohertz up to 100 kHz. For currents at frequencies above 100 kHz same limits applied as at 100 kHz. Fig. 43 shows a graph of the current limitation versus frequency from IEC 60601-1. Fig. 42 depicts the required electrical isolation.

Simplified general architecture of the required device can seen on Fig. 44 and more detailed picture on Fig. 45.
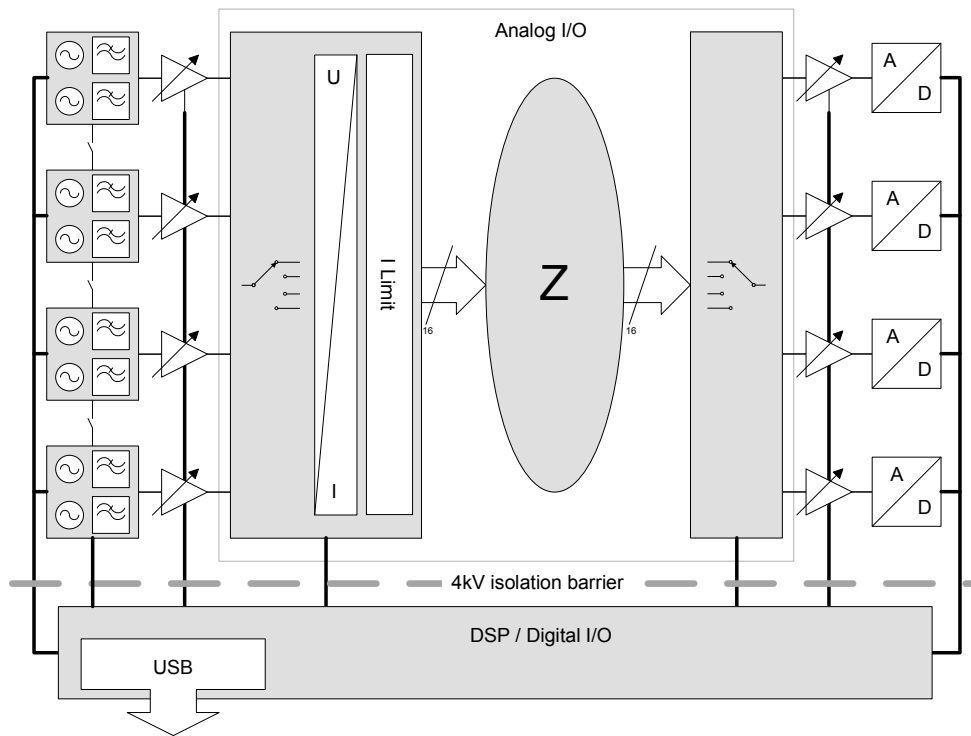
Fig. 44. Simplified general architecture of the EBI spectroscope for intracardiac measurements (Annus, Kuusik, Land, Märtens, & Ronk, 2006).

Device consists of four excitation signal sources, each incorporating two DDS circuits with low pass filters, and grouping switch matrix. Excitation sources are followed by signal conditioning differential amplifiers, and resulting waveforms are output to crosspoint switch matrix. Voltage on selected outputs is thereafter converted into current. Current sources with frequency dependent current limiting (Fig. 40) are completing the output channel.

Input signal is picked up by high input impedance amplifiers, right channels are selected with next crosspoint switch, signals are conditioned with fully differential amplifiers, and simultaneously converted into digital domain by four parallel analog to digital converters (ADC).

IMPEDANCE ELECTRODES

Patient cable(s)

$\dot{Z}$

19-pin Redel Connector
Surge Arrester

Output selector

Input selector

8x16 Analog Switch Array

Overvoltage protection circuits

VCC 1
VCC 2
VCC 3
VCC 4
VCC 5
VCC 6
VCC 7
VCC 8
VCC 9
VCC10
VCC11
VCC12
VCC13
VCC14
VCC15
VCC16

Overvoltage protection circuits

8x16 Analog Switch Array

AD7621 16-bit

Pre-selectoral circuits

G1
f_{1lo} f_{1hi}
G2
Σ

G3
f_{2lo} f_{2hi}
G4
Σ

G5
f_{3lo} f_{3hi}
G6
Σ

G7
f_{4lo} f_{4hi}
G8
Σ

A/D

A/D

F P G A

A/D

A/D

Configuration Control Code
(re-coded)

Control code to the Output Selector

Control code to the Input Selector

µC

8 DDS ICs 9834
Control code to the generators 1...8

µC

µC

µC

I^2C

DDS reset

DDS reset

Main clock
50 MHz

Auxiliary Channel

AUXILIARY INPUTS

26-pin Redel Connector
Surge Arrester

Auxiliary Channel Board

Galvanic isolation
4kV

12 channels
4-input MUX/DACs ADS1256s (TI/BB)
G=1...64   24-bit output 7.5 kS/s
1024 times oversampling

USB

D S P
8 input **MUX**
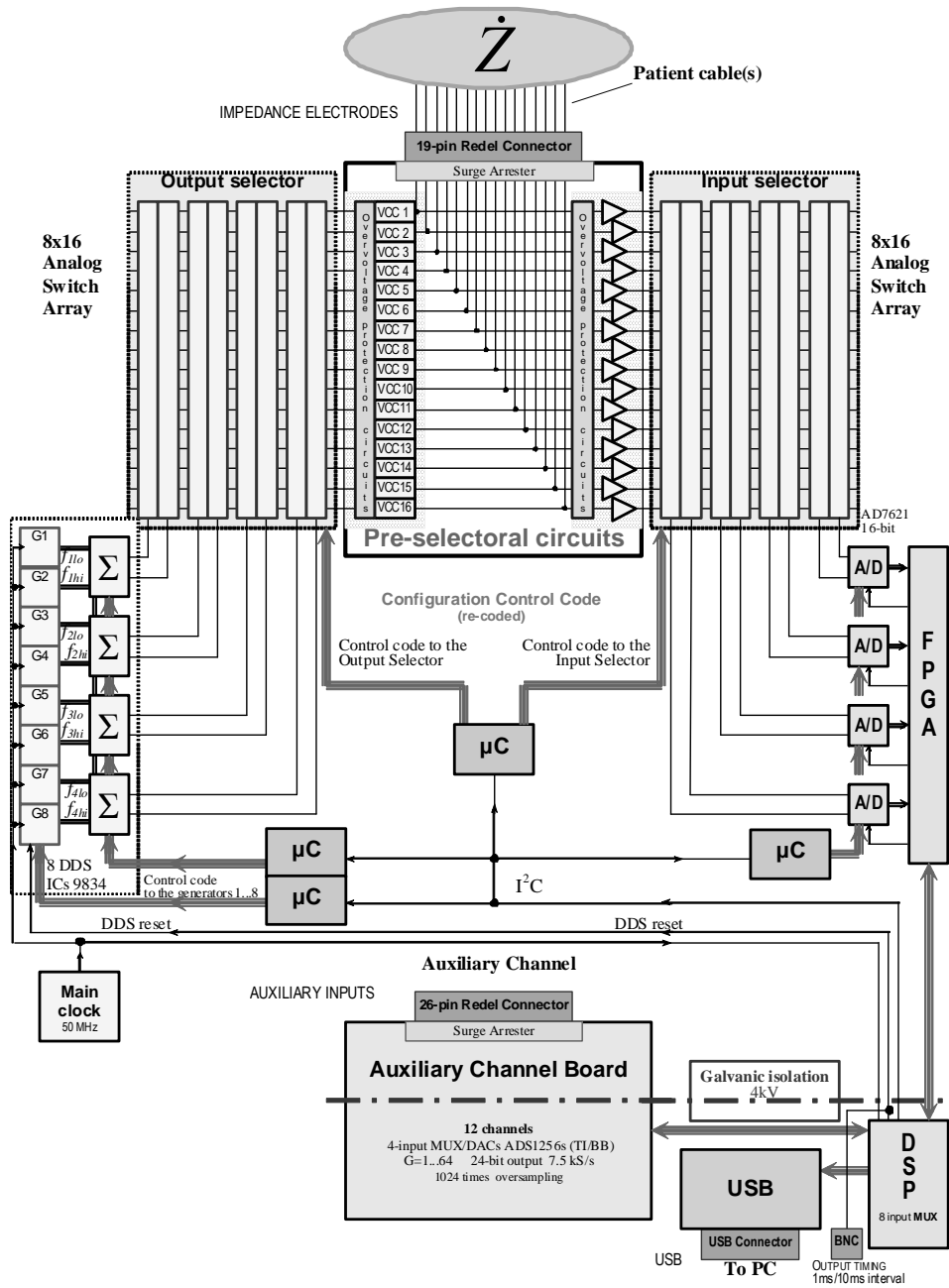
USB Connector

BNC

USB

To PC

OUTPUT TIMING
1ms/10ms interval

Fig. 45. Detailed block diagram of the EBI spectroscope for intracardiac measurements.

Given a selected RMS excitation current, I in μA, the full-scale impedance in ohms had to be selectable from *640/I, 1280/I, 2560/I, 5120/I,* and *10240/I*. This equates to 64, 128, 256, 512, and 1024Ω at 10μA and to 640, 1280, 2560, 5120, and 10240Ω at 1μA excitation current. The instrument's impedance measurements accuracy was required to be within 1% of the selected full-scale range for each of the full-scale input impedance ranges, and the resolution of the impedance measurements at least 1% of the full-scale for all of the operable full-scale ranges of the device. Digitalization in measurement channels was required with at least 16 bit resolution, and RMS noise at digitization had to be within 4 ADC bits for any input gain setting.

2.2   **Practical design decisions**

Since 4000VAC isolation barrier was required inside instrument, decision had to be made as where should it be. In order to minimize digital noise leakage to sensitive analog electronics isolation barrier was placed between signal processing unit, and analog mainboard. Such a leakage could potentially have devastating effect on the measurement results, since many digital signals are synchronous to the measurement signals. Isolation barrier is comprised of 6 iCoupler® digital isolators ADuM2402 from Analog Devices. These relatively low power, bidirectional, 3 and 5V compliant, high data rate: dc to 90 Mbps (NRZ) isolators with precise timing characteristics are also compliant with IEC 60601-1 requirements. The ADuM2402 iCoupler digital isolators are ideally suited for medical applications that require IEC 60601-1-certified isolation to protect patients and equipment. These products are available in wide-body, surface-mount packages with 8 mm creepage and clearance distances as required per IEC 60601-1. Power from the unprotected side is supplied through four TRACOPOWER THP-3 series DC/DC converters. These converter modules provide reinforced insulation. Input to output isolation voltages are rated for 4000 VAC. The products come with industrial and medical safety approvals, and provide ultra-wide input ranges including appropriate 18-36 VDC range. Placement of isolation barrier and isolators on mainboard can be seen on Fig. 46.
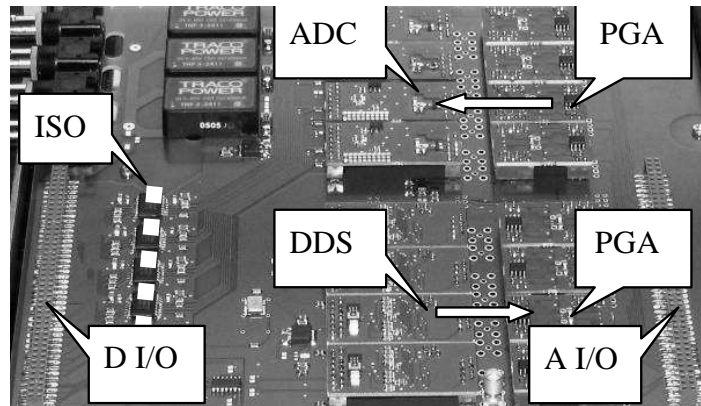
Fig. 46. Main board of the realized impedance analyzer: D I/O – Digital Input/Output module connector, ISO – Isolation barrier, ADC – Analog to Digital Converter module, PGA- Programmable Gain Amplifier module, DDS – Direct Digital Synthesizer module, A I/O – Analog Input/Output module connector (Annus, Kuusik, Land, Märtens, & Ronk, 2006)

Single patient connector, as required, has to carry both the input and output signals for all four channels. Front end switching had to be provided to permit multiplexing between different available electrodes, to make it possible to map each of the 16 impedance input-output conductors to any arbitrary set of pins on the impedance connector. Further is desirable to perform the multiplexing as rapidly as possible, in order to enable "simultaneous" measurements over many electrode configurations. It was desired to be able to program automatic multiplexing sequences for use within an experiment. The goal was to be able to excite current on any set of 2 or more of the 16 electrodes, and to measure voltage on any set of 2 or more of the 16 electrodes. The system has to be designed to minimize the crosstalk between frequency signals encoded on a single channel, and between signals on different measurement channels. If signal frequencies are to be adjusted for minimization of crosstalk, the system shall select appropriate frequencies automatically.

While reasonable requirements from usage point of view they are probably the most controversial ones. Arbitrary multiplexing between electrodes implies that both the input amplifiers and current generators shall be inside the device, since each lead can assume a role of both the current source, and voltage pickup. Together with single connector requirement it forms a complex of problems. First reason is simply mechanical. Since device shall have 16 lead wires to electrodes, cable becomes bulky and not flexible enough. Worst problem is associated with close placement of leads. If operating on frequencies up to some megahertz is considered, then cross coupling and capacitive loading from leads is almost unavoidable, and could potentially destroy measurement. Nevertheless Lemo Redel

2P series CKBM19GLNA 19-pin connector was used, as required, and two Intersil CD22M3494 16x8x1 BiMOS-E Crosspoint Switches introduced (Fig. 47).
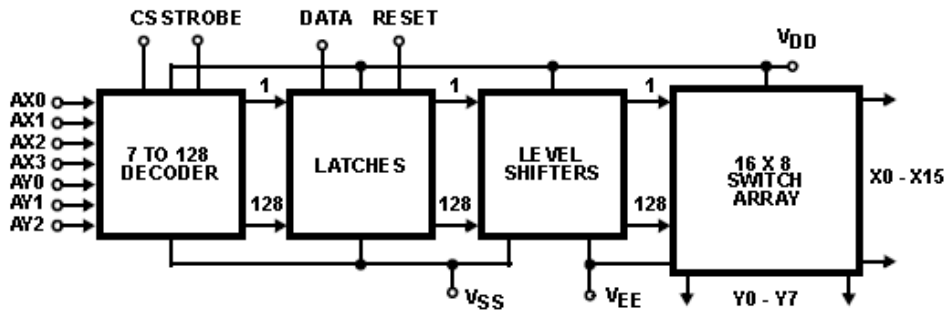

Fig. 47. Block diagram of the Intersil CD22M3494 16x8x1 BiMOS-E Crosspoint Switch from manufacturers datasheet.

One for mapping of the four differential output channels to the arbitrary current source, and one for selecting the signal from 16 input voltage pickups arbitrarily into four differential measurement channels. CD22M3494 is an array of 128 analog switches capable of handling signals from DC to 50 MHz (-3dB 14V), with low r_{ON}, guaranteed r_{ON} matching, and with analog signal input voltage equal to the supply voltage. Most importantly CD22M3494 has very low crosstalk. Because of the switch structure, input signals may swing through the total supply voltage range. Any number or combination of connections may be active at one time. However each connection must be made or broken individually. All switches may be reset by taking the reset input from a zero state to a one state and then returning it to its normal low state.

Four fully independent excitation and response channels were implemented, as required. On the excitation side eight DDS circuits AD9834 from Analog Devices were chosen as excitation sources. Two in each channel. AD9834 is a 75 MHz low power DDS device capable of producing high performance sine outputs. AD9834 consumes only 20 mW of power at 3 V, and is an almost ideal candidate for power-sensitive applications. Block diagram of the AD9834 is on Fig. 48. Each channel in the instrument has two DDS sources with following 5th order low pass filter with 18 MHz cutoff frequency, and switching circuitry. For each channel, the excitation signal amplitude is independently selectable in the range of 1-10μA RMS. At higher frequencies, the current may be increased to values above 10μA RMS and still satisfy the electrical safety requirements (Fig. 43). Excitation signal amplitude is selected by two means.
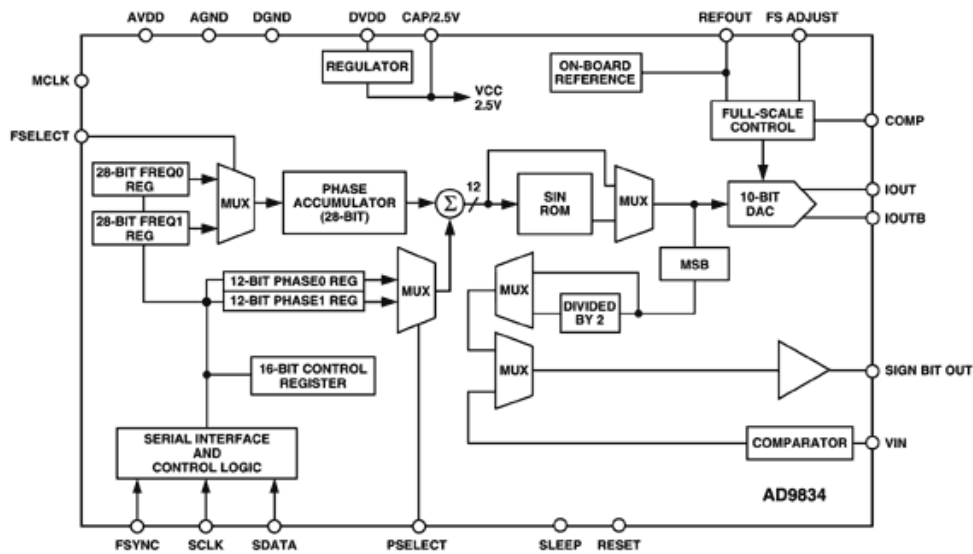
Fig. 48. Block diagram of AD9834 DDS chip from manufacturers datasheet.

In each channel one dual digital to analog converter (DAC) MAX5721 (Fig. 49) from Maxim Integrated Products is driving full scale inputs (FS Adjust) of the AD9834 DDS circuits.

The MAX5721 is 10-bit, low-power, buffered voltage-output, digital-to-analog converter with 20MHz serial peripheral interface (SPI) compatible serial interface. DAC outputs employ on-chip precision output amplifiers that swing rail-to-rail. The MAX5721's reference input accepts any voltage in the range from 0V to VDD. In power-down the reference input is at high impedance, further reducing the system's total power consumption. The MAX5721 on-chip power-on reset (POR) circuit resets the DAC outputs to zero and loads the output with a 100kΩ resistor to ground. This provides additional safety since the measurement current is off on power-up. Ultra-low power (supply current 135µA at VDD = +5.5V) MAX5721 has guaranteed 10-Bit monotonicity (±1 LSB DNL). Additionally the output current setting is achieved by controlling the gain of an amplifier stage following DDS module. It has digital 3 bit gain control.
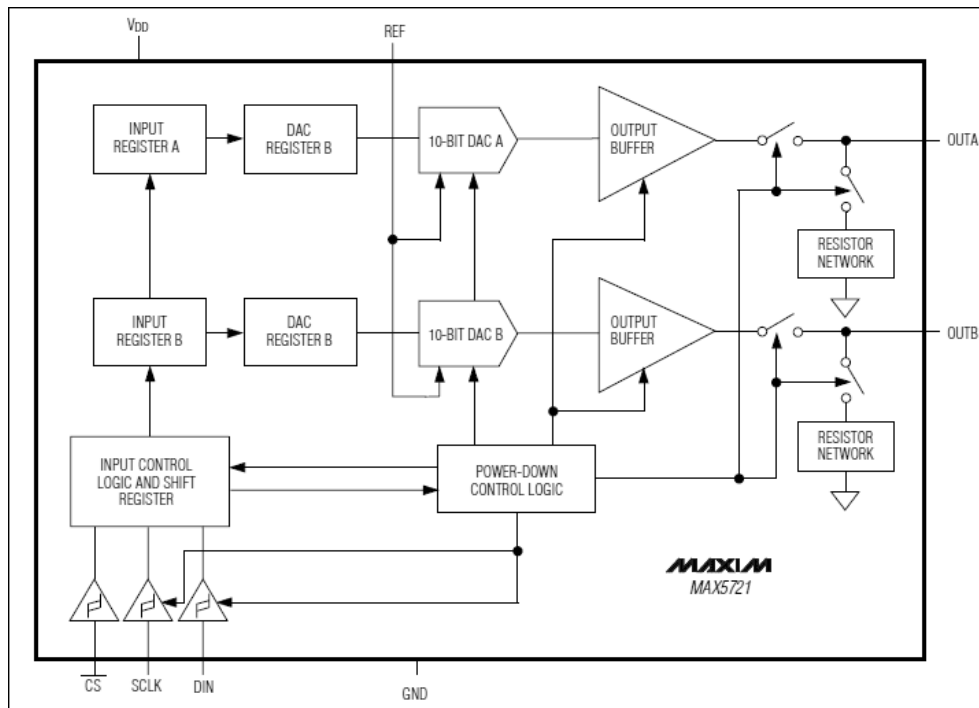
Fig. 49. Block diagram of the MAX5721 digital to analog converter from manufacturers datasheet.

An AD7621 (Fig. 50) from Analog Devices PulSAR family of successive approximation (SAR) converters was chosen for digitalization of the response signals. The AD7621 is a 16-bit, 3 MSPS, charge redistribution SAR, fully differential analog-to-digital converter. It offers ± 2 LSB (± 30 ppm of full scale) integral and differential linearity errors (INL/DNL), no missing codes, and at least 87,5 dB signal-to-noise ratio (including distortion). Typical total harmonic distortion (THD) of the AD7621 is below -103 dB @ 100 kHz, and it operates from a single 2,5 V power supply. This combination of speed and accuracy is achieved while consuming just 70 mW at 3 MSPS. The SAR architecture ensures that there are no pipeline delays. The part contains a high speed, 16-bit sampling ADC, an internal conversion clock, an internal reference buffer, error correction circuits, and both serial and parallel system interface ports.
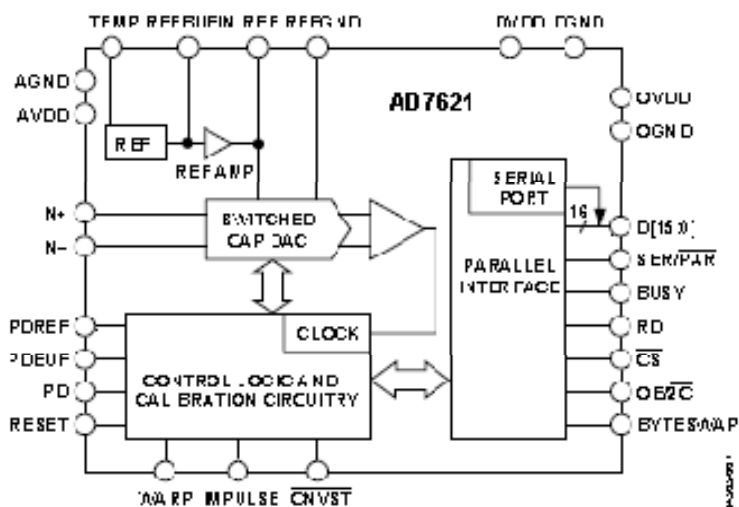
- 61 -

Fig. 50. Block diagram of the AD7621 converter from manufacturers datasheet.

Real sampling rate achieved in final device was 100 kilo samples per second. It was limited by the computing power of the used digital signal processor. Since maximum required measurement frequency is 1MHz, then the sample rate may look at the first glance inadequate. According to Nyquist–Shannon sampling criterion a bandlimited analog signal that has been sampled can be perfectly reconstructed from an infinite sequence of samples only if the sampling rate exceeds $2B$ samples per second, where B is the highest frequency in the original signal. In fact additional margin is required due to non ideal antialiasing filters. Fortunately when sampling known signals, which are generated on site, an under-sampling can be used, provided that aliasing effects are accounted for. Limiting factor in case of the undersampling is the input bandwidth of the converter, which in case of AD7621 is 50 MHz (–3 dB), more than enough for 1 MHz signal.

2.3   Instrument Control

As described previously several components in protected area of the instrument require digital programming. Two crosspoint switches need information regarding the electrode configuration in the front end module. Each of them having 4 digital lines for setting switches. There are eight amplifiers on the mainboard, four in each direction. Amplification of the amplifier module is set by four bit parallel digital word. Further down the line four DDS modules have two DDS circuits, one DAC

circuit, and two switches each. DAC and DDS circuits are programmed over SPI interface, and two switches share common digital control line. All in all it would imply usage of 4+4+8*4+8*3+4*3+4= 80 digital control lines. It is clearly not feasible to pass all of them separately over the isolation barrier. Decision has been made to include several microprocessors at relevant locations to adjust settings over common Inter-Integrated Circuit (I^2C) control bus. I^2C has many advantages. It requires only two bidirectional digital lines, Serial Data Line (SDL) and Serial Clock (SCL), to control all the aspects of the device. Secondly: I^2C is addressable bus and carries its own clock. It makes possible to selectively freeze and wake up relevant microcontrollers, thus effectively eliminating digital noise from them during the operation of the device. Connection hierarchy inside the device is on Fig. 51. There are 5 physical I^2C devices:

a. Atmel AVR based slave controller to manage input/output crosspoint switches
b. Atmel AVR based slave controller to manage gains of output amplifiers
c. Atmel AVR based slave controller to manage gains of input amplifiers
d. Atmel AVR based slave controller to manage frequencies of DDS'es and output voltages of DAC's
e. DSP based master controller

Four physical AVR controllers are divided into 12 logical subsystems with separate I^2C Addresses (write address). Eight logical I^2C slaves for each of the DDS, output amplifier manager, output crosspoint switch configurator, input crosspoint switch configurator, and input amplifier manager. DDS_n-DAC_n manager conveys code words to determine phase, frequency, and amplitude of the individual signals. It also selects outputs from the individual DDS-DAC modules – differential output of the DDS is either connected to summing bus or directly to an output amplifier input. Amplifier manager sets gains of the individual fully differential amplifiers, and enables or disables individual amplifiers. Crosspoint switch commutator ensures that right input and output channels are connected. Maximum 4 differential connections per switch. Each time new data is received old connections are all disconnected.

In current version data to and from the I^2C subsystem is directly pipelined to the LabVIEW based user interface. Two main tasks to be performed are reading and writing internal registers of the I^2C slaves. Current version supports writing in fix format packets, and reading from addressed internal registers.
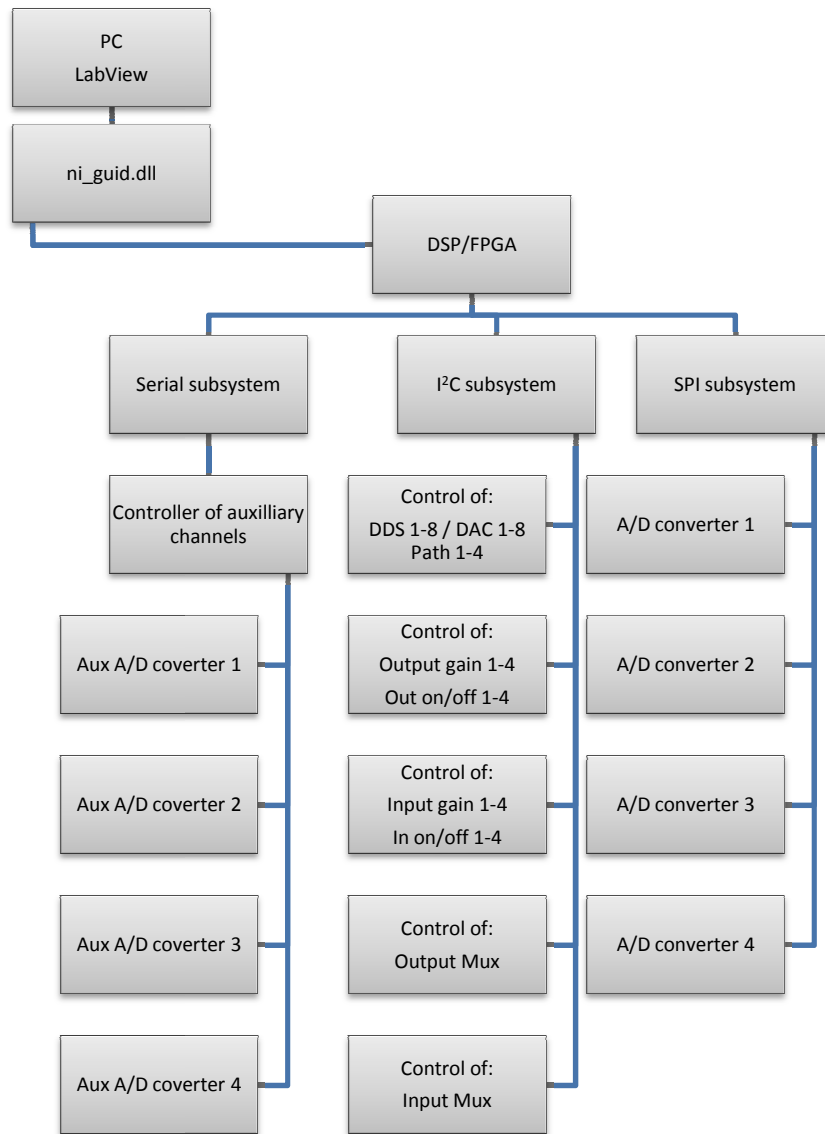
Fig. 51. Data path to interconnected objects inside measurement unit.

Information regarding masters success or failure, while doing described operations, is pipelined directly to LabVIEW. User intervention is required if 10 repeated attempts did not succeed.

2.4 Sampling, signal processing and communications

As discussed earlier sampling in all four ADC channels is parallel. Sampling points are generated in the digital side with the aid of FPGA circuit. There are several tasks performed by the FPGA. First of all it generates the sample rate for the impedance measurement. In all of the measurement channels it is set to be 1kHz. It is crucial to synchronize all tasks performed inside instrument to this 1 ms sampling period. For synchronization with outside devices separate digital output is provided. Secondly ADC sampling clock is needed, together with serial data communication with each of the four ADC's. Next four serial streams are desterilized, and passed over to digital signal processor.

Step by step following happens: From main 48MHz clock 1ms reset pulses are derived initiating measurement cycles. It resets all the excitation generating DDS circuits each time, in order to guarantee full synchronization of all the signals. Sampling signal, generated with the aid of the dedicated DDS circuit on digital side, initiates the conversion cycle for all AD converters. At the end of all of the conversion cycles, 16 bits of the ADC serial output data is simultaneously clocked into FPGA registers, using 24MHz clock, and an interrupt output is set. After receiving an interrupt signal DSP initiates 4 read pulses for retrieving ADC measurement data over the 16 bit parallel bus in burst mode. Interrupt signal will be reset at the beginning of the next ADC measurement cycle when any of the four busy signals goes high.

From that it is clear that most of the clocking, and signaling is generated on the digital side of the instrument. To pass it over to ADC, and DDS circuits on the analog side they have to pass isolator circuits. Already not the best jitter parameters of the signals, due to relatively high jitter inherent to FPGA circuits (33 to 50 ps) (Brannon & Barlow, 2006), degrade even further. It is rather unfortunate, since sampling performance is degraded as well. Generally signal to noise ratio of the sampling circuits depends heavily on the phase noise and jitter of the sampling signal:

$$SNR = -20\log(2\pi f t_a), \tag{2.1}$$

Where f is the frequency of the signal to be sampled and t_a is the so called aperture jitter in RMS. If 10 MHz input sinusoid is sampled with ideal ADC, then for SNR of ca 96 dB, corresponding to 16 bit resolution, total RMS aperture jitter should be below roughly 250 fs. There are other contributions to SNR, such as quantization

noise and thermal noise. For more adequate picture these noise sources can be combined into single equation:

$$SNR = -20log\sqrt{\left[(2\pi f t_a)^2 + \left(\frac{1+\epsilon}{2^N}\right)^2\right]}, \qquad (2.2)$$

Where f is the analog input frequency. t_a is the combined aperture uncertainty for the ADC and the clock oscillator (jitter), ϵ here is the composite RMS DNL in LSBs, including thermal noise, and N is the resolution in number of bits. So in reality even better clock source is required for the same performance in terms of SNR. Given aforementioned parameters and constraints solution for the problem is not a trivial one. Nevertheless relatively good results can be achieved by placing good quality clock oscillator near the converters, and using as few as possible gates between the oscillator and converters. Solution adopted was to place main low RMS jitter 48 MHz clock source on the analog side, and synchronize signals from digital side with two low jitter D triggers. Two main signals need cleaning: namely ADC sampling clock, and 1 ms impedance sampling period. Digital side clock is coming from analog circuitry over the isolation barrier, and is then used to generate all the clocking signals needed.

Form one side ADC sampling rate is limited by the capabilities of the converter itself, from another by the signal processing power of the DSP circuitry. By using TMS320F2811 DSP chip from Texas Instruments maximum achievable rate to calculate four times eight (four channels, eight frequencies) complex discrete Fourier transforms (DFT) was limited to 100 points per each millisecond. Therefore full capability of the ADCs was unfortunately not utilized, and maximum sampling rate was only 100 kHz.

All aspects of the instrument operation are controlled via an integrated graphical software application on the host computer. Application software was created in National Instruments LabVIEW graphical programming environment. It allows required flexibility, and easy redesign. Later is needed due to the experimental nature of the device. USB connection to host PC was provided by FTDI's popular USB UART/FIFO family member FT2232. This device features two multi-purpose UART/FIFO controllers which can be configured individually in several different modes. Each measurement channel did simultaneously and automatically decode the real & imaginary parts of the frequency components of the corresponding excitation signal. In reality it gives roughly 3 megabit per second data stream through USB interface, and that is unfortunately on the very limit of the FTDIs circuitry.

2.5 Full boxed device and subassemblies

Standard plastic EURO CASE 3HE from OKW was chosen, with outer dimensions 260*250*143mm, and internal metallization layer for shielding. For easy testing and occasional redesign all the subcomponents were put on separate PCB's. Analog mainboard subassembly is shown on Fig. 46, digital signal processing module on Fig. 52, and analog front end subassembly on Fig. 53. Outside view is on Fig. 54, and operator screen fragments are on Fig. 55.
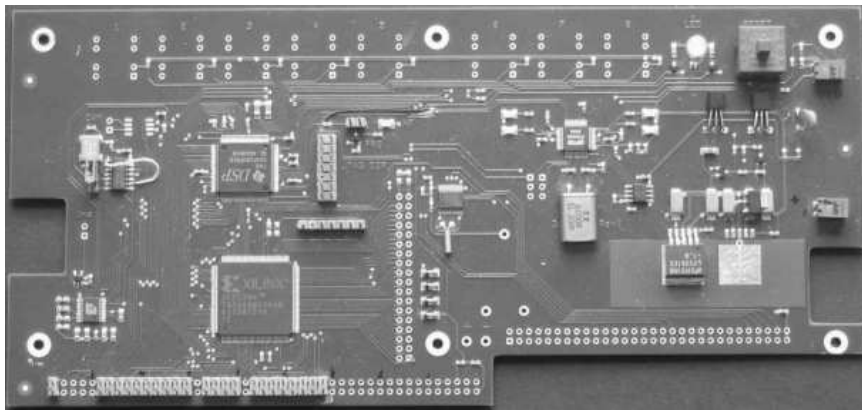

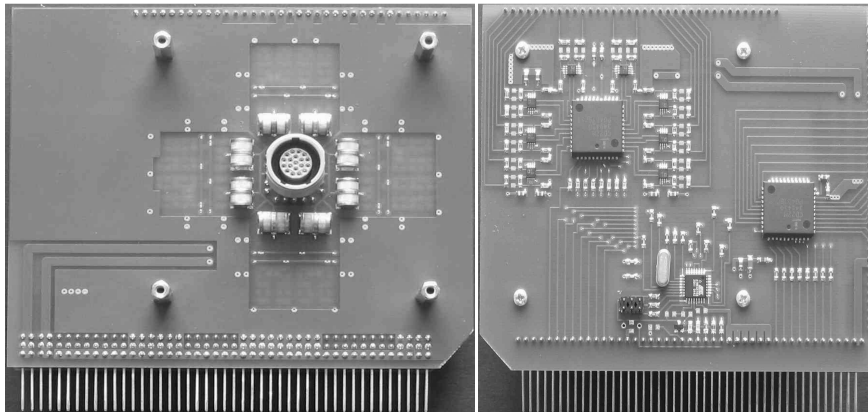Fig. 52. Digital signal processing and communication module.

Fig. 53. Analog front end module. On the left side front view with protecting surge arresters is shown, and on the right side back view of the module with two crosspoint switches, and microcontroller.

Fig. 54. Outside view of the first device, front view in the left, and backside on the right.
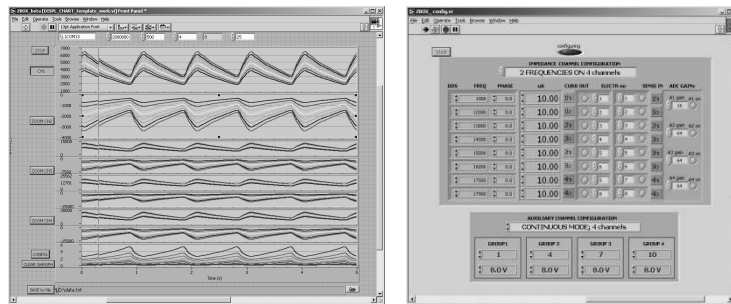

Fig. 55. Operator interface on PC. On the left picture is the measurement window, and on the right configuration window is shown.

2.6 **Test fixture and test results**

Electrical components do vary in their parameters, and consequently each and every device will have somewhat different parameters. Also ambient temperature and temperature inside the instrument will have an effect on the parameters. To achieve precision measurements, and avoid troublesome manual tuning of the instrument, an automatic test procedure was devised, and special test fixture designed. Inside shielded enclosure of the test fixture (Fig. 56) ring of 16 precision resistors is formed and attached to the connector with 100 mm wires.

Fig. 56. Instrument with test fixture (aluminum enclosure on the right) attached.

Three purely resistive rings (with three different values 10Ω, 100Ω, and 1kΩ) can be used. Arbitrary resistor in the ring can be modulated by connecting in parallel 100, and 1000 times bigger resistors. After connecting the test fixture to the device an automatic test cycle is initiated in LabVIEW environment. Real gain values of the amplifiers, output parameters of the current sources and frequency characteristics of the appearing filter elements are automatically measured, and correcting values are stored. Two main contributors in frequency domain are coupling capacitors together with related impedances, and low pass filter in front of the ADC. Analog circuitry will add certain summary delay to the signal, which should be taken into account as well. Measured and un-compensated magnitude and phase characteristics of the instrument can be seen on figures Fig. 57, and Fig. 59. Measurements were taken with precision 100 ohm resistors in test fixture. Same magnitude and phase characteristics after compensation in the LabVIEW software is applied can be seen on Fig. 58, and Fig. 60. It is worth noting good similarity between different measurement channels shown on Fig. 58. Considerable improvement both in magnitude and phase characteristics is clearly visible. Magnitude is well within 1% of the ideal 100 ohm value, and phase deviation has been reduced from tens of degrees to under 1 degree. Empirical compensation coefficient for summary delay is 632 ns. Filter with -3dB point at 95 Hz is inserted for compensating the low pass filter formed by the coupling capacitors. To compensate for low pass filter in front of the ADC a 160 kHz inverse filter is employed, and compensation for apparent 6,8 MHz low pass filter is applied. Arbitrary automatic gain compensation is performed as well.

Fig. 57. Measured and un-compensated magnitude characteristics of the instrument.

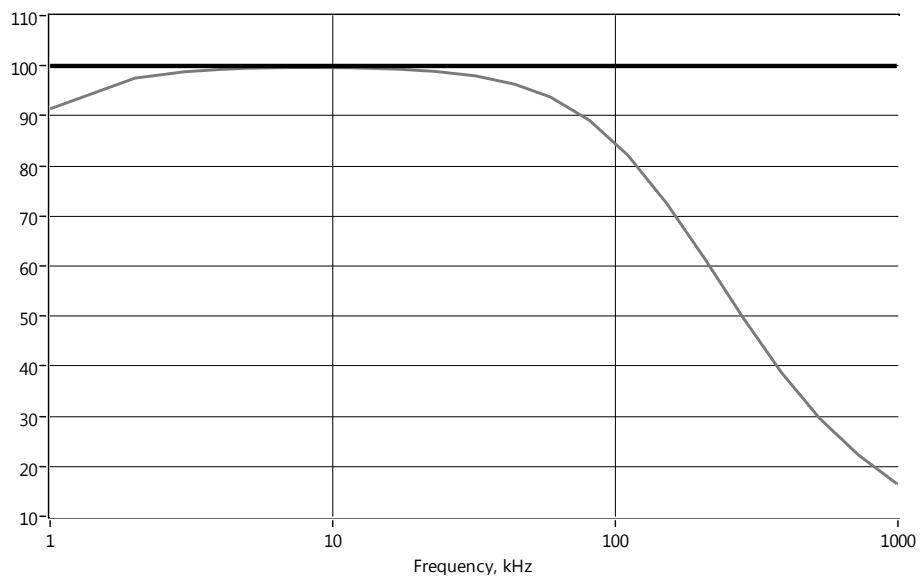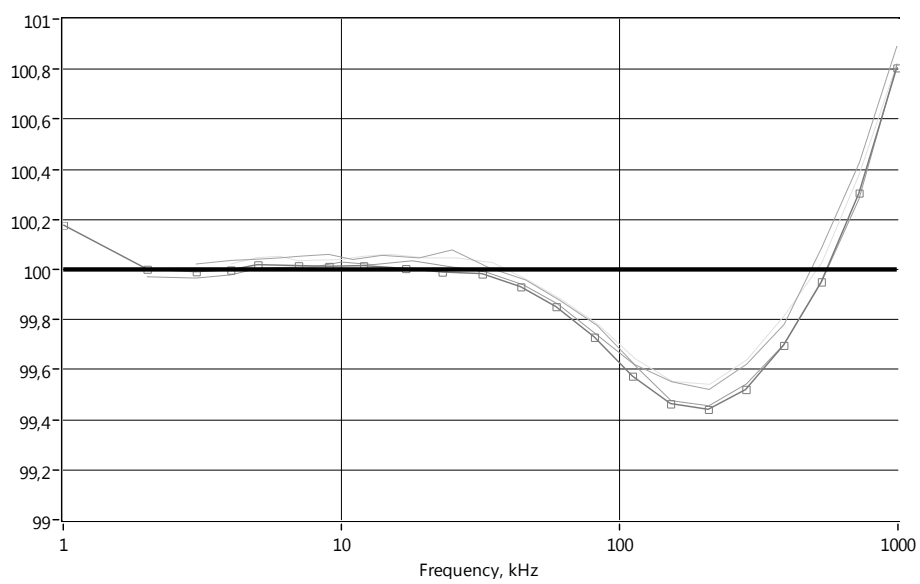Fig. 58. Compensated magnitude characteristics of the instrument.
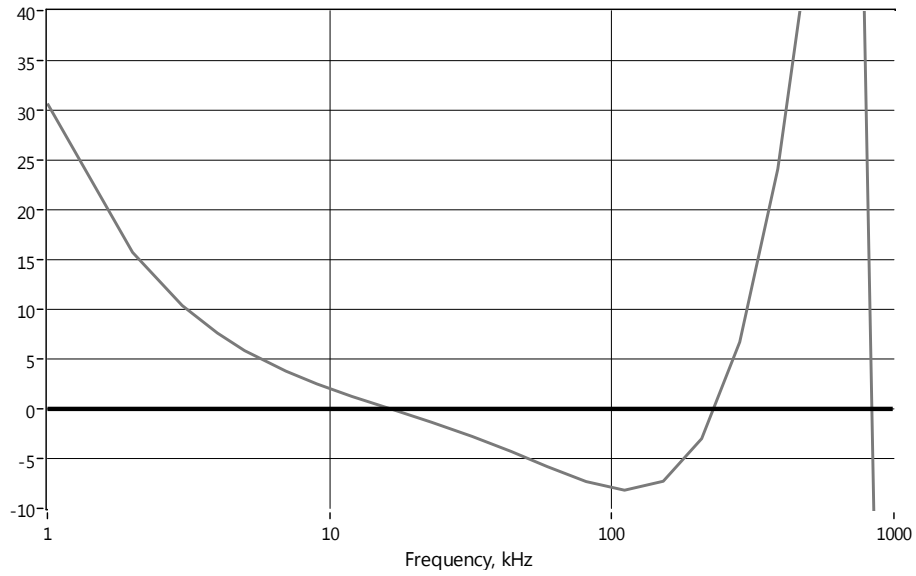
Fig. 59. Measured and un-compensated phase characteristics of the instrument.
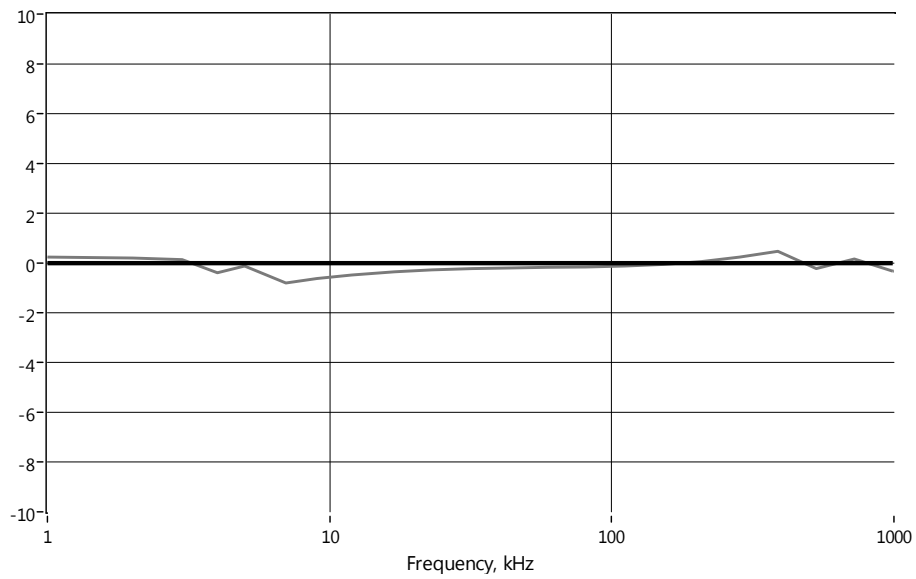
Fig. 60. Compensated phase characteristics of the instrument.

Later when calculating values of the real and imaginary parts of the impedance these correcting values are automatically applied. For comparison on Fig. 61, and

Fig. 62 magnitude and phase characteristics of an ordinary 1% resistor are shown. They were measured with Wayne Kerr Electronics precision impedance analyzer 6500P. It can be clearly seen that even an ordinary resistor behaves reasonably well for calibration within frequency range from 1kHz to 1MHz.
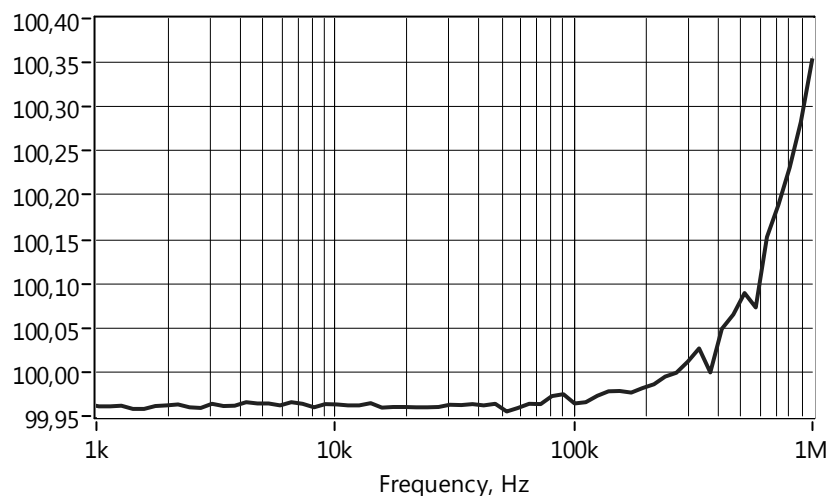
Fig. 61. Magnitude characteristics of the 100 Ω resistor.
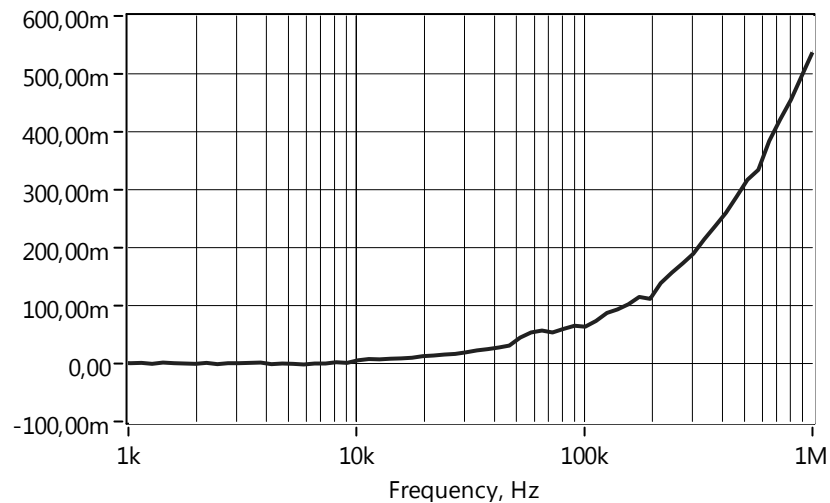
Fig. 62. Phase characteristics of the100 Ω resistor.

Therefore it can be concluded, that measurements after the calibration are well within required accuracy limits (within 1% of the selected full-scale range for each of the full-scale input impedance ranges) at different frequencies from kilohertz to megahertz. By modulating values of the test resistors it was confirmed that the

resolution of the impedance measurements of at least 1% of the full-scale range, for all of the operable full-scale ranges of the device, is achieved. Clearly distinguishable modulation could be observed above the noise level on the measured impedance components even at higher operating frequencies and without additional filtering (Fig. 63).

Fig. 63. Fragment of the operator screen showing noise level and 1 % modulation at 1 MHz excitation frequency. Re and Im values are in ohms.

3

3.1 **Results, conclusions, and first improvements**

Tests carried on with the apparatus allow to conclude that main requirements were fulfilled, and in some cases even surpassed. Nevertheless optimization is warranted in many areas. As the device is rather complex, and with demanding requirements, design decision was made not to optimize for power consumption, but for performance. Resulting average power cons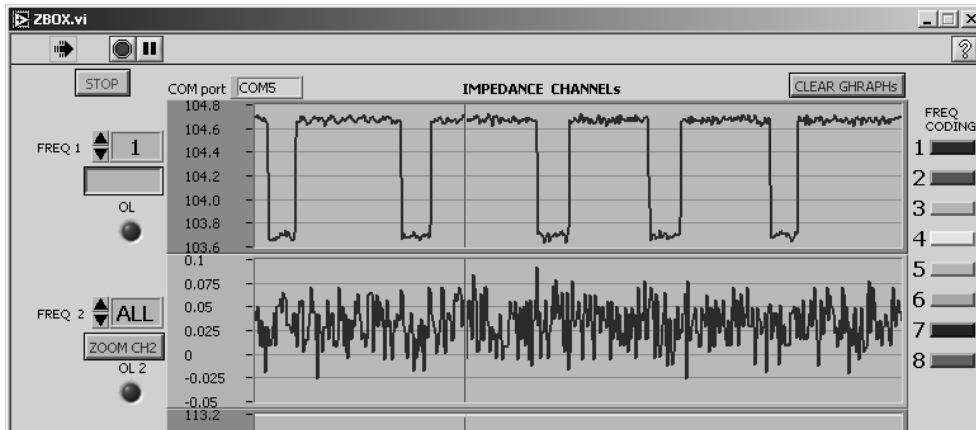umption of the device is in roughly 25W. While it is rather large number in itself, adverse effects from the raising temperature inside the device worsen the situation further. It warranted multipoint temperature measurement inside the device in order to compensate for changing parameters.

Second problem associated with power supplies is related to noise of the free running DC-DC converters. While it was hoped that it would not interfere much with the measurement results due to its asynchronic nature, reality showed that measurements at frequencies higher than some hundred kilohertz were increasingly noisy. Simple solution was proposed to enhance the signal to noise ratio at higher frequencies. It is well known in analog FM communication area, and is called there pre-emphasis, and de-emphasis. In essence higher frequency components are increased in excitation part of the device, and correspondingly RC low pass filter just before the analog to digital converters is responsible for the reciprocal conversion. In context of the impedance measurements it is quite natural, since higher signal levels are allowed at higher frequencies (Fig. 43). Also increase in amplitude, and corresponding phase characteristics are easy to realize just by programming the DDS circuits accordingly. The biggest drawback is in the temperature dependence of the analog RC filter. In order for the pre-emphasis, and de-emphasis idea to work flawlessly both should be matched with high precision. Smallest errors in magnitude and phase are immediately apparent in impedance measurement results. Fortunately usage of high quality components, and aforementioned temperature compensation, together with automatic calibration procedure, reduced these errors to negligible level.

Third problem is related to the original specification of the device. It is certainly user friendly to have everything in one single box, and it is tempting to have full freedom when choosing electrodes, frequencies, and signal levels. And the device was working as expected when the testing was done at the terminals, and by the professionals. Sad truth is, that as soon as longer cables are used, high frequency parameters will degrade. Furthermore level of freedom in configuring of the device appeared to be one of the major obstacles in using it, and often resulted in misconfiguration.

And last but not the least of the problems were issues related to the usage of the USB interface. The driver supplied by the FTDI was not up to the task of guaranteeing sustained 3 megabit per second data transfer to the PC. Low level system programming was required, in order to improve the situation, but during longer periods, working for days during experiments, system still ultimately could collapse at the end.

3.2 Lessons learned from design of similar devices

Two devices for multifrequency impedance measurement will be briefly discussed. First of them is combined multichannel ECG/ICG measurement unit (Min, Parve, Ronk, Annus, & Paavle, Synchronous Sampling and Demodulation in an Instrument for Multifrequency Bioimpedance Measurement, 2007). Upper frequency limit at 1 MHz is similar to previously described device. However there are also major differences. First only one analog to digital converter assembly is used for all channels. It requires fast multiplexing between different inputs. Secondly all the excitation, sampling, signal processing and communication tasks are handled by single FPGA. Thirdly optical Ethernet connection is used instead of the USB. And finally active current sources, based on Analog Devices AD8129/30 differential-to-single-ended amplifiers, were used. Functional block diagram of the unit is shown on the Fig. 64. Since the resolution of the very fast AD converter (160 Msps, used at half speed) did not fully satisfy design requirements also sample based compensation was employed. Together with fast input multiplexing it required very high bandwidth amplifiers. By using optical Ethernet most of the safety concerns vanished, and at the same time communication speed was increased manyfold compared to USB1.1. In comparison with previous design following can be stated. Sample based compensation together with fast input multiplexing, while tempting, complicates design considerably. Usage of the

multiple analog to digital converters, one for each physical input channel, seems to be more preferable.
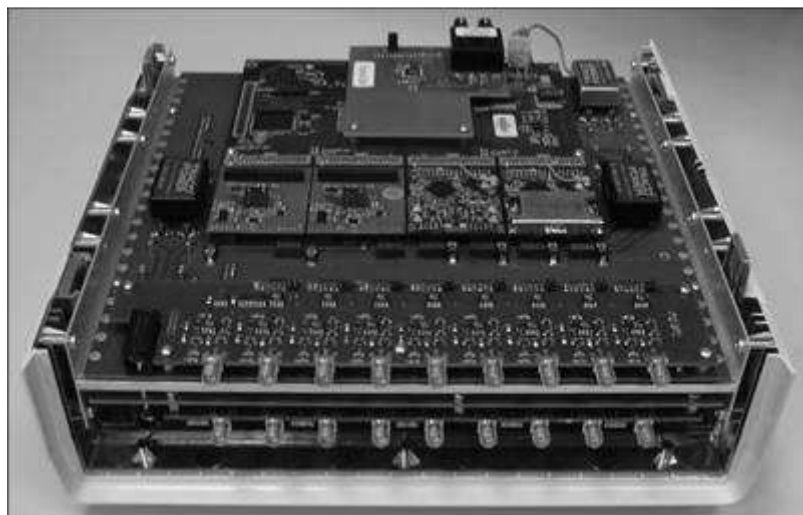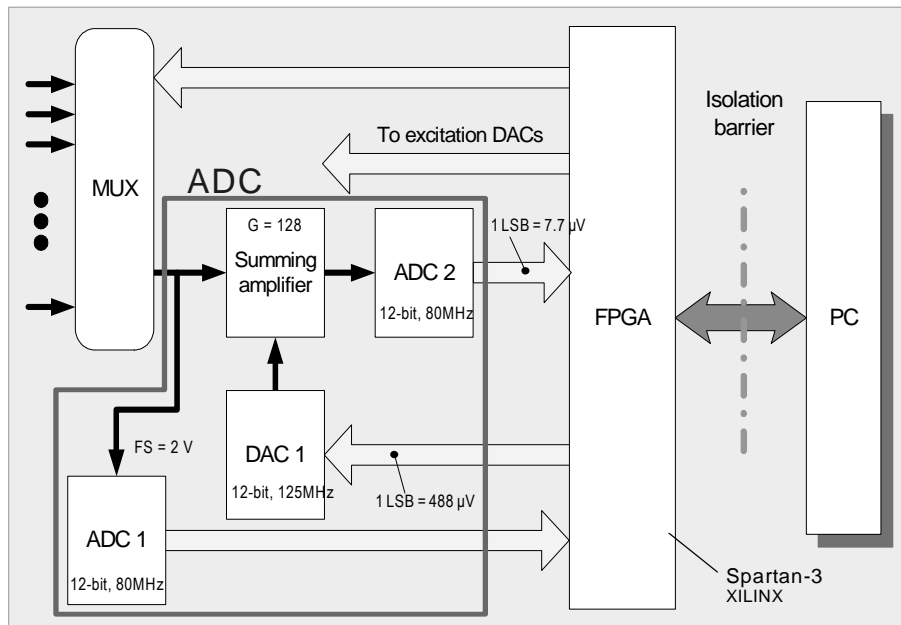
Fig. 64. Functional block diagram and picture of the ICG/ECG measurement unit. (Min, Parve, Annus, & Paavle, 2006)

Ethernet is preferable connection medium in multichannel devices. Together with optical cabling it will provide for speed, isolation, and also for the reliability of the

communication link. Usage of the single FPGA instead of the multichip solution seems to be viable. When printed circuit board is designed correctly, then noise leakage to analog side is not very dangerous, and is certainly less disturbing then noise impact from nearby DC-DC converters. When measuring impedances under kiloohm, and with microampere range currents, then active current sources have very little advantage over much simpler resistive current source. Problems with capacitive loading from cabling were evident as well, since the multiplexed active current sources were inside the device. Active shield driving, while useful, can be source of severe stability issues.

Second device of interest is battery powered tissue monitor with Bluetooth interface (Fig. 65).
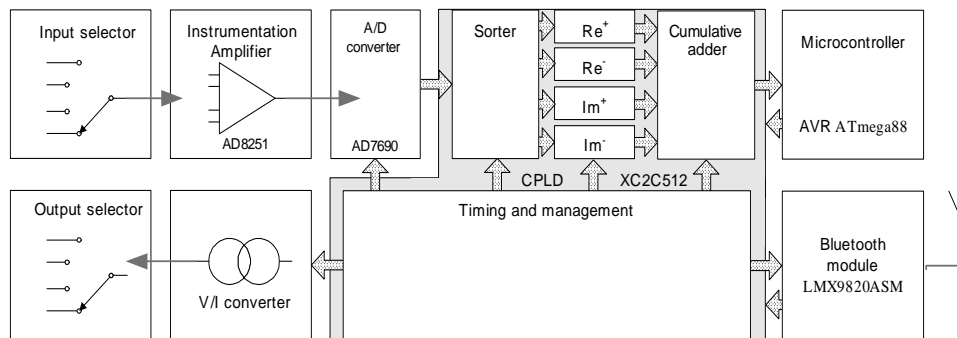
Fig. 65. Functional block diagram and picture of the tissue monitor unit.

Shortened square waves were utilized for measurement, and simple four transistor current source (Fig. 41) used. Communication task was handle by Atmel AVR microcontroller, sampling and signal pro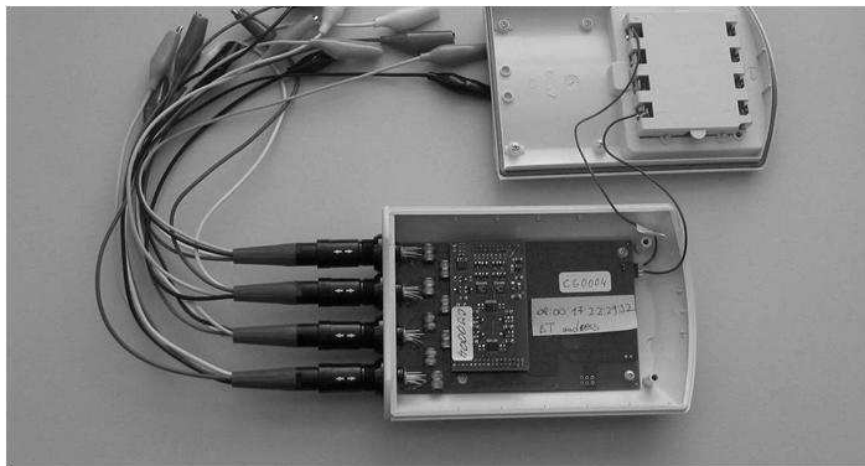cessing with low power FPGA. Four parallel channels had separate front end amplifiers, and were multiplexed to single analog to digital converter. It was deliberately slower than previously described devices, completing one measurement cycle in 100 ms time. Maximum frequency for measurement was limited to 100 kHz. It is possible to place the unit close to the electrodes due to the compact size, and cabling is effectively reduced to very short leads. Battery power and RF interface together allow full isolation from surrounding equipment. Therefore safety concerns are greatly reduced, and are focused only on input and output stage design of the unit. It is interesting to see the current consumption of this battery powered unit (Fig. 66).
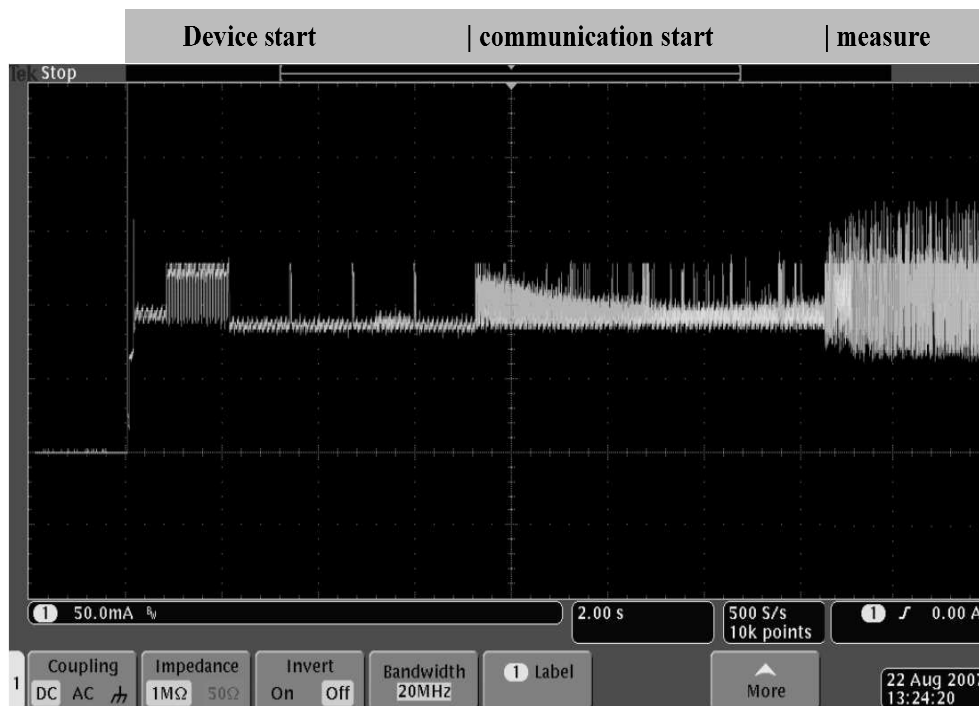
Fig. 66. Current consumption of the tissue monitor. Measured with Tektronix TCP0030 120 MHz current probe on the accumulator wire.

Average power consumption is well within 100 mA measured with Agilent 34410A multimeter. From that the Bluetooth communication consumes about 15 mA, Atmel AVR based communications controller about 10 mA, 12 MHz system oscillator about 2 mA, four instrumentation amplifiers AD8251 from Analog Devices about 4x5=20 mA, power supply circuits about 10 mA, design errors

count for roughly 10 mA, and only approximately 30 mA can be contributed to signal processing. It suggests that, even when sampling at higher frequency, parallel signal processing in FPGA circuit can be made reasonably efficient.

3.3   Revisions and directions for future development

All in all following shortcomings need addressing in consequent models:

Signal processing capability of the used single digital signal processor should be enhanced, in order to utilize analog to digital converters capabilities. Among the possibilities is development of the dedicated signal processor based on the FPGA, currently in process (Ellervee, Annus, & Min, 2009). Also signal processing algorithm needs revisiting in this context. The numerical synchronous detection (NSD) based approach (Annus, Kuusik, Land, Märtens, & Ronk, 2006) needs more complicated sampling but less computation than the DFT based approach. It is important that NSD enables to obtain the desired results at every sample more easily. By applying averaging methods, also the averaged results with lower noise level can be achieved. The NSD based approach with its special sampling system can be easily applied in a system with M simultaneously working SISO (single input – single output) tissue impedance measurement channels and eliminates interference between these channels. It suits also for alternating (cyclic) measurement of the responses to the excitations from M outputs at every input. NSD approach based parallel signal-processing channels of the MIMO (multiple input-multiple output) system can be efficiently realized on the FPGA. Sampling based synchronous demodulation with shortened square wave is an interesting alternative. Simple sorting, occasional shifting and summing operations are fast, and can be also massively parallel in FPGA.

At the highest possible sampling frequencies the noise suppression achieved by means of the discrete Fourier transformation was not excellent with the current sample rate. The noise was largely caused by DC-DC converters and masked the small (fraction of the %) modulations caused by the varying bioimpedance. It was improved by introduction of the first order analog low pass filters in front of the converters, and sufficiently low noise level was achieved at the output. As a result 1% modulation of the 100-ohm base impedance has been clearly distinguished. Nevertheless it is not the best possible solution for the future. One possible way to reduce the problem is usage of accumulators instead of DC-DC converters.

Major drawback of the analyzer's current realization is its high current consumption (due to parallel multichannel and non optimized structure in the analog part and also due to power consumed by digital signal processing). The goal is to reduce the analyzer's power consumption of at least 10 times, which makes it possible to supply it entirely from USB port of the connected PC or form small battery. Appealing solution is to reduce channel number in single device, and to make the design more modular, each module (channel) consuming less power, and also delivering less data.

It is also quite clear that active probing has to be introduced. Adverse effects from cabling, including noise pickup, attenuation and phase errors at higher frequencies can be drastically reduced by placing at least the current source and voltage pickup amplifier in the close vicinity to the electrodes. Possibility to multiplex signals arbitrarily is lost by doing so, but increased performance and ease of operation overweight that manyfold. For testing purposes input module with crosspoint switches has been replaced with active probes near the electrodes. This implementation was tested with encouraging results.

By using accumulators isolation barrier can be shifted outside the device. Highly appealing solution is usage of optical Ethernet instead of USB (Min, Parve, Annus, & Paavle, 2006). Ethernet is both more reliable and with overall higher sustained throughoutput. By moving to the Ethernet whole range of solid TCP IP based solutions becomes usable. Some advantages of the Ethernet include: UPnP, SNMP, DHCP, etc. enabled automatic discovery, addressing, asset management, and network management; serving up web pages, UI, manuals, and support; unlimited range, unlimited number of nodes; multiple media choices, from CAT5 cable to wireless to glass, giving integrators unprecedented connectivity and isolation options and more. Among them is also LAN eXtensions for Instrumentation (LXI). By introducing LXI protocol, and boundary clock system together with IEEE 1588 Precision Timing Protocol (PTP), very good synchronization of many devices becomes possible, even worldwide if required (The LXI Consortium, 2009). Some performance data regarding maximum resolution of synchronization capabilities can be found in (Benetazzo, Narduzzi, & Stellini, 2007). Second viable solution is to use Bluetooth based RF link instead. It is already certified for usage in medical instruments, and suggested in Continua health alliance Version One Design Guidelines. Third possibility to be explored is usage of recently introduced USB 3.0 standard. It is both much faster than previous counterparts, and allows much higher current to be drawn from the host device.

3.4 Modular bioimpedance spectroscopy device

Based on previous experience following structure can be suggested for single channel multifrequency bioimpedance measurement unit (Fig. 67). On excitation side single four channel DDS chip AD9959 from Analog Devices is suggested. It allows simultaneous excitation at four frequencies, amplitude regulation, and allows experimentation with chirp pulses as well. It is followed by filter, signal conditioning, and resistive current source. On the input side signal is amplified by instrumentation amplifier and then synchronously sampled by AD764 from Analog Devices. It is 18-bit, 2 MSPS, charge redistribution SAR with fully differential input, and operates from a single 2.5 V power supply. Central to the unit is low phase noise clock generation and distribution unit in close vicinity to the DDS and AD converter. Parallel signal processing on eight frequencies simultaneously is handled by dedicated FPGA based structure (Ellervee, Annus, & Min, 2009). It can be encapsulated in small enclosure, battery powered, and used directly near the electrodes. To use many of these modules in parallel a common external 1 ms synchronization should be available.
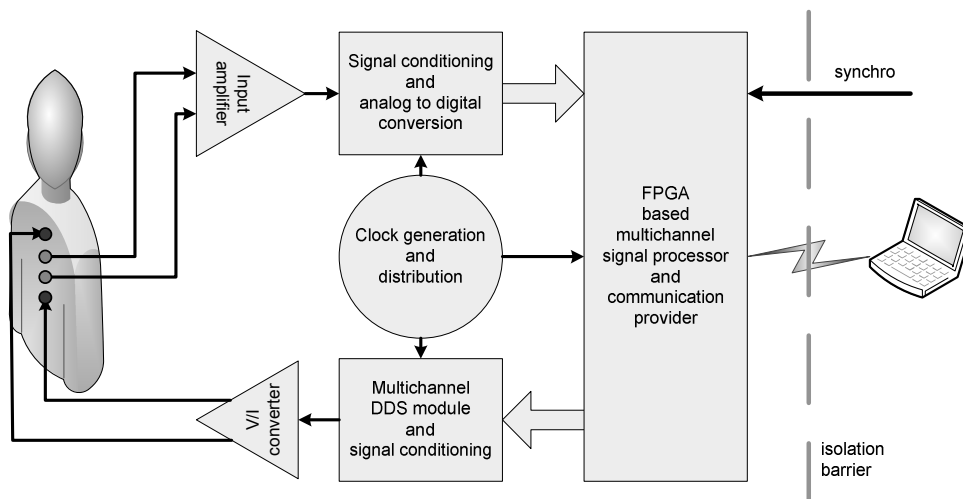
Fig. 67. Functional block diagram of the suggested multifrequency unit.

3.5   **Towards the future**

Research continues in several directions. First of all both time duration, and frequency band optimized signals are investigated. Starting with different chirps (Fig. 68) up to more exotic custom designed waveforms. Signal processing can be based on of the correlation and FFT (Fig. 69), or ultimately also customized.
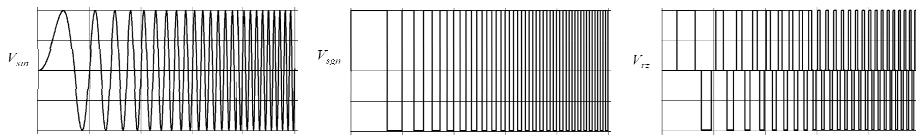
Fig. 68. Different chirp signals (Min, Pliquett, Nacke, Barthel, Annus, & Land, 2008).
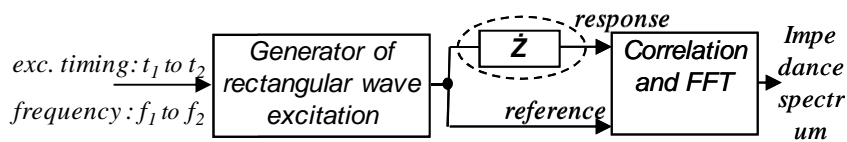
Fig. 69. Simplified block diagram of the suggested chirp based measurement unit.

Totally new and interesting approach is based on DASP technology (Bilinskis, 2007). Direct Analog to Digital Event converter (DADEC), utilizing input signal comparison with sine waves, is very promising for distributed measurement systems.
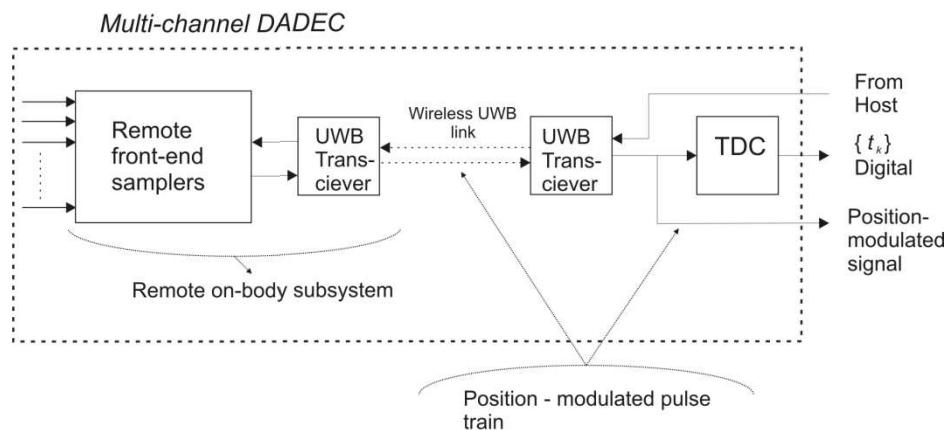
Fig. 70. Possible functional block diagram of the multichannel DADEC system.

3.6 Conclusions

Methods for fast and efficient measurements have been investigated by author, and new solutions proposed, including specific waveforms. New methods and algorithms have been investigated and proposed for synchronous sampling and signal processing. Efficient partition between analog and digital signal processing has been investigated, and solutions suggested. Many articles have been published internationally, including participation in writing of the article which received the best paper award of TUT in engineering in 2007 (Min, Parve, Ronk, Annus, & Paavle, Synchronous Sampling and Demodulation in an Instrument for Multifrequency Bioimpedance Measurement, 2007)

Author has participated in design and development of the device for multisite, multifrequency intracardiac impedance spectroscopy. New methods have been successfully applied, and are partly waiting to be introduced in coming designs. Based on achieved results several international patent applications have been published, and one national patent has been granted. Author has introduced contemporary design solutions into the analog part of the measurement system, as well as into sampling and signal processing. The developed instrument suits well for research in laboratory conditions, and has been successfully applied in several high profile locations worldwide.

Main contributions by the author:

- New synchronous sampling patterns;
- New waveforms for energy efficient synchronous signal processing;
- Several tested current source designs;
- Development of the frequency dependent current limitation circuitry;
- Circuit for speedy DDS amplitude changes;
- Design of the analog side circuitry for the described device.

Considering acquired experience new solutions have been proposed and tested. Further development of the low-power versatile impedance spectroscopy devices continues. Design of an application specific integrated circuit (ASIC) based current source (Kasemaa & Annus, 2008) for efficient generation of the above described shortened square wave signals is currently in progress.

Achieved results should ultimately advance the art of synchronous measurements, enhance medical diagnostics and lower the costs in healthcare sector.

References

Agilent Technologies, Inc. (2009). *Agilent Impedance Measurement Handbook 4th Edition.* Agilent Technologies.

Annus, P., & Kipper, R. (2007). *Patent No. P200700045.* Eesti.

Annus, P., Krivoshei, A., Min, M., & Parve, T. (2008). Excitation Current Source for Bioimpedance Measurement Applications: Analysis and Design. *Instrumentation and Measurement Technology Conference Proceedings, 2008. IMTC 2008. IEEE* (pp. 848-853). Victoria: IEEE.

Annus, P., Kuusik, A., Land, R., Märtens, O., & Ronk, A. (2006). A Digital Multichannel Bioimpedance Analyser: Signal Processing Task and its Solution. *Proc. of the IEEE Instrumentation and Measurement Technology Conference IMTC2006* (pp. 1405 - 1409). Sorrento: IEEE-Inst Electrical Electronics Engineers Inc.

Annus, P., Lamp, J., Min, M., & Paavle, T. (2005). Design of a bioimpedance measurement system using direct carrier compensation. *Proceedings of the 2005 European Conference on Circuit Theory and Design, ECCTD05. III*, pp. 23-26. Cork: IEEE.

Annus, P., Min, M., & Ojarand, J. (2008). Shortened square wave waveforms in synchronous signal processing. *Proc. of 2008 IEEE Instrumentation and Measurement Technology Conf.* (pp. 1259-1262). Victoria: IEEE.

Annus, P., Min, M., & Ojarand, J. (2009). *Patent No. WO 2009/138093 A1.*

Benetazzo, L., Narduzzi, C., & Stellini, M. (2007). Analysis of Clock Tracking Performances for a Software-only IEEE 1588 Implementation. *Instrumentation and Measurement Technology Conference Proceedings, 2007.* (pp. 1-6). Warsaw: IEEE.

Bertemes-Filho, P., Brown, B. H., & Wilson, A. J. (2000). A comparison of modified Howland Circuits as current generators with current mirror type circuits. *Physiol. Meas.* , 1-6.

Bilinskis, I. (2007). *Digital Alias-free Signal Processing.* Chichester: Wiley.

Birkett, A. (2005, 12 5). Bipolar current source maintains high output impedance at high frequencies. *EDN* , pp. 128-130.

Bombelli, R. (1569). *L'algebra.* Bologna.

Boone, K. G., & Holder, D. S. (1996). Current approaches to analogue instrumentation design in electrical impedance tomography. *Physiol. Meas.* , 229-247.

Bordeau, S. P. (1982). *Volts to Hertz: The Rise of Electricity.* Minneapolis: Burgess Intl Group.

Born, I. (1971). *The Born-Einstein Letters.* New York: Walker and Company.

Brannon, B., & Barlow, A. (2006). *AN-501 Aperture Uncertainty and ADC System Performance.* Norwood: Analog Devices, Inc.

Brittain, J. E. (2006). Electrical Engineering Hall of Fame - Arthur E. Kennelly. *94* (9), 1772-1775.

Bush, V. (1940). Bibliographical Memoir of Arthur Edwin Kennelly 1861-1939. *Bibliographical Memoirs , XXII*.

Chen, C.-Y., Lu, Y.-Y., Huang, W.-L., & Cheng, K.-S. (2006). The Simulation of Current Generator Design for Multi-Frequency Electrical Impedance Tomograph. *Proceedings of the 28th IEEE EMBS Annual International Conference* (pp. 6072-6075). New York: IEEE.

Cohn, M., & Lempel, A. (1977). On fast M-sequence transforms. *IEEE Transactions on Information Theory* , 135- 137.

Cole, K. S. (1928). Electric Impedance of Suspensions of Spheres. *The Journal of General Physiology* , 29-36.

Cole, K. S., & Cole, R. H. (1941). Dispersion and Absorption in Dielectrics. *Journal of Chemical Physics , 9,* 341-351.

Cushing, R. (1999). *A Technical Tutorial on Digital Signal Synthesis.* Analog Devices.

Duhamel, P., & Vetterli, M. (1990). Fast Fourier Transforms: A Tutorial Review and a State of the Art. *Signal Processing , 4* (19), 259-299.

Ellervee, P., Annus, P., & Min, M. (2009). High Speed Data Preprocessing for Bioimpedance Measurements: Architectural Exploration. *Proc of the 27th NORCHIP Conference.* Trondheim: IEEE.

Fricke, H. (1925). The Electric Capacity of Suspensions With Special Reference to Blood. *The Journal of General Physiology* , 137-152.

Gabor, D. (1946). Theory of Communication. *J. IEE , 93* (26), 429-457.

Gabriel, S., Lau, R. W., & Gabriel, C. (1996). The Dielectric Properties if Biological Tissues. *Phys. Med. Biol.* , 2251-2269.

Geddes, L. A. (1996, october). Who Introduced the Tetrapolar Method for Measuring Resistance and Impedance? *IEEE Engineering in Medicine and Biology*, pp. 133-134.

Gordon, R. (2007). *Modelling of Cardiac Dynamics and Intracardiac Bioimpedance.* Tallinn: TUT Press.

Graeme, J. G. (1973). *Applications of operational amplifiers: third-generation techniques.* New York: McGraw-Hill.

Grimnes, S., & Martinsen, O. G. (2008). *Bioimpedance and Bioelectricity Basics.* Oxford: Elsiver.

Grimnes, S., & Martinsen, O. G. (2006). Sources of Error in Tetrapolar Impedance Measurements on Biomaterials and Other Ionic Conductors. *Journal of Physics* , 9-14.

Heideman, M. T., Johnson, D. H., & Burrus, S. C. (1984, October). Gauss and the History of the Fast Fourier Transform. *IEEE ASSP Magazine* , pp. 14-21.

Hong, H., Rahal, M., Demosthenous, A., & Bayford, R. H. (2007). Floating voltage-controlled current sources for electrical impedance tomography. *Circuit Theory and Design, 2007. ECCTD 2007. 18th European Conference on* (pp. 208-211). Seville: IEEE.

Horowitz, P., & Hill, W. (1989). *The Art of Electronics* (Vol. I). Cambridge: Cambridge University Press.

Houston, E. J., & Kennelly, A. E. (1895). *Alternating Electric Currents.* New York: The W.J. Johnston Company.

IEC. (n.d.). IEC 60601-1 Medical Electrical Equipment. Part 1: General requirements for safety.

Jerri, A. J. (1977). The Shannon Sampling Theorem-Its Various Extensions and Applications: A Tutorial Review. *Proceedings of the IEEE* , pp. 1565-1596.

Johnson, D. H. (2001, August 11). *Origins of the Equivalent Circuit Concept.* Retrieved from www.ece.rice.edu/~dhj/paper1.pdf

Johnson, J. B. (1928). Thermal Agitation of Electricity in Conductors. *Physical Review* , *32* (1), 97-109.

Karvonen, S., Riley, T., & Kostamovaara, J. (2001). A low noise quadrature subsampling mixer. *The 2001 IEEE International Symposium on Circuits and Systems, 2001. ISCAS 2001.* (pp. 790-793). Sidney: IEEE.

Kasemaa, A., & Annus, P. (2008). CMOS current source for shortened square wave waveforms. *Electronics Conference, 2008. BEC 2008. 11th International Biennial Baltic* (pp. 119-120). Tallinn: IEEE.

Kennelly, A. E. (1893). Impedance. (pp. 175-232). New York: American Institute of Electrical Engineers.

Krivoshei, A. (2009). *Model Based Method for Adaptive Decomposition of the Thoracic Bioimpedance Variations Into Cardiac and Respiratory Components.* Tallinn: TUT Press.

Kubicek, W. G., Karnegis, J. N., & Patterson, R. P. (1966). Development and evaluation of an impedance cardiac output system. *Aerosp Med* , 1208-1212.

Kubicek, W. G., Patterson, R. P., & Lillehei, R. C. (1970). Impedance cardiography as a non-invasive method to monitor cardiac function and other parameters of the cardiovascular system. *Ann NY Acad Sci* , 724-732.

Kuhlberg, A., Land, R., Min, M., & Parve, T. (2003). PWM Based Lock-In Bioimpedance Measuremnt Unit for Implantable Medical Devices. *XVII IMEKO World Congress.*

Lotman, J. (2005). *Kultuur ja plahvatus.* Tallinn: Varrak.

Martinsen, G. O., & Grimnes, S. (2005). Cole Electrical Impedance Model-Critique and an Alternative. *IEEE Transactions on Biomedical Engineering* , *52* (1), 132-135.

Min, M., Annus, P., Kuusik, A., Land, R., Parve, T., Ronk, A., et al. (2007). *Patent No. WO2007/121756 A2.*

Min, M., Kink, A., Land, R., & Parve, T. (2006). *Patent No. US2006/0100539 A1.* United States of America.

Min, M., Land, R., Märtens, O., Parve, T., & Ronk, A. (2004). A sampling multichannel bioimpedance analyzer for tissue monitoring. *Engineering in Medicine and Biology Society, 2004. IEMBS '04. 26th Annual International Conference of the IEEE* (pp. 902-905). San Francisco: IEEE.

Min, M., Ollmar, S., Gersing, E. (2003). Electrical Impedance and Cardiac Monitoring – Technology, Potential and Applications. *International Journal of Bioelectromagnetism, Vol. 5, No. 1*, pp. 53-56.

Min, M., Paavle, T., Annus, P., & Land, R. (2009). Rectangular wave excitation in wideband bioimpedance spectroscopy. *Proceedings of the 2009 IEEE International Workshop on Medical Measurements and Applications* (pp. 268-271). IEEE Computer Society.

Min, M., Parve, T., & Ronk, A. (1992). Design Concepts of Instruments for Vector Parameter Identification. *IEEE transactions on instrumentation and measurement, 41* (1), 50-53.

Min, M., Parve, T., Annus, P., & Paavle, T. (2006). A Method of Synchronous Sampling in Multifrequency Bioimpedance Measurements. *Proc. of the 23rd IEEE Instrumentation and Measurement Technology Conference (IMTC/06)* (pp. 1699 - 1703). Sorrento: IEEE Operations Center.

Min, M., Parve, T., Ronk, A., Annus, P., & Paavle, T. (2007). Synchronous Sampling and Demodulation in an Instrument for Multifrequency Bioimpedance Measurement. *IEEE Transactions on instrumentation and Measurement* , 1365-1372.

Min, M., Pliquett, U., Nacke, T., Barthel, A., Annus, P., & Land, R. (2008). Broadband excitation for short-time impedance spectroscopy. *Physiological Measurement* , *29*, S185-S192.

Northrop, R. B. (2004). *Analysis and Application of Analog Electronic Circuits to Biomedical Instrumentation.* Boca Raton: CRC Press.

Nyquist, H. (1928). Thermal Agitation of Electric Charge in Conductors. *Physical Review , 32* (1), 110 - 113.

Ohm, G. S. (1827). *Die galvanische Kette : mathematisch bearbeitet.* Berlin: Riemann.

Paavle, T., Annus, P., Kuusik, A., Land, R., & Min, M. (2007). Bioimpedance monitoring with improved accuracy using three-level stimulus. *Circuit Theory and Design, 2007. ECCTD 2007. 18th European Conference on* (pp. 412-415). Seville: IEEE.

Pallas Areny, R., & Webster, J. G. (1993). Bioelectric impedance measurements using synchronous sampling. *IEEE Transactions on Biomedical Engineering , 40* (8), pp. 824-829.

Patterson, R. P., Kubicek, W. G., Kinnen, E., Witsoe, D. A., & Noren, G. (1964). Development of an electrical impedance plethysmography system to monitor cardiac output. *Proc of the First Ann Rocky Mountain Bioengineering Symposium*, (pp. 56-71).

Pease, R. A. (2008). *A Comprehensive Study of the Howland Current Pump.* National Semiconductor Corporation.

Schwan, H. P. (1999). The Practical Success of Impedance Techniques from an Historical Perspective. In *Electrical Bioimpedance Methods: Applications to Medicine and Biotechnology* (pp. 1-12). New York: New York Academy of Sciences.

Seoane, F., Bragos, R., & Lindecrantz, K. (2006). Current source for multifrequency broadband electrical bioimpedance spectroscopy systems. A novel approach. *Engineering in Medicine and Biology Society, 2006. EMBS '06. 28th Annual International Conference of the IEEE* (pp. 5121 - 5125). New York: IEEE.

Soares, L. R., Oliveira, H. M., Cintra, R. J., & Campello de Souza, R. M. (2003). Fourier Eigenfunctions, Uncertainty Gabor Principle And Isoresolution Wavelets. *XX Simposio Brasiliero De Telecomunicacoes.* Rio De Janeiro.

The LXI Consortium. (2009). *LXI | LAN eXtensions for Instrumentation | Home.* Retrieved 2009, from http://www.lxistandard.org/

Udal, A., Kukk, V., & Velmre, E. (2009, 6). Critical Analysis of Uncertainty Relations Based on Signal Duration and Spectrum Width. *ELEKTRONIKA IR ELEKTROTECHNIKA* , pp. 31-34.

Wang, C., Xu, M., & Wang, H. (2005). Mixing Frequency Biology Impedance Measurement with Virtual Reference Point. *Instrumentation and Measurement Technology Conference, 2005. IMTC 2005. Proceedings of the IEEE* (pp. 1407-1410). Ottawa: IEEE.

Weber, E., & Nebeker, F. (1994). *The evolution of electrical engineering : a personal perspective.* New York: IEEE Press.

Webster, J. G. (1997). *Medical Instrumentation: Application and Design* . Boston: Wiley.

Wei, Y., & Zhang, Q. (2000). *Common Waveform Analysis. A New and Practical Generalization of Fourier Analysis.* Boston, Dordrecht, London: Kluwer Academic Publishers.

Velmre, E. (1971, 1). Tallinast võrsunud avastaja. *Horisont* .

WHO. (2009). *Cardiovascular diseases (CVDs).* (WHO Media centre) Retrieved from http://www.who.int/mediacentre/factsheets/fs317/en/index.html

von Hippel, A. R. (1988). The Dielectric Relaxation Spectra of Water, Ice, and Aqueous Solutions, and their Interpretation. *IEEE Transactions on Electrical Insulation , 23* (5), 790-840.

Vujić, J. (2006). Nikola Tesla: Electrifying Legacy. *Scientific-Technical Review , LVI* (2), 3-9.

APPENDIXES

A Digital Multichannel Bioimpedance Analyser: Signal Processing Task and its Solution.

Annus, P.; Kuusik, A.; Land, R.; Märtens, O.; Ronk, A. (2006).

In: Proc. of the IEEE Instrumentation and Measurement Technology Conference IMTC2006: IEEE Instrumentation and Measurement Technology Conference, Sorrento, Italy, April 24-27, 2006. USA: IEEE-Inst Electrical Electronics Engineers Inc, 2006, 1405 - 1409.

Design of a Bioimpedance Measurement System Using Direct Carrier Compensation.

Annus, Paul; Lamp, Jürgen; Min, Mart; Paavle, Toivo (2005).

Shortened square wave waveforms in synchronous signal processing.
Annus, Paul; Min, Mart; Ojarand, Jaan (2008).
In: 2008 IEEE International Instrumentation and Measurement Technology Conference Proceedings: 2008 IEEE International Instrumentation and Measurement Technology Conference (I2MTC 2008), 12-15 May 2008, Victoria, British Columbia, Canada, 2008. , 2008, 1259 - 1262.

Patent application, 12.05.2008, **Method and device using shortened square wave waveforms in synchronous signal processing**, Paul Annus, Mart Min, Jaan Ojarand

Excitation Current Source for Bioimpedance Measurement Applications: Analysis and Design.
Annus, P.; Krivoshei, A.; Min, M.; Parve, T. (2008).
2008 IEEE International Instrumentation and Measurement Technology Conference (I²MTC 2008), 12-15 May 2008, Viktoria, British Columbia, Canada. , 2008, 848 - 853.

Patent, 15.12.2009, **Sümmeetriline vooluallikas**, Paul Annus, Rein Kipper

Synchronous Sampling and Demodulation in an Instrument for Multifrequency Bioimpedance Measurement.
Min, M.; Parve, T.; Ronk, A.; Annus, P.; Paavle, T. (2007)
IEEE Transactions on instrumentation and Measurement, 56(4), 1365 - 1372.

Patent application: Method and device for multichannel multifrequency analysis of an object; Omanik: ELIKO Tehnoloogia Arenduskeskus OÜ; Autorid: Mart Min, Paul Annus, Antti Haapalainen, Alar Kuusik, Raul Land, Toomas Parve, Ants Ronk; Prioriteedinumber: US60/745488; Prioriteedikuupäev: 24.04.2006

ELULOOKIRJELDUS

Eesnimi	Paul
Perekonnanimi	Annus
Sünniaeg (pp.kk.aaaa)	30.04.1962
E-mail	paul.annus@eliko.ee

Teenistuskäik

Töökoht ja amet

2005 - ... Tallinna Tehnikaülikool, Infotehnoloogia teaduskond, Elektrooni-kainstituut; doktorant

2004 - ... ELIKO Tehnoloogia Arenduskeskus OÜ; Projektijuht

Haridustee

1980 - ...   Tallinna Polütehniline Instituut

1982 - 1987   Budapesti Tehnikaülikool

Teadusorganisatsiooniline ja -administratiivne tegevus

2006 - ...   IEEE liige

Keeled

Eesti

Inglise

Ungari

Vene

Teadustegevus

Teaduskraadi info

magistrikraad, 1987, diplomitöö elektroonikast, Budapesti Tehnikaülikool

doktorant, (juh) Mart Min, Toomas Parve, Tallinna Tehnikaülikool, Infotehnoloogia teaduskond, Elektroonikainstituut

Teaduspreemiad ja -tunnustused

2008; TTÜ 2007.a. parima artikli preemia tehnika ja tehnoloogia alal – M. Min, T. Parve, A. Ronk, P. Annus, T. Paavle. Synchronous Sampling and Demodulation in an Instrument for Multifrequency Bioimpedance Measurement. IEEE Trans. I&M, vol.56, no.4.

Teadustöö põhisuunad

Loodusteadused ja tehnika, Elektrotehnika ja elektroonika (bioimpedantsi uuringud)

Jooksvad projektid

Mitmekomponendiliste ja mitme kandjaga mõõtesignaalide süntees ja analüüs: signaalide sünkroon- ja adaptiivtöötluse meetodite ja vahendite arendus

Missioonikriitiliste sardsüsteemide elektroonsed komponendid ja alamsüsteemid

Eureka ITEA2 D-MINT

Juhendatud väitekirjad

Ruiqi Zhang, magistrikraad (teaduskraad), 2009, (juh) Paul Annus, Digital Watermarking Technique Based on DCT (Diskreetsel koosinus transformatsioonil baseeruvad digitaalsed vesimärgid), Tallinna Tehnikaülikool, Infotehnoloogia teaduskond, Elektroonikainstituut

CV

First name: Paul

Last name: Annus

Date of birth (mm/dd/yyyy)   04/30/1962

E-mail   paul.annus@eliko.ee

Career

Institution and position held

2005 - ... Tallinn University of Technology , Faculty of Infotechnology, Department of Electronics; doctoral student

2004 - ... ELIKO Competence Centre in Electronics-, Info- and Communication Technologies; Project Manager

Education

1980 - ...   Tallinn University of Technology

1982 - 1987   BME

Administrative responsibilities

2006 - ...   IEEE member

Languages

Estonian

English

Hungarian

Russian

Research activity

Degree information

Master's Degree, 1987, diploma in electrical engineering (M.Sc. degree), Budapesti Tehnikaülikool

PhD Student, (sup) Mart Min, Toomas Parve, Tallinn University of Technology , Faculty of Infotechnology, Department of Electronics

Honours & Awards

2008; The best paper award of TTU in technics and technology in 2007 – M. Min, T. Parve, A. Ronk, P. Annus, T. Paavle. Synchronous Sampling and Demodulation in an Instrument for Multifrequency Bioimpedance Measurement. IEEE Trans. I&M, vol.56, no.4.

Field of research

Natural Sciences and Engineering, Electrical Engineering and Electronics (bioimpedance)

Current grants & projects

Synthesis and analysis of multi-component and multi-carrier measurement signals: development of methods and means for synchronous and adaptive signal processing

Electronic components and subsystems for mission critical embedded systems

Eureka ITEA2 D-MINT

Dissertations supervised

Ruiqi Zhang, Master's Degree, 2009, (sup) Paul Annus, Digital Watermarking Technique Based on DCT, Tallinn University of Technology , Faculty of Infotechnology, Department of Electronics

List of Publications

Ellervee, P.; Annus, P.; Min, M. (2009). High Speed Data Preprocessing for Bioimpedance Measurements: Architectural Exploration. The 27th NORCHIP Conference, Trondheim, Norway, Nov. 2009.

Min, Mart; Paavle, Toivo; Annus, Paul; Land, Raul (2009). Rectangular Wave Excitation in Wideband Bioimpedance Spectroscopy. In: Proc. 4th International Workshop on Medical Measurements and Applications (MeMeA2009): International Workshop on Medical Measurements and Applications (MeMeA), Cetraro, Italy, May 29-30, 2009. IEEE Operations Center, 2009, 268 - 271.

Paavle, Toivo; Min, Mart; Annus, Paul; Birjukov, Andrei; Land, Raul; Parve, Toomas (2009). Wideband Object Identification with Rectangular Wave Chirp Excitation. In: Proc. of European Conference on Circuit Theory and Design 2009 (ECCTD'09): ECCTD'09 European Conference on Circuit Theory and Design 2009, Antalya, Turkey, August 23-27, 2009. IEEE, 2009, 421 - 424.

Min, Mart; Pliquett, Uwe; Nacke, Thomas; Barthel, Andreas; Annus, Paul; Land, Raul (2008). Broadband excitation for short-time impedance spectroscopy. Physiological Measurement, 29(6), 185 - 192.

Kasemaa, Argo; Annus, Paul (2008). CMOS current source for shortened square wave waveforms. In: Proceedings of the 11th Biennial Baltic Electronics Conference: 2008 International Biennial Baltic Electronics Conference (BEC2008) Tallinn, Estonia, October 6-8, 2008. , 2008, 119 - 120.

Annus, P.; Krivoshei, A.; Min, M.; Parve, T. (2008). Excitation Current Source for Bioimpedance Measurement Applications: Analysis and Design. 2008 IEEE International Instrumentation and Measurement Technology Conference (I²MTC 2008), 12-15 May 2008, Viktoria, British Columbia, Canada. , 2008, 848 - 853.

Annus, Paul; Min, Mart; Ojarand, Jaan (2008). Shortened square wave waveforms in synchronous signal processing. In: 2008 IEEE International Instrumentation and Measurement Technology Conference Proceedings: 2008 IEEE International Instrumentation and Measurement Technology Conference (I2MTC 2008), 12-15 May 2008, Victoria, British Columbia, Canada, 2008. , 2008, 1259 - 1262.

Märtens, Olev; Min, Mart; Land, Raul; Liimets, Aivar; Trampärk, Harri; Annus, Paul (2008). TMS320F2811-based Multi-frequency Multi-channel Bioimpedance Measurement Device. In: Proc. of the 3rd European DSP Education and Research Symposium: 3rd European DSP Education and Research Symposium EDERS 2008, Tel Aviv, Israel, 18th June. , 2008, 179 - 183.

Min, M.; Parve, T.; Ronk, A.; Annus, P.; Paavle, T. (2007). Synchronous Sampling and Demodulation in an Instrument for Multifrequency Bioimpedance Measurement. IEEE Transactions on instrumentation and Measurement, 56(4), 1365 - 1372.

Annus, P.; Kuusik, A.; Land, R.; Haldre, E.; Min, M.; Parve, T.; Poola, G. (2007). An energy efficient wearable tissue monitor. In: IFMBE Proceedings ICEBI 2007 "13th International Conference on Electrical Bioimpedance and the 8th Conference on Electrical Impedance Tomography", Vol. 17, 2007, Graz, Austria: 13th International Conference on Electrical Bioimpedance and the 8th Conference on Electrical Impedance Tomography, Graz, Austria, August 29th - September 2nd 2007. (Toim.) Hermann Scharfetter; Robert Merwa. Berlin Heidelberg: Springer-Verlag, 2007, (IFMBE Proceedings; 17), 240 - 243.

Min, M.; Annus, P.; Land, R.; Paavle, T.; Haldre, E.; Ruus, R. (2007). Bioimpedance Monitoring of Tissue Transplants. In: Proc. of the IEEE Instrumentation and Measurement Technology Conference IMTC 2007: IEEE Instrumentation and Measurement Technology Conference IMTC 2007,Warsaw, Poland, May 1-3, 2007. Warsaw, Poland: IEEE Operations Center, 2007, 1 - 4.

Paavle, T.; Annus, P.; Kuusik, A.; Land, R.; Min, M. (2007). Bioimpedance Monitoring with Improved Accuracy Using Three-Level Stimulus . In: Proc. of European Conference on Circuit Theory and Design 2007 (ECCTD'07): European Conference on Circuit Theory and Design 2007 (ECCTD'07), Seville, Spain, Aug.26-30, 2007. , 2007, 412 - 415.

Min, M.; Pliquett, U.; Nacke, T.; Barthel, A.; Annus, P.; Land, R. (2007). Signals in bioimpedance measurement: different waveforms for different tasks. In: IFMB Proceedings ICEBI 2007 "13th International Conference on electrical Bioimpedance and the 8th Conference on Electrical Impedance Tomography", Vol.17, 2007, Graz, Austria: 13th International Conference on Electrical Bioimpedance and 8th Conference on Electrical Impedance Tomography 2007, ICEBI 2007, Graz, Austria, August 29th - September 2nd 2007. (Toim.) Hermann Scharfetter; Robert Merwa. Berlin Heidelberg: Springer-Verlag, 2007, (IFMBE Proceedings; 17), 181 - 184.

Land, R.; Annus, P.; Min, M. (2007). Time-Frequency Impedance Spectroscopy: Excitation Considerations. In: Proc. of the 15th IMEKO TC4 International Symposium on Novelties in Electrical Measurements and Instrumentations: 15th IMEKO TC4 International Symposium on Novelties in Electrical Measurements and Instrumentations, Iasi, Romania, September 18-22, 2007. (Toim.) Cretu, M.; Sarmasanu, C.. CERMI Publishing House, 2007, 328 - 331.

Annus, P.; Kuusik, A.; Land, R.; Märtens, O.; Ronk, A. (2006). A Digital Multichannel Bioimpedance Analyser: Signal Processing Task and its Solution. In: Proc. of the IEEE Instrumentation and Measurement Technology Conference IMTC2006: IEEE Instrumentation and Measurement Technology Conference, Sorrento, Italy, April 24-27, 2006. USA: IEEE-Inst Electrical Electronics Engineers Inc, 2006, 1405 - 1409.

Min, M.; Parve, T.; Annus, P.; Paavle, T. (2006). A Method of Synchronous Sampling in Multifrequency Bioimpedance Measurements. In: Proc. of the 23rd IEEE Instrumentation and Measurement Technology Conference (IMTC/06), Sorrento, Italy, 24-27 April, 2006: Instrumentation and measurements technology conference (IMTC/06), Sorrento, Italy, 24-27 april 2006. IEEE Operations Center, 2006, 1699 - 1703.

Märtens, O.; Min, M.; Land, R.; Annus, P. (2006). Multi-frequency and Multichannel Bio-impedance Measurement Solution. In: Proceedings of 7th Nordic Signal Processing Symposiun (NORSIG 2006): 7th Nordic Signal Processing Symposiun (NORSIG 2006), Reykjavik, Iceland, June 7-9, 2006. Reykjavik, Iceland: IEEE Operations Center, 2006, 1 - 4.

Annus, Paul; Lamp, Jürgen; Min, Mart; Paavle, Toivo (2005). Modelling, Design and Test of a Bioimpedance Measurement System with Carrier Compensation. Scientific Proc. of Riga Technical University (22 - 25). Riga: Riga Technical University

Annus, Paul; Lamp, Jürgen; Min, Mart; Paavle, Toivo (2005). Design of a Bioimpedance Measurement System Using Direct Carrier Compensation. In: Proc. of the European Conference on Circuit Theory and Design (ECCTD´05, IEEE Publ), Aug.29-Sept.02, 2005, Cork, Ireland, 2005, vol. III: European Conference on Circuit Theory and Design (ECCTD´05, IEEE Publ), Aug.29-Sept.02, 2005, Cork, Ireland, 2005. , 2005, 23 - 26.

Ronk, A.; Annus, P.; Kuusik, A.; Land, R.; Märtens, O. (2005). Digital multichannel bioimpedance analyser: signal processing approaches. In: Proceedings of the International Federation for Medical and Biological Engineering: 3rd European Medical & Biological Engineering Conference; IFMBE European Conference on Biomedical Engineering EMBEC'05, Prague, Czech Republic, November 20-25, 2005. Prague, Czech Republic: EMBEC'05 & IFMBE, 2005, 4pgs.

Patents and patent applications

Patent application: Laiaribaline impedantsi analüsaator; Omanik: ELIKO Tehnoloogia Arenduskeskus OÜ, Tallinna Tehnikaülikool; Autorid: Mart Min, Toivo Paavle, Raul Land, Paul Annus, Toomas Parve; Prioriteedinumber: US61/103061; Prioriteedikuupäev: 06.10.2008

Patent application: Method and device using shortened square wave waveforms in synchronous signal processing; Omanik: ELIKO Tehnoloogia Arenduskeskus OÜ, Tallinna Tehnikaülikool; Autorid: Paul Annus, Mart Min, Jaan Ojarand; Prioriteedinumber: US61/052467; Prioriteedikuupäev: 12.05.2008

Patent: Sümmeetriline vooluallikas; Omanik: ELIKO Tehnoloogia Arenduskeskus OÜ; Autorid: Paul Annus, Rein Kipper; Prioriteedinumber: P200700045; Prioriteedikuupäev: 29.08.2007

Patent application: Method and device for multichannel multifrequency analysis of an object; Omanik: ELIKO Tehnoloogia Arenduskeskus OÜ; Autorid: Mart Min, Paul Annus, Antti Haapalainen, Alar Kuusik, Raul Land, Toomas Parve, Ants Ronk; Prioriteedinumber: US60/745488; Prioriteedikuupäev: 24.04.2006